Order Number 9510663

# Effects of channel fading on a direct sequence-spread spectrum signal at 2 GHz

Ghassemzadeh, Saeed Seyed, Ph.D.

City University of New York, 1994



U·M·I
300 N. Zeeb Rd.
Ann Arbor, MI 48106

# EFFECTS OF CHANNEL FADING ON A DIRECT SEQUENCE-SPREAD SPECTRUM SIGNAL AT 2 GHz

by

SAEED S. GHASSEMZADEH

A dissertation submitted to the Graduate Faculty in Engineering in partial fulfillment of the requirement for the degree of Doctor of Philosophy.

The City University of New York.

1994

This manuscript has been read and accepted for the Graduate Faculty in Engineering in satisfaction of the dissertation requirement for the degree of Doctor of Philosophy.

September 1, 1994
DATE

Professor Donald L. Schilling
Chairman Examining Committee

Sept. 1, 1994
DATE

Dean Gerard Lowen
Executive Officer

Professor J. Barba

Professor S. Maric

Professor T. N. Saadawi

Dr. J. Garodnick

Supervisory Committee

**THE CITY UNIVERSITY OF NEW YORK**

# ABSTRACT


## EFFECTS OF CHANNEL FADING ON A DIRECT SEQUENCE SPREAD SPECTRUM SIGNAL AT 2 GHz

by

**SAEED S. GHASSEMZADEH**

Advisor: Professor Donald L. Schilling

This dissertation considers the most critical parameter in a Personal Communication System; Multipath Fading, and its impact on system performance.

It is shown that the received power loss due to fading (the fade margin before despreader) increases dramatically as the signalling bandwidth decreases below 11 MHz. In particular, comparing the fade margins of 1 MHz and 15 MHz bandwidth signals reveal a difference in fade margin of approximately 10 dB.

Further, it is shown that the multipath observed in practice had almost all of its energy concentrated in a time interval of less than 1 μsec ( for high antenna heights ) with the largest, most significant signal components about 100-200 ns apart. For low antenna heights the excess delay is concentrated

in a time interval of less than 500 n sec with main signal components 40 nsec apart.

The suburban experiments performed to evaluate the fade margins after, despreading, reveal an increase in fade margin of 15 dB with probability 0.001, for a one finger receiver. The variations tend to decrease less when the chip rate is increased. Since, a wider band spread spectrum system can resolve most of the multipath returns, it can use a coherent RAKE receiver to lower its fade margin by up to 14 dB. This improvement cannot be achieved by narrowband CDMA systems which typically have bandwidths less than 10 MHz.

It is also shown that in a particular environment, if a distant multipath signal is present, and if this reflection is delayed by more than 1μs compared to the main return, then a narrowband spread spectrum system can use RAKE to collect this added power. It should be noted, however, that a narrowband system must collect this extra energy since its main signal rays suffer from severe multipath fading independent of the other delayed signals. However, locations having a main and a distant multipath signal, which exceeded 1 μsec delay and which was of amplitude comparable to that of the primary return, were found to be confined to a very low probability of existence within a prescribed cell.

Indoor measurements reveal that there are 5 dominant returns when a 24 Mchips/s system is used. The typical excess delay was 350 nsec and individual components were often 40 nsec apart. It was shown that a coherent RAKE receiver with five fingers could improve the fade margin by approximately 9 dB. Again this improvement cannot be achieved by a narrowband system since such a system could not distinguish between the multipath returns.

## ACKNOWLEDGMENTS

I am forever indebted to my supervisor, Professor Donald L. Schilling, for his excellent guidance, continuous support and for believing in me throughout the course of this study. I am grateful to Dr. Joseph Garodnick for sponsoring the experiments and for his invaluable input during the research.

Special thanks to all InterDigital employees specially John Bird, Ceaser Carrero, Constantine Constantopoulos, Shu Chu, Chris Kalaigian, Ken Robison, Avi Silverberg who helped me during the preparation of the equipment. Special thanks also go to Donald Grieco, Zion Hadad, Dr. Fred Bruno, Dr. Gary Lomp, Dr. Emannuel Kanterakis and Dr. Kourosh Parsa for their invaluable discussions about this dissertation. Thanks to all of you for making it happen!

I thank City University of New York for supporting me financially throughout this work. I would also like to thank, my City University Colleagues, Dr. Vinko Erceg and Dr. Maxwell Taylor for helping me during the measurements and Mr. Hussain Arshad for undertaking the difficult driving duties during the measurements in New York City.

I cannot thank enough to repay the love, patience, encouragement and generosity given to me by my family. THANK YOU EVER SO MUCH.

Finally, to Sharon my wife, thanks for all your love, support and patience. Thanks for giving me the most delicious fruit of life, Sara Nicole, and joining me in this venture and making a success of it. I dedicate this work to both of you.

# TABLE OF CONTENTS

## LIST OF TABLES

## LIST OF FIGURES

# 1. Introduction

Over the past decade the interest in wireless communication has been nothing but spectacular. A goal of wireless communication is to make communication truly personal, so that anyone can place a call from anywhere at anytime, through a nationwide wireless network. The future of mobile communication systems relies highly upon the techniques of network planning and mobile radio design which will enable efficient and economical use of the spectrum assigned to industry by the regulatory agencies such as the United States FCC.

To encourage mobile radio deployment, the FCC in 1974 allocated 40-MHz of the spectrum in the 800- to 900- MHz band for development of advanced high-capacity systems. As a result, an analog FM technique called the Advanced Mobile Phone Service (AMPS) cellular system was proposed based on the reuse of assigned channel frequencies in a cellular planned network. It was designed and tested by the Bell Telephone Laboratories. In 1986, the FCC allocated an additional 5 MHz to each band adding 83 more channels to each band. This system, currently in use, has a low capacity and like all narrowband wireless techniques does not perform well in the presence of fading. Therefore, users do not experience a wired line type of service; i.e., dropped calls, lower voice quality and limited services are most common in an

AMPS network.

The revolution in mobile and portable technologies has continued non-stop in the past decade since cellular was first authorized. Personal communications requirements in the United States are rapidly changing as our society becomes more mobile and the demand for instantaneous communication increases.

There is a steadily increasing consumer and business interest in new mobile services and technologies for numerous, sometimes incompatible, applications. These include wireless PBX, smaller, lighter, portable cellular phones, multi-channel cordless phones, and services that facilitate contacting an individual instead of a particular station. In 1992, the FCC issued a policy statement on Personal Communication Services (PCS) and opened a proceeding designed to make available spectrum in the 2 GHz band for a variety of emerging technologies including PCS. Subsequently, cellular mobile telecommunications manufacturers and carriers became interested in new digital cellular and microcellular technologies which provide higher capacity, more user services, higher data rate and better voice quality than AMPS. The proposed microcellular system increases the number of users dramatically [1-4]. To allow multiple users to simultaneously communicate over a fading channel with higher capacity, spread-Spectrum (SS) techniques

have been proposed for use in mobile radio to realize higher spectral efficiency [5], and are strongly being considered for use in cellular and microcellular communication systems [4, 6-8]. The bandwidth of the SS signal plays an important role in system capacity, voice quality, and fading behavior of the signals. Variations in the received signal's amplitude are called signal fading or multipath fading. The prerequisite for the design specification of any wireless communications system is having knowledge of the mobile radio fading channel characteristics in various environments and signalling bandwidths. This requirement was the main factor behind the research presented herein.

In the following sections, we describe the problem and previous work. A description of spread spectrum signals, multipath fading channel parameters, RAKE receiver and received envelope characterization is given in Chapter 2. Chapter 3 presents an overview of various channel sounding techniques. Chapter 4 describes the experimental equipment, set-up and procedures. In Chapter 5, the method of data processing is explained and the results are discussed. Finally, the conclusion of the work is discussed and future work is presented.

### 1.1. Statement of the problem

Because of multipath propagation phenomena (See Figure 1.1), when the

base station transmits to the mobile unit (or vice-versa), the signal takes various paths to the receiver. These signals, each with random amplitude, phase and delay, add vectorially to form the combined received signal. Therefore, in a mobile environment, there are significant variations in the received signal's envelope.

As we mentioned earlier, the bandwidth of the SS signal plays an important role in the fading behavior of the channel as experienced by the mobile receiver. This bandwidth is directly proportional to the chip rate of the SS signal and inversely proportional to duration of its chips (the spread spectrum bits are referred to as "chips"). This means that as the chip rate of the system decreased the signal bandwidth decreases while the chip duration increases. As a result, the probability of incoming multipaths within a chip is more likely. As the number of multipaths within the chip increases, the frequency and depth of the fades also increase. The statistics of these fades are a function of the chip rate used in the SS system as well as the environment which the system operates in. The knowledge of these statistics helps the system engineers to understand the fading channel better and to determine optimum methods of circumventing the impairments caused by the multipath fading. In fact, the envelope statistics can be used in designing the APC and in calculation of spill-over power to adjacent cells.

To date, there are no propagation measurements available which compares the received envelope variation as a function of chip rate in different environments. In this work, we are mainly concerned with the effects of channel fading on the received envelope of the SS signals as the chip rate of the system is varied. These effects will be analyzed in terms of statistics of received envelope variations and the ability of the receiver to resolve the multipaths in order to improve its performance. The channel effects will be analyzed for both before and after despreading of the received SS signal. Although, it is not the scope of this work to model the channel, an attempt is made to model the envelope variations of the received signal. This will be done by fitting various cumulative distributions to the measured data. This work is the result of designing a "channel sounder" such that it will enable us to find:

1. The statistics of received envelope variations before despreading as a function of signalling bandwidth. This envelope is the envelope of the sum of all the rays that are present at the receiving antenna.
2. The statistics of the received signal envelope after despreading as a function of signalling bandwidth. This is the envelope of the ray that the SS system is synchronized with.
3. The effect of chip rate on the receiver's observation of channel's excess delay and its impact on the communication system.

## 1.2. Previous work

Although wideband measurements had been performed as early as the 1950 [31], it is the work of Cox at 910 MHz in New York City around 1972 which is referred to as the first definitive study for wideband mobile channel characterization. Cox's study [19-21] concentrated heavily on presenting average delay profiles, frequency correlation and separation, and two dimensional delay-Doppler scattering functions. However, one shortcoming of the work was that it never investigated the envelope variations of the cross-correlator output for different signalling bandwidths.

Channel measurements are devided into two catagories: Narowband and wideband measurements. Narrowband (CW) measurements have been performed in attempt to characterize the UHF channel in factories [16]. In [16], Rappaport's indoor measurements indicated 30-35 dB fading dynamic range over distances of a few wavelength which translates to 20-30 dB fades below the mean signal power. The distribution of the fast fades were reported as Rayleigh. In a light clutter, when the receiver is in the line-of-sight of transmitter, Rappaport found that the fast variations of the envelope can be modeled by a Rician with K value of 2 dB. However, the distribution of the envelope was found to be log-normal with $\sigma$ = 6 dB hold well for obstructed factory paths. Other researcher who have performed wideband (10-11 MHz) measurements in buildings [22, 24, 25, 27], in and

around houses [18] have reported less envelope variations when a wider band signal was used.

Bultitude [22-24], used a 40 Mchips/s SS signal for its indoor measurements at 910 MHz and 1.75 GHz. He found that the envelope of the despreader output was also Rician distributed with K value of 8 dB. But its average delay profile showed a delay spread of no more than 400 nsec. This means that a 10 finger coherent RAKE can be used by a wider band CDMA system to improve its fade margin whereas a narrower band CDMA (say 1 Mchips/s) could not resolve the multipath and use of a RAKE receiver would not be of any advantage.

Demery [30] used a 10 Mchips SS signal in his channel sounder at 880 MHz. He found the same results for urban area where the envelope of the despreader output exhibited Rayleigh behavior. In fact, in [30], he shows that the envelope of the first 10 returns have the same behavior. Other researchers [20, 21, 23, 26] concur with Demery that the envelope suffers from the Rayleigh fading in Urban areas. However, non of them have tried to investigate the effect of changing the wideband sounding rate on the SS signal. It should be noted that while the above mentioned researchers investigated same chip rate at different frequencies, to date, no measurements have been made to determine how the channel fading caused

by multipath propagation affects the transmitted signal as the chip rate of the signal is varied.

# 2. Theory

## 2.1. Spread Spectrum Signals And Systems

Spread spectrum is a technique in which the spectrum of the transmitted signal is spread over a wide range of frequencies; much wider, in fact, than the minimum bandwidth required to transmit the information being sent. As a result, the power per unit frequency decreases so that the wave form barely interferes with any other signal operating in the same frequency band [9-11]. Spread spectrum techniques have been long established and used for antijam and multipath rejection applications as well as for accurate ranging and tracking and are currently being used in military communications [12-14].

Spread Spectrum is typically designed to be "transparent" to other users. This means that spread spectrum signals are designed to provide negligible interference to the communication of other existing users, and indeed, it is difficult to detect if a spread spectrum signal is present. This is known as the Low Probability of Detection (LPD) characteristic of the spread spectrum signal which allows transmission between users of a spread spectrum network without the existing users experiencing significant interference. Spread spectrum is also "jam" or interference resistant. A spread spectrum receiver spreads the spectrum of the interfering signal and hence reduces the interference so that it does not noticeably degrade system

performance. It is this feature of interference reduction that makes spread spectrum useful for commercial communications, i.e., the spread spectrum wave forms can be overlaid on top of existing narrowband signals [7].

Direct Sequence-Spread spectrum (DS-SS) achieves a spreading of the spectrum by modulating the original signal with a very wideband signal relative to the data bandwidth. This wideband signal is normally chosen to have two possible amplitudes, ±1, and they are switched, in a pseudo-random manner, periodically. Thus, at each equally spaced time interval, a decision is made as to whether the wideband modulating signal should be ±1. The generation of such a decision is done electronically and approximately random which is known a priori to the transmitter and receiver. The resulting signal is a high rate NRZ (Non-Return-to-Zero signal, also called bi-phase signal), Pseudo-Random Noise (PN) binary sequence having the values ±1.

A Direct Sequence-Binary Phase Shift Keying (DS-BPSK) spread spectrum signal is one where a carrier is modulated by the spread signal explained above. Since the second modulation has the effect of "chopping" the original data bits, PN "bits" are also referred to as "chips". The PN code sequences can be generated many ways including a Maximal-Length (ML) shift-register with feedback. Maximal length codes are a class of cyclic codes and

have good autocorrelation properties. The length of the code sequence, L, is determined by the number of the shift register stages, m, as follows:

$$L = 2^m - 1 \tag{2-1}$$

The code period is $T = LT_c$ where $T_c$ is the PN chip period. Figure 2.1 shows the autocorrelation of a PN code of length 255 when a chip rate of 25 MHz is used. Periodic ML-PN sequences exhibit a periodic autocorrelation which is represented as follows:

$$\varphi(\tau) = \begin{cases} 1 - \left\lfloor \dfrac{L+1}{L} \right\rfloor \left| \dfrac{\tau}{T_c} \right| & \text{for } |\tau| \le T_c \\ \dfrac{-1}{L} & \text{for } T_c < |\tau| < T - T_c \end{cases} \tag{2-2}$$

Spread spectrum signals, in general, are defined as either "narrowband" or "broadband" spread spectrum signals. Within the context of this dissertation the narrowband signals are those with bandwidth smaller than the coherence bandwidth of the channel in which the system is operating. Broadband spread spectrum signals are those with bandwidth greater than the coherence bandwidth of the channel. It should be noted that the part of the signal's bandwidth in which all frequencies fade together, almost simultaneously, is called the "coherence bandwidth".

## 2.2. Multipath Fading Channels And Their Parameters

Multipath fading is the single parameter of the mobile channel which can cause maximum signal degradation in any wireless communications system.

In general, there are many parameters which can be used to characterize multipath fading. Some of these parameters are: Average Fade Duration (AFD), fade rate, Level Crossing Rate (LCR), magnitude and phase of the received signal's envelope, delay spread ($\tau_m$), RMS delay spread, coherence bandwidth and coherence time.

In an outdoor environment, propagation, dissipation, dispersion, scattering, refraction and absorption of electromagnetic waves occur due to the presence of buildings, trees, cars, and people; whereas, in an indoor environment, it is widely due to the presence of ceilings, walls, furniture, equipment, utility-facilities and people inside the building. These obstacles result in the transmitted signal taking multiple paths to the receiver. Each of these signals (multipaths) arrive from a different direction; therefore, each is delayed with respect to the others and has a different power. This phenomenon is called multipath propagation. If all the energy arrives at the receiver as a result of scattering, then the received signal envelope is treated as a Rayleigh random process. However, when some of the signal energy arrives at the receiver via a specular path, the received signal envelope is a Rician random process. The probability distribution function (pdf) of the envelope of various random processes which this work was compared with is listed below:

**Nakagami-m:**

The expression for this distribution function is given by:

$$p_R(r) = \frac{2}{\Gamma(m)}\left(\frac{m}{\Omega}\right)^m r^{2m-1} \exp\left(\frac{-mr^2}{\Omega}\right) \qquad m \geq \frac{1}{2},\ r \geq 0 \qquad (2-3)$$

where m is the measure of the signal variability, $\Omega$ is the mean-square value of r, and $\Gamma(m)$ is defined as:

$$\Gamma(m) = \begin{cases} \int_0^\infty t^{m-1}e^{-t}dt & \text{for } m > 0 \text{ and } m \notin I \\ (m-1)! & \text{for } m > 0 \text{ and } m \in I \end{cases}$$

We chose Nakagami-m as one of the distributions because the computational complexity is reduced considerably when compared with the Rician distribution. For values of m=0.5 and m=1, it is equal to one-sided Gaussian and Rayleigh distribution, respectively.

**Rayleigh:**

When all the energy arrives at the receiver from scattering then the received signal envelope is treated as a Rayleigh random process[15]. The Rayleigh distribution function is defined as:

$$p_R(r) = \frac{r}{\sigma^2} \cdot e^{-\frac{r^2}{2\sigma^2}} \qquad r \geq 0 \qquad (2-4)$$

where $\sigma^2$ is the variance of the random variable r.

**Rician:**

In some situations, there exists a line-of-site (LOS) path to the receiver, or at least a strong dominant specular component in non line-of-site (NLOS) such that its level is equal or above the sum of the rest of the multipaths.

This results in fading characteristics exactly like those of sine wave plus additive Gaussian noise. Hence, Rician distribution will be a good approximation to the received envelope variations. Rician distribution is defined as:

$$p_R(r) = \frac{1}{2\sigma^2} \cdot e^{-\left(\frac{r^2}{2\sigma^2} + K\right)} I_0\left(\frac{rs}{\sigma^2}\right) \qquad r \geq 0 \qquad (2\text{-}5)$$

where $I_0(\bullet)$ is the modified bessel function of the first kind and zero-order. $\sigma^2$ is the nonspecular multipath power and K is defined as the ratio of the peak specular component power to nonspecular multipath power:

$$K = \frac{s^2}{2\sigma^2}$$

Figure 2.2 illustrates the effect of variable K in the Rician distribution. Clearly, as the multipath power increases, the variation in the signal increases. Also note that when there is no dominant signal component; i.e., s = 0, then the Rice distribution reduces to Rayleigh distribution.

Figure 2.3 illustrates the multipath scattering phenomena where there are three scatterers present. These incoming radio waves combine vectorially at the receiver to give a resultant signal which can be large or small depending on the distribution of phases ( a time dependent random variable) among the received rays. It should be noted that spread spectrum signal exhibits low correlation to a second signal ray if the two rays are received delayed from one another by more than a chip time. If the delay is

less than chip time, the signals are substantially correlated and will add or subtract depending upon their carrier phase.

Clearly, due to multipath, a receiver at any location can receive signals that differ in power by order of magnitude from that at another location only a short distance away where all received signals have phases that can add up constructively. It should be noted that if the delay exceeds a chip duration where signals are essentially uncorrelated, their powers will add. In this case, the delayed signals appear as interference to the SS receiver and add to its noise floor. Multipath fading is the major limitation to the performance of the mobile communication systems both for indoor and outdoor environment.

If one could transmit an extremely sharp impulse over a multipath medium, the received signal would appear as a train of impulses. The overall spread in time of arrival of these impulses, $\tau_m$, is called the "delay spread" or "multipath spread". Clearly, to observe a multipath spread, the time differentials between the paths must be large with respect to the time scale characteristics of the signal modulation; i.e., the time differentials are significantly larger than the period of the highest "significant" frequency component of the signal. Delay spread inflicts a waiting period which determines when the next bit must be transmitted by the transmitter in

order to avoid intersymbol interference. The delay spread of a channel can be measured from the Delay Power Spectrum (i.e., Multipath profile). Figure 2.4 shows the delay power spectrum of the channel at a particular location. It tells us how much power each multipath return carries and what is its relative delay with respect to the first return (shortest path). The delay power spectrum represents the signal's power for each multipath as a function of path delay. It can be measured by transmitting very narrow pulses (wideband signal) and cross-correlating the received signal with a delayed version (usually by a few KHz) of itself. Later, it will be shown that the delay spread measurement gives us vital information for designing the signalling and the system that will resolve the multipaths received from a single antenna. That part of the signal's bandwidth, in which all frequencies fade together, almost simultaneously, is called the Coherence Bandwidth. This bandwidth is inversely proportional to the delay spread of the channel. Within this bandwidth, all frequency components of the signal fade in the same manner. This is when the signal is said to be "flat-fading".

The envelope fluctuation caused by multipath fading can be classified as either short-term or long-term. The short-term fluctuation which is mainly caused by local scatterers is known as fast fading. This is due to the fast changing environment surrounding the mobile receiver (e.g., in outdoor

environment, large trucks passing by the mobile or heavy traffic.). Long-term fading or shadowing is due to relatively large earth or man-made structures obstructing the direct line-of-sight (LOS) of communication. In Chapter 5, we will show how to estimate the statistics of the fast variations by extracting the slow variations from the received envelope. We define the Fade Margin as the power loss in the received envelope due to fading with probability of a fade occurring below a prescribed level and Fade Rate as the rate at which fades of a given depth occur.

## 2.3. Use Of RAKE Receiver To Combat Multipath Fading

Use of RAKE receivers often arises in spread spectrum systems to collect more of a desired signal's energy. A RAKE receiver is based on using signals having bandwidths greater than the coherence bandwidth of the channel. Such a signal with bandwidth W can resolve the multipath components and provide the receiver with several independently fading signal paths. A RAKE receiver can be thought of as a tapped delay line receiver or as a number of spread spectrum receivers (often called "fingers") incorporated to operate in parallel. Each of them are synchronized to a distinct uncorrelated ray, assuming each ray is delayed from one another by more than a chip.

RAKE receiver attempts to collect the signal energy from all the received

signal paths that fall within the span of the delay line and carry the same information. These received signals can then be combined coherently (each finger is synchronized to a distinct multipath return) or non-coherently (each finger is not synchronized to a multipath) to increase the signal-to-noise ratio(SNR).

For example, if the three signals, shown in Figure 2.3, are of same amplitude but delayed more than a chip time from one another, a 9.4 dB increase in signal-to-noise ratio is attainable if they are added coherently. Clearly, the amount of improvement depends on the number of RAKE's fingers, the amplitude of the multipath returns and the combining method used by the RAKE receiver. It should, also, be noted that the RAKE can only help when the rays are uncorrelated i.e., delayed by more than a chip. Incoming rays which have path delay differences of less than a chip are not resolvable by the RAKE receiver and therefore the use of RAKE has no advantage in this situation.

## 2.4. Channel Envelope Characterization

The signal from the transmitter to the receiver takes multiple paths. These signals, each with random amplitude and phase, add vectorially to form the combined received signal. Therefore, the received signal undergoes significant variations (i.e., by variations we mean fast fading only). Figure

2.5 illustrates the close-in (solid arrows) and far-out (dotted arrows) multipath phenomena for an arbitrary chip duration. The transmit signal for a direct sequence spread spectrum BPSK modulated carrier is defined as:

$$s(t) = d(t) \cdot g(t) \cdot \cos(\omega_0 t - \theta_0)$$

For channel envelope characterization, we have omitted the transmission of data by setting d(t) to 1 for all t's. This will not effect the channel behavior in any way. Hence, s(t) becomes:

$$s(t) = g(t) \cdot \cos(\omega_0 t - \theta_0) \qquad (2\text{-}6)$$

g(t) is defined as the pilot-PN code, $\omega_0$ is the carrier frequency and $\theta_0$ is the phase of the carrier. This signal will take multiple paths (in this case N paths) to the receiver. Therefore, the received signals for each path can be defined mathematically as:

$$r_1(t,d_1) = A_1(t,d_1) \cdot g(t-\tau_1) \cdot \cos\left[\omega_0(t-\tau_1) + \theta_0 - \theta_1(t)\right]$$

$$r_2(t,d_2) = A_2(t,d_2) \cdot g(t-\tau_2) \cdot \cos\left[w_0(t-\tau_2) + \theta_0 - \theta_2(t)\right]$$

□

$$r_N(t,d_N) = A_3(t,d_N) \cdot g(t-\tau_N) \cdot \cos\left[\omega_0(t-\tau_N) + \theta_0 - \theta_N(t)\right]$$

The total received signal is then given by:

$$R(t) = \sum_{i=1}^{N} A_i(t,d_i) \cdot g(t-\tau_i) \cdot \cos\left[\omega_0(t-\tau_i) + \theta_0 - \theta_i(t)\right] \qquad (2\text{-}7)$$

where N is the total number of paths in the channel, $\tau_i$ is the delay associated with the $i^{th}$ path, $A_i$ is the gain of the $i^{th}$ path, $d_i$ is the $i^{th}$ path

length and $\theta_i(t)$ is the phase associated with the $i^{th}$ path. The total power $P_s(t)$ in the envelope of R(t), is defined as follows:

$$P_s(t) = |R(t)|^2 = \left| \sum_{i=1}^{N} A_i(t_i, d_i) g(t-\tau_i) \cdot \cos\left[\omega_0(t-\tau_i) + \theta_0 - \theta_i(t)\right] \right|^2$$

$$= \left(A_1(t,d_1)g(t-\tau_1)\right)^2 + \cdots + \left(A_N(t,d_N)g(t-\tau_N)\right)^2$$

$$+ \sum_{i=1}^{N} \sum_{\substack{j=1 \\ j \neq i}}^{N} A_i(t,d_i) A_j(t,d_j) g(t-\tau_i) g(t-\tau_j) \cos\left[\omega_0(\tau_i - \tau_j) + \theta_i(t) - \theta_j(t)\right]$$

After averaging the envelope, the power in dB units becomes:

$$\overline{P_s(t)}\Big|_{dB} = 10 \cdot \log_{10} \overline{|R(t)|^2} = 10 \cdot \log_{10} \left[ \left(A_1(d_1)\right)^2 + \left(A_2(d_2)\right)^2 + \cdots + \left(A_N(d_N)\right)^2 \right.$$

$$\left. + \sum_{i=1}^{N} \sum_{\substack{j=1 \\ j \neq i}}^{N} A_{ij}(d_{ij})\, \alpha_g(\tau_{ij}) \cos\left(\omega_0(\tau_i - \tau_j) + \Theta_{ij}\right) \right] \qquad (2\text{-}8)$$

where

$$\Theta_{ij} = \theta_i(t) - \theta_j(t)$$

$$A_{ij}(d_{ij}) = A_i(d_i) A_j(d_j)$$

$$\alpha_g(\tau_{ij}) = \overline{g(t-\tau_i)g(t-\tau_j)}$$

$$\tau_{ij} = \tau_i - \tau_j$$

$$\overline{g(t-\tau_i)g(t-\tau_j)} = \begin{cases} 1 - \left[\dfrac{L+1}{L}\right]\dfrac{\tau}{T_c} & \text{for } |\tau_i - \tau_j| < T_c \\ \dfrac{-1}{L} & \text{for } |\tau_i - \tau_j| > T_c \end{cases}$$

It is important to note that the power fluctuations observed in this received envelope are for the spread signal. The only terms which contribute to the fluctuations in equation (2-8) are the cosine term ( a function of the path delays and the phase of each signal path) and the chip rate of g(t). The

variations due to path gains are considered to be much slower with respect to the chip duration of the SS signal.

To illustrate what is really happening, let's consider the transmission of infinitely long chip duration, or the equivalent of the transmission of a CW signal. We expect signal variation of 20-30 dB for this type of signalling independent of the environment. This is only because close-in multipaths exist inside each chip. These rays are correlated with each other and, at the receiver, depending on their phases, they add-up or subtract from each other to cause severe multipath fading. The fluctuations of this type of envelope is Rayleigh distributed [15].

As the chip rate of the SS signal is increased, a smaller percentage of the close-in multipaths will fall within a chip. As a result, the chip overlap from the close-in rays will decrease. Hence, the fluctuations tend to decrease and its distribution becomes more Rician. This behavior changes as the environment changes. For example. when using low antenna height, in urban areas like downtown Manhattan, N.Y. where the structure of the buildings and streets are like a wave guide, there is always a specular component present at the receiver. Therefore the variation of the envelope is expected to be Rician. This behavior holds somewhat true for suburban areas as well. Since there are more open areas in suburban environment,

the power of specular component may be weaker in suburban than urban which tends to increase the variations in the envelope. It should be noted that when the SS receiver can resolve all the close-in multipaths (i.e., infinite transmit bandwidth and all the energy of the system arrives via one specular path) the received envelope will sustain no variations due to multipath.

For indoor environment, the path differences in multipath returns are small (i.e., 1 feet $\approx$ 1 nsec) with respect to the chip duration of the system. For example, a 5 MHz DS-CDMA system can only resolve multipaths which have path differences of greater than 200 feet. As a result, when this system operates in an indoor environment, many close-in rays fall within its chips which cause the envelope of each individual multipath return fade severely and independent of one another. The fading in the envelope of sum of all multipaths will be less severe than the envelope of an individual ray. This is one of the reasons why broadband CDMA is superior to the narrower band CDMA systems when operating in an indoor environment.

Next, we will consider the envelope at the output of the despreader where the receiver is synchronized only to one of the incoming rays. Depending on the chip duration, there maybe many close-in rays within the single chip. Generally, the number of close-in rays is random. Assuming that the

receiver is locked to the first ray in Figure 2.1, the despreader output envelope can be written as:

$$P_{des}(t) = \left|\sum_{i=1}^{k} r_i(t)\right|^2 = \left|\sum_{i=1}^{k} A_i(d_i)\, g(t) g(t-\tau_i) \cos(\omega_0 (t-\tau_i) + \theta_0 + \theta_i(t)\right|^2 \qquad (2\text{-}9)$$

where k is a random variable between 1 and N depending on the chip duration. After averaging:

$$\overline{P_{des}(t)}\Big|_{dB} = 10 \cdot \log_{10} \overline{\left|\sum_{i=1}^{k} r_i(t)\right|^2} = 10 \cdot \log_{10} \left[ (A_1(d_1))^2 + (A_2(d_2))^2 + \cdots + (A_k(d_k))^2 + \sum_{i=1}^{k} \sum_{\substack{j=1 \\ j \neq i}}^{k} A_{ij}(d_{ij})\, a_g(t_{ij}) \cos(w_0 (t_i - t_j) + Q_{ij}) \right] \qquad (2\text{-}10)$$

The envelope of this received signal again is a function of the chip rate, the power of each multipath and the distribution of their phases at the receiver. Let us look at the situation when we are operating in Line-of-Site (LOS). Suppose there are N multipaths returns. The shortest return (direct path) is known to have a Rician envelope. On the other hand, by Central Limit Theorem, other paths have Rayleigh distributed envelopes. Now depending on the chip duration and which ray the receiver is locked to, many of the Rayleigh distributed multipaths and/or including the specular path fall inside the chip. Let us say that the receiver is locked to the first ray which includes the specular and many other multipaths with delays less than or equal to chip time. Also, assume that the multipaths have power comparable to the shortest return. Then the sum of all these rays have an envelope which is Rayleigh distributed. However, if the multipaths have

power which are less than the shortest return, then depending on the power of multipaths, the variation becomes Rician with some K value. This means that as power in the multipaths weakens, the received envelope statistics becomes more Rician distributed. This situation is also true when the mobile operates in NLOS region. However, the power of shortest return is already attenuated by shadowing or other obstructions which makes it a weaker Rician.

The fading due to multipath observed in this work is rarely wider than 10-MHz for indoor (See Figures 2.6 and 2.7 which represent the power spectral plots using a spectrum analyzer in two different buildings) and 5-MHz for outdoor environment (See Figures 2.8 and 2.9 which represent the power spectral plots using a spectrum analyzer in suburban and urban environment, respectively). As a result of these findings, we will demonstrate that there are major advantages to using broader band spread spectrum systems over narrower band spread spectrum systems.

In the case of a narrowband system, the probability of incoming multipaths within a chip is more likely. Therefore, a RAKE receiver would help such a system's performance if, in addition to the main signal ray, a second set of signal rays could arrive (as a result of a distant reflection) with some delay greater than chip time. For example, it is probable that during a certain

time, in a particular environment, the first-received signal may fade and become very small, while the delayed rays which fade independently, may become larger in amplitude. Now, if a RAKE receiver was not used, then the probability of a bit being in error (BER) could be very high. But, if RAKE was used, the longer path signal could have been resolved, and added more energy to $E_b/N_o$ and improve the BER.

Throughout this work, the variations of the spread or unspread received SS signal envelope will be investigated. These statistics will describe how the fading is changing as the chip rate of the system is varied. Therefore, the experiments will be performed in various environments (indoor, suburban, Urban).

# 3. An Introduction On Channel Sounding Techniques

When we require the impulse response of a system, we excite that system by an impulse $\delta(t)$. We can treat the mobile channel the same way. However, we need a very narrow pulse (very wide band signal) to excite the mobile propagation channel. Since all practical communications systems are bandlimitted, therefore, in this thesis, we view the channel as what the receiver of a system perceives it to be. This means that the observation of the channel is limited by duration of the received pulses by the receiver.

To build the channel sounder, we have studied many designs. In the following sections, we discuss various methods of building channel sounders.

## 3.1. Periodic Pulse Sounding

In order to observe the time-varying behavior of the channel, periodic pulse sounding must be used. The pulse repetition must be greater than the largest observable delay in the channel. The pulse duration determines the minimum observable path difference between the multipaths, while the pulse period determines the maximum delay for which a multipath echo can be unambiguously resolved. Young and Lacy [31] used this method of sounding where they employed an envelope detection technique in the receiver to observe the envelope variation of the multipath returns.

One of the major limitations inherent in this kind of sounding is that it requires a high peak-to-mean power ratio to provide adequate weak multipath detection. Furthermore, since the pulsed transmitters are peak power limited, it is wise to use a channel sounder which provides pulse compression; hence the pulse compression technique.

### 3.2. Pulse Compression Technique

The basis for all pulse compression sounding systems is derived from the fact that the impulse response of a linear system can be evaluated using white noise, and some method of correlation processing. That is, if white noise, n(t), is applied to the input of a linear system, h(t), and if the output of that system, x(t), is cross-correlated with a delayed replica of the input, n(t-$\tau$), then the resulting cross-correlation coefficient is proportional to the impulse response of the system, h($\tau$). The following system block diagram illustrates the theory behind the pulse compression technique:

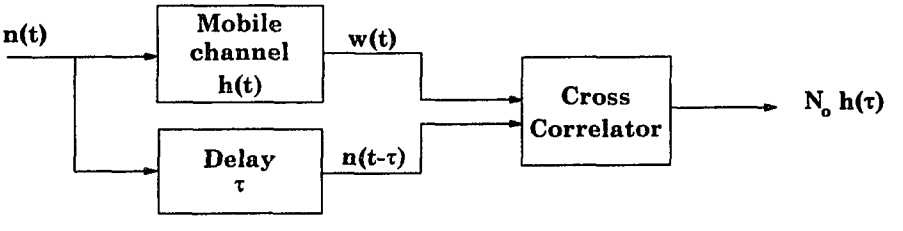


It is important to note that the output of the channel is given by the convolution of the n(t) and the impulse response of the channel, h(t). This is equivalent to:

$$w(t) = \int h(\zeta)n(t-\zeta)d\zeta \qquad (3\text{-}1)$$

and the output of the cross-correlator is given by:

$$\begin{aligned} E[w(t)n^*(t-\tau)] &= E\left[\int h(\zeta)n(t-\zeta)n^*(t-\tau)d\zeta\right] \\ &= \int h(\zeta)R_n(t-\zeta)d\zeta \\ &= N_0 h(t) \end{aligned} \qquad (3\text{-}2)$$

Since, in practice, white noise cannot be used for actual channel sounding (i.e. infinite transmit bandwidth), the actual experimental system must use bandlimitted waveforms which have characteristics such as white-noise. For this reason, maximal length pseudo-random binary sequences (often called m-sequences or PN sequences) are used which are known for having excellent periodic autocorrelation properties (See eq. 2-2) as shown in Figure 2.1. The length of the sequence, m, determines the processing gain of the measuring system and the maximum measurable multipath return time delay. The clock rate of the PN sequence determines the minimum resolvable path difference. In the following two sections, we will discuss the various methods of pulse compression technique.

### 3.3. Convolution Matched-Filter Method

In this method, the channel sounder receiver uses a filter which is matched to the PN-sequence used at the transmitter. Therefore, if x(t) is the transmitted signal, the output of the matched-filter can be represented as:

$$y(t) = x(t) * h(t) * x(T - t) \qquad (3 - 3)$$

where x(T–t) is the impulse response of the matched-filter. The convolution of the x(t) and x(T–t) is given by:

$$r(t) = \int x(\alpha)x(T - t + \alpha)d\alpha \qquad (3 - 4)$$

and the convolution of h(t) and r(t) is given by:

$$\begin{aligned} y(t) &= \int h(\beta)r(t - \beta)d\beta \\ &= \iint h(\beta)x(\alpha - \beta)x(T - t + \beta)d\beta d\alpha \\ &= \int h(\beta)R_x(t - T - \beta)d\beta \end{aligned} \qquad (3 - 5)$$

note that if the autocorrelation function $R_x(t–T)$ is approximately a delta function, then the output of the matched-filter becomes the impulse response of the channel as function of real time.

One of the advantages of the matched-filter method is that the need for local regeneration of the m-sequence is eliminated. This minimizes the need for synchronization of the receiver to the transmitter. However, since the system is operating in real time, it becomes very costly in terms of memory. Also, as the length of the m-sequence gets longer the group delay of the filter increases too.

### 3.4. Swept Time Delay Cross Correlation Method

In this method, the correlation process is performed by a single correlator

[19]. The received signal is correlated with an m-sequence identical to that used at the transmitter, but clocked at a slightly slower rate (usually a few kHz). As a result, the output samples of the swept time delay cross-correlator are the samples of the impulse response of the channel. By reducing the locally generated m-sequence rate by k Hz, the bandwidth of the cross-correlator output is reduced by a factor of :

$$K = \frac{\text{chip rate}}{k}$$

which means the features of K impulse responses of the channel are within each delay profile. If the maximum anticipated multipath return delay is represented by D, then the slower m-sequence clock must be reset every KD seconds.

Care must be taken in choosing the values of D and K such that KD is at least less than ½ wavelength at mobile speed of V m/sec. This will insure that the K individual responses do not alter significantly in their multipath structure. This bandwidth reduction then enables the user to sample the response at a much lower rate than the chip rate of the system. Accurate time delay and Doppler shift in the channel can then be measured by this type of the sounder. Cox[19], who invented this channel sounder, was the first experimentalist to simultaneously measure these two quantities.

# 4. The Experimental Equipment and Location

We need a channel sounder such that its receiver can measure the excess delay of the channel as we vary the chip rate of the system. Its receiver should also be able to measure the envelope fluctuations of an SS signal before and after despreading. The receiver stays in synchronization with the transmitted signal. Therefore, the need to transmit a second signal called "pilot" is apparent. After locking to the pilot code, the receiver will track the frequency and phase of the carrier and use that information to despread the data.

A transmitter and a receiver were designed and built to measure the amplitude of the received envelope before and after despreading. The channel sounder operated at 1956 MHz. The reason for utilizing this frequency is that the FCC has chosen this frequency band for future applications in PCS. Also, we can compare the measurement results at this frequency with the work by other investigators [16-31]. In the following sections, we describe the transmitter and the receiver structures used throughout this research.

## 4.1. Transmitter

The channel sounder transmitter structure is shown in figure 4.1. The

transmitter employed a Direct Sequence Binary Phase Shift Keying (DS-BPSK) spread spectrum modulation technique, with a chip rate of 24-Mchips/sec, and a carrier frequency of 1956-MHz. The transmitter transmits two different PNs of length 8000, one for the pilot and one for the data; which we will refer to as pilot PN and data PN, respectively. The need to change the chip rate without changing the transmitter/receiver set-up was very important. Therefore, to change the chip rate, we only changed the data PN code by repeating each chip of the original system chip rate, N times to achieve a chip rate of 24/N Mchips/s. For example, if an 8-Mchips/s rate was desired, each of the original data PN chips of the 24 Mchips/s system was repeated 3 times. As a result, it would appear that the data PN's chip rate has been slowed down by a factor of 3. This is the same as transmitting a 1 Mchips/s or a 2-MHz wide SS signal. The same PN code sequence had to be provided at the receiver for despreading the new set of data.

This modulated signal is then translated to the RF frequency by mixing it with a 1799-MHz crystal oscillator. The RF signal is then amplified to produce an average radiated power of 1W. The 30 dBm radiated power is adjusted with an RF attenuator to keep the typical received signal level more than 10 dB above the receiver noise floor for all measurement locations. The side lobes were removed by filtering the transmitted signal

with a 48-MHz bandpass filter centered at 1956-MHz (See figure 4.2). The transmitting and receiving antennas were omni-directional quarter wavelength dipoles and were adjusted to 2.5 meters and 1.8 meters from the floor, for indoor measurements, respectively.

### 4.2. Receiver

Figure 4.3 shows the receiver configuration for measurements before the despreader. Following front-end filtering and amplification, the received signal is translated to 85-MHz by mixing with an 2041-MHz local oscillator. The 85-MHz IF signal is then amplified and passed through a filter which corresponds to the transmitted signal bandwidth. The filters had bandwidths of 2, 11, 22, 30 and 48-MHz and were adjusted to have equal insertion loss to ease the calibration process. An 85-MHz Logarithmic-Amplifier (LOG-AMP) with 76 dB dynamic range was then designed and built to detect the envelope of the received signal. The output of the LOG-AMP was then passed through a 2-KHz low-pass filter followed by an A/D. This receiver was equipped with a specially designed wheel which was supplied with a photo interrupt sensor acting as a switch, such that the A/D's sampling time of the received envelope was at every centimeter (i.e. one data point per centimeter). The sampled data was then stored on the hard disk of a PC-AT computer for later analysis.

The receiver was placed on a industrial cart or in a van for indoor and outdoor measurements, respectively.

The receiver for measurements after the despreader had a configuration which was more complicated than structure of the one before the despreader. This additive complexity was due to acquisition and tracking circuitry. A fully operational DS-BPSK spread spectrum system (designed and developed by InterDigital Communications Corp.) had already existed. With a few minor changes to this system, we made it possible to observe the channel's behavior.

Figure 4.4 shows the receiver configuration for measurements after the despreader. Here, the signal following front-end filtering and amplification is translated to 85-MHz IF frequency. The AGC then provides the despreader with a constant signal power through a 60 dB dynamic range (-40 dBm to -100 dBm). This is a crucial stage for locking of the signal. The AGC used in our receiver had a 1 ms time constant and was 48-MHz wide. The effect of AGC on the despread signal is only known if the amount of the gain or attenuation provided by the AGC is known. We, therefore, sampled the AGC control voltage continuously, at 1 ms intervals.

After the despreader, the signal is filtered and amplified. The envelope of

the despread signal is detected with the LOG-AMP and is made available for collection at the A/D terminal. A 10-bit A/D sampled this signal every 1 ms. The data was saved on the RAM- drive (speed of 70 nsec) of a 486-50 MHz PC-AT and then saved on the hard drive for later analysis. To extract the AGC effect from the collected data after despreader, the system was calibrated and a calibration table was made. The values in this table provided a one-to-one relationship between the input power at the antenna and the amount of gain provided by the front-end of the receiver (including the AGC). This gain is then subtracted from the detected despreader output power to indicate the true power at the antenna. During the calibration of the system, it was noted that a 200 mv DC noise existed due to system. This translated to 0.5 dB error with probability 0.001. Therefore, the effect of this noise was included in all the calibration tables. The calibration tables were then checked before the actual measurements took place to verify the integrity of the measuring system.

To obtain the delay spread of the channel, again more modification had to be made to the receiver. The transmitter was exactly as before except for the fact that the data PN code was now changed for measurements of different chip rates as described previously.. Figure 4.5 shows the receiver configuration used for delay spread measurements. The signal, following front-end filtering and down conversion to IF frequency, is despread. In

order to observe the delay spread of the channel, we transmitted the same data PN code that the receiver is synchronized with, continuously. At the receiver, upon achieving lock; we cross-correlated the received signal with the delayed replica of the same transmitted code being locally generated at the receiver. In Figure 4.5, the multiplexer chooses the output of each delay element every 2.7 msec. The delay length is set to be 10.2 μsec. Therefore, maximum unambiguous path delay observable by this system was set to 10.2 μsec. The multiplexer is then reset every 0.7 seconds. The despreader output was filtered and integrated 2.5 msec. This sliding-correlator output is then digitized and saved on the hard drive of a PC-AT for later analysis.

### 4.3. Location

The experiment was performed for outdoor and indoor environments. For indoor environments, the first set of measurements was taken at the InterDigital Communications Corp. office building (site-A) in Port Washington, Long Island, New York. This building was a typical, small office building with a rectangular dimensions of 45m by 25m. The interior of the building had a standard 3m high dropped-ceiling structure on each floor. Measurements were recorded down corridors, around corners and inside each room. The offices had desks, chairs, computers, glass windows (1.2m by 1.5m) and, like any busy office, the people inside the building were constantly in motion. Figure 4.6 shows the floor plan of this building where

wide lines denote drywalls with aluminum studs that extend from floor to ceiling placed every 40 cm. The narrow lines represent 2 m tall soft partitions.

The second set of indoor measurements were taken on the 6th floor of the NAC building (site-B) located at the City College of New York in New York City (See Figure 4.7). It is a very large, solid building with some of the basic outdoor features of site-A. However, the interior walls of site-B were made of concrete blocks. The classrooms had ceiling height of 3m with no windows. Students populated the narrow hallways ( approx. 7 feet wide). At some locations, the corridors resembled as a maze and therefore prohibited a line-of-sight between the receiver and the transmitter.

For outdoor experiments, the first set of experiments were performed in a dense, urban area in downtown Manhattan with the location of the transmitting antenna along the side of 19th street and Second avenue (site-C). Figure 4.8 illustrates the location of the transmitter and street configuration. The streets are laid out in a rectilinear grid system and are lined by tall buildings with an average height of 30m. Each block is approximately 75m long. The width of the main streets are approximately 30m and 20m, respectively. There is dense mobile and pedestrian traffic which is slowly moving.

A second set of data was gathered for a suburban area in a residential neighborhood of Port Washington (site-D) in Long Island, New York. The main difference between the two environments was the relative height of the buildings and the traffic congestion. Figure 4.9 illustrates the street configuration and the transmitter/receiver locations at the test site. The average height of the houses in this neighborhood was approximately 10m. For all measurements, over 500,000 data points were taken for each signalling bandwidth.

Two sets of delay spread measurements were performed in New York City. We first looked at the received multipath from a base station located on the roof of a building located on 23rd Street near sixth Avenue (site-E) in Manhattan. This location was chosen since it is approximately 10 blocks away from the Empire State Building, a distance of approximately 0.5 mi equivalent to 2.5 μs delay. This would guarantee excess delays of at most 3 μsec in the channel. Omni-directional antennae was used at the receiver and transmitter, although a few experiments were also performed with a 90 degree directional antenna at the base station. The receiver on the street was then moved from 17th Street to 28th Street and from Broadway to eighth Avenue. We then looked at the received multipath from a base station located on the 9th floor of a building located at the corner of 68th Street and Central Park West (site-F). A 90 degree directional antenna was used to

transmit a SS signal at 2-GHz. The receiver equipped with an Omni-directional antenna was then moved around the Central Park Area. This experiment was carried out to observe if the excess delays over 1 μs are strong with respect to the first returns. The measurements were taken at 100 intersections and between two side streets while driving either on Central Park West (going north) or on Fifth Avenue (going south) or on Central Park South (going west). Figures 4.9 and 4.11 show the test areas chosen for these two sets of measurements.

## 5. Data Analysis and Experimental results

As discussed in section 2.2, the received envelope consists of two types of fluctuations: small-scale and large-scale. This is equivalant to :

$$R_s(t) = s(t) \cdot l(t) \tag{5.1}$$

where s(t) and l(t) represent the small and large-scale fluctuations, respectively. To analyze the fast variations in the measured data, s(t) and l(t) must be separated from each other. A moving average technique [29] was used to estimate $l(t_n)$, at a time $t_n$, from S samples of the envelope using the following equation:

$$l(t_n) = \frac{1}{S} \cdot \sum_{m=\frac{-(s-1)}{2}}^{\frac{(s-1)}{2}} P_s(m+n) \tag{5.2}$$

where $P_s(m+n)$ represents the samples of the received envelope. The averaging window size, S, is large enough so that small-scale fluctuation is still present but not so large such that the large-scale fluctuation is lost in the process of averaging. The averaging window size was set to approximately 10 wavelengths. After finding l(t), it was then possible to estimate s(t) by dividing the received envelope by l(t). The CDF of s(t) is then computed by using the following procedure over the whole dynamic range of the received envelope:

1. Count the number of samples below current threshold level.

2. Divide the count in 1, by the total number of samples in the envelope. (Note: Over 50,000 samples of the envelope were used for evaluation of each CDF).
3. Add one dB to the threshold and go to step 1.

This procedure is then repeated until the end of a each file has been reached. Although there are several techniques used to display the distribution functions in the literature, a logarithmic vertical scale is useful because it clearly indicates the likelihood of very low signal levels (deep fades) indicated by the left tail of the distributions. Therefore, logarithmic vertical scale is used for presentation of all CDFs throughout this work.

In the following sections, we present the results of extensive wideband measurements performed, within buildings/offices, and outdoors in the suburbs and in New York City. The experiments were designed in a variety of diverse locations. A great deal of attention was given to the range, orientation of antenna and street position, so that data for different chip rates are comparable.

## 5.1. Fade Margin

### 5.1.1. Before despreader

Figures 5.1, 5.3, 5.5, and 5.7 show the probability of the average received signal power differing from the mean signal power by more than a specific amount, called the "fade margin". For example, in Figure 5.1, the data was taken in a suburban neighborhood of Port Washington, N.Y.. For a bandwidth of 11 MHz (i.e., chip rate = 5.5 Mchips/s using BPSK modulation), the probability that the received signal's power will fade more than 12.5 dB from its mean value is 0.001. The results shown in this figure for the bandwidths of 22, 30 and 48 MHz are similar. However, the fading for bandwidths less than 11 MHz and for a CW signal show that very large fade margins are needed.

Comparing the results of suburban areas with urban areas (in microcellular and low antenna height), we note that the fade margins are lower for urban than suburban areas. This is expected in urban areas where the antenna height is low with respect to average height of the surrounding buildings. Buildings and streets form a "canyon", acting as a waveguide to let the signals through. This canyon structure accounts for the reception of multipaths from one direction rather than every direction. Subsequently, less multipaths arrive at the mobile antenna. On the other hand, in the suburban area under study (a residential neighborhood of

Port Washington, NY), where the average building height is approximately the same as the transmitting antenna height and there are many open fields such as backyards and spaces between houses which account for multipath arrival from every direction at the receiver.

Nevertheless, the most interesting feature of our results is apparent. As we anticipated, the results show that fading is significantly reduced as the chip rate of the system is increased. For suburban and urban areas, distribution about median path loss is approximately Rician distributed with K value equal to 10 and 12 dB, respectively. We also observed that the fade minima in the received envelope was sharper than the fade maxima. This phenomena makes it difficult to model the envelope variation with only one distribution. For example, earlier analysis in [32] have shown that two distributions were needed to model the envelope statistics, one for below and the other for above the median path loss. However, later analysis show that the Nakagami-m distribution gives a tighter fit to the measured data. Nakagami-m distribution is preferred over Rician distribution since its computational complexity is greatly reduced. The Nakagami-4.5 and Nakagami-7 fit the data best for both below and above median in suburban and urban areas, respectively (See Figure 5.9).

It should be noted that if the spread spectrum system was to use a coherent RAKE receiver, the envelope of the RAKE's output would sustain variations which are better than that of the signal before the despreader. Therefore, it is not true to say, statistics of the fast variations before despreader serve as an upper bound for improvement achieved when a coherent RAKE receiver is used at the receiver. In fact, depending on the number of fingers of the RAKE and the environment, a coherent RAKE receiver will be able to collect even more energy than what we observed in this study. It should also be noted that CW is not considered as wideband channel measurement; however, it provided a means of understanding the effect of infinite chip duration and enabled us to compare our results to other researchers where applicable (for example, Rappaport results in [16]. To understand the implication of such results on the system performance, an example will follow.

For the sake of argument, we will compare two microcellular DS-BPSK SS systems with chip rates of 1 Mchips/s and 24 Mchips/s called system A and B, respectively. We will assume that the minimum acceptable received signal is -100 dBm and the remote is to be serviced over 99% of the cell. Based on the results of Figure 5.2, 1% of time system B requires a 6 dB fade margin. This means 99% of time the signal envelope will suffer from fast fading of no more than 6 dB. It should be noted that if the cell is

designed such that the mean received power is approximately -94 dBm from the cell edge, then 99% of time the received power is equal to -100 dBm. Therefore, the cell radius is set such that the receiver receives -94 dBm at the cell edge. On the other hand, system A will suffer from 14 dB deep fades below its mean received power (See Figure 5.1). Therefore, at the receiver, the received power is at -108 dBm. To overcome this power loss, either the cell radius must be reduced or the transmit power must be increased by 8 dB. The former will make the cell coverage smaller and the latter will increase the interference noise in the adjacent cells by 8 dB and consequently the BER will increase too.

Figures 5.2, 5.4, 5.6, and 5.8 are redrawn plots of figures 5.1, 5.3, 5.5 and 5.7 for three different probabilities, 0.001, 0.01 and 0.1. Note that there is a variation in fade margin of less than 1 dB for bandwidths exceeding 20-MHz. Also, note that variation increase dramatically for bandwidths less than 20-MHz. Clearly, narrowband spread spectrum systems, having bandwidths of about 2-MHz require a fade margin of 14-18 dB with probability of 0.1% depending on the environment. Therefore, narrowband systems require more transmit power to overcome the fading due to multipath returns. As a result, they introduce more interference to their own users and adjacent cells. It is interesting to note, that if this narrowband system is to be used in conjunction with a current cellular

system by increasing its transmit power it would jam (interfere with) those frequencies used in cells located on the second tier.

Tables 5.1 and 5.2 summarize the fade margin requirements for outdoor environments and for probabilities, 0.001, 0.01 and 1. Note that in urban environment, there is a variation in fade margin of less than a few dB for bandwidths exceeding 11-MHz as oppose to suburban areas.

| | FADE MARGIN, dB | | |
|---|---|---|---|
| | 0.1% | 1% | 10% |
| CW | 22.5 | 17 | 8 |
| 2 MHz | 17 | 14 | 7 |
| 11 MHz | 12.5 | 9 | 4 |
| 22 MHz | 9.5 | 6.5 | 3.75 |
| 30 MHz | 9 | 6.25 | 3.5 |
| 48 MHz | 8.75 | 6 | 3 |

**Table 5.1: Fade Margin Requirements in Suburban areas for various bandwidths.**

| | FADE MARGIN, dB | | |
|---|---|---|---|
| | 0.1% | 1% | 10% |
| CW | 20 | 14 | 7 |
| 2 MHz | 14.5 | 11 | 6 |
| 11 MHz | 9 | 7.5 | 4 |
| 22 MHz | 7.5 | 5.5 | 3 |
| 30 MHz | 7 | 5 | 2.75 |
| 48 MHz | 6.5 | 4.5 | 2.5 |

**Table 5.2: Fade Margin Requirements in Urban areas for various bandwidths.**

In an indoor environments, the channel performance deteriorates even more than outdoor as the bandwidth of the SS system is decreased. This is because the differential path delays due to scattering around the receiver are relatively small (e.g., 10- 20 ft equivalent to 10-20 nsec) with respect to the chip duration of SS signal. As a result, most multipath arrive at the receiver less than a chip time away from each other. Indeed, the indoor experiments performed in sites A and B show improvement in fade margin as the chip rate of the system is increased. For example, in Figure 5.6, the data was taken in NAC building of City College where omni-directional antenna was used. For a chip rate of 5.5 MHz, the probability that the fade margin exceeds 12 dB is 0.001. This fade margin is increased by 4 dB when the rate is reduced by a factor of 4. On the other hand, when the chip rate is increased by a factor of 4 the fade margin is reduced by 4 dB. This improvement in fade margin is what makes the broader band CDMA system perform better than narrower band CDMA systems. Statistics of fades for various bandwidths in other indoor locations such as site A are shown in Figure 5.5. Again, it is seen that spread spectrum signals with bandwidths in excess of 11 MHz have almost the same fade margin. It is clear from these results that the fade margin is decreased as the chip rate is increased.

Rappaport [16] reported a dynamic fading range of 30 dB in office buildings, when a CW signal was used. Our data confirms Rappaport's

results. It also reveals a dynamic range, seen by the receiver, of no more than 9 dB with probability of $10^{-2}$ when using signals with bandwidth greater than 11 MHz. The results clearly show that spread spectrum systems using chip rates less than 11 MHz and no other form of diversity can have instantaneous power losses which could exceed 15 dB with probability of 1%. Tables 5.3 and 5.4 summarize the fade margin requirements for indoor environment.

| | FADE MARGIN, dB | | |
|---|---|---|---|
| | 0.1% | 1% | 10% |
| CW | 24 | 14.5 | 6.5 |
| 2 MHz | 16 | 12 | 6 |
| 11 MHz | 12 | 8 | 4 |
| 22 MHz | 9 | 6.5 | 3 |
| 30 MHz | 8.5 | 6.25 | 2.75 |
| 48 MHz | 8 | 6 | 2.5 |

**Table 5.3: Fade Margin Requirements at NAC Building before the despreader for various bandwidths.**

| | FADE MARGIN, dB | | |
|---|---|---|---|
| | 0.1% | 1% | 10% |
| CW | 22.5 | 17 | 8 |
| 2 MHz | 17.5 | 14 | 7.5 |
| 11 MHz | 12 | 9 | 4.5 |
| 22 MHz | 8.75 | 6.75 | 3.5 |
| 30 MHz | 8.5 | 6.5 | 3 |
| 48 MHz | 8 | 6 | 3 |

**Table 5.4: Fade Margin Requirements at IDC Building before the despreader for various bandwidths.**

Figure 5.10, illustrates the distribution fits for two indoor locations under study. It is interesting to note that the statistics of data has not changed even though the locations has. It is shown that the Nakagami-5 is a good approximation to the indoor data. Rician distribution with K=10 dB, also make a good approximation. However, for simulation purposes the Nakagami-m is preferred over Rician for its computational simplicity.

### 5.1.2. After Despreader

To observe the behavior of the one finger SS receiver, we performed many experiments in residential neighborhood of Port Washington, NY. An omni directional antenna was used to transmit a SS signal at 2GHz. The receiver was moved in NLOS region at speed of 5 mph $\approx$ 220 cm/s. Over each 22 m path, 10,000 points were gathered at 1 ms intervals. The slow variation was removed from the data as described earlier in this chapter. This experiment was also repeated for other chip rates.

Figure 5.12 shows the fade margins of various chip rates after the despreader. As we expected, the fade depths have increased dramatically. The envelope variation of the locked ray behaves as a Rayleigh random process. We believe that the reason behind this is that components scattered by the houses arrive at the mobile within a very short delay with respect to the system's chip duration. Because of this small delay, and the

fact that the returns have power comparable to that of the shortest return, the variations become very large. However, these variations become less when the chip rate is increased.

In [17, 19, 25, 30] where 1.25 Mchips/s and 10 Mchips/s SS signals were used, the researchers found that the output envelope of the single correlator is Rayleigh distributed. Demery [30] shows that the first 10 returns have statistics even worse than Rayleigh. Our results confirms this for the first return and further points out that the envelope does start to deviate away from the Rayleigh distribution as the chip rate is increased. In Figure 5.12, for example, the envelope is best approximated by a Rician distribution with a K value of 1 to 2 dB). It may be argued that one or two dB of K value is not much of a Rician distribution. However, this is a significant improvement, for if we examine the delay spread measurements performed at the same site (See Figure 5.28), we note that a 24 Mchips/s system can decrease its fade margin by even more dB's by using a RAKE to collect the power from the far-out multipaths. This cannot be done by a narrower band CDMA systems simply because it cannot resolve the multipaths. Table 5.5 summarizes the fade margin requirements for the envelope of the despreader output.

Indoor measurements at site A, also point out the same fact that in order

to resolve more multipaths we must use wide band signals. Figure 5.10 shows the fade margin statistics for various chip rates under study. Note that the change in fade margin, although small in comparison with Rayleigh, is apparent. Table 5-6 summarizes the fade margin requirements after the despreader for indoor environment under study.

| | FADE MARGIN, dB | | |
|---|---|---|---|
| | 0.1% | 1% | 10% |
| 2 MHz | 26.5 | 21 | 8 |
| 6 MHz | 26.5 | 21 | 8 |
| 12 MHz | 26.5 | 17.5 | 7.5 |
| 24 MHz | 26 | 17.5 | 7 |
| 48 MHz | 24 | 16 | 4.5 |

**Table 5.5: Fade Margin Requirements after the despreader, in suburban environment for various bandwidths.**

| | FADE MARGIN, dB | | |
|---|---|---|---|
| | 0.1% | 1% | 10% |
| 2 MHz | 27.5 | 17.5 | 7 |
| 6 MHz | 26.5 | 17.5 | 7 |
| 12 MHz | 26 | 16 | 7 |
| 24 MHz | 24.5 | 15 | 6 |
| 48 MHz | 22 | 13.5 | 5 |

**Table 5.6: Fade Margin Requirements after the despreader, in Indoor environment for various bandwidths.**

## 5.2. Delay Spread

Figures 5.13-5.19 illustrate the average multipath returns seen by the

mobile receiver at site-E. These plots show the power in each multipath return as a function time and distance. In each of these plots, each small division represents 40 ns (i.e., the interval between 0 and 10 represents 400 ns). Since signal power can vary over small portions of the wavelength, measurements were taken every centimeter and displayed over the wavelength. Over 500 snap shots were collected at different intersections and streets in a 1 mile radius around the transmitter.

Figures 5.13 and 5.14 show the delay profile when transmitter used an Omni-directional antenna whereas in Figures 5.15 and 5.16 the transmitter used a directional antenna, having a 90 degree beam width, aimed at the Empire State Building. The reason for using two different antennas was to see the effect of directionality of the antenna on the excess delay observed in the environment.

In each case, we see that the multipaths exceeding 1 μs do not carry any significant power in the environment under test. Figure 5.13 shows two equal multipath signals 200 ns apart. These results show that a spread spectrum having a chip rate less than 5 Mchips/s, "sees" the most "close in" multipath signals. These signals can add up to produce deep fading. In this case, a RAKE receiver could not help the narrower band system since there are no "far out" multipath returns in excess of 1μs with a significant amount

of energy for RAKE to collect. Hence, such a narrowband system could not operate acceptably within the coverage area without some type of instantaneous power compensation to overcome the severe fading imposed on its system. One ramification of this action, again, is the excess power "spilled over" to adjacent cells, causing burst interference to its own users and the cellular users (if the system is to be used in conjunction of a cellular system). These results show that the narrower the bandwidth of the spread spectrum signal the greater the number of uncorrelated rays which can occur within a chip time. Hence the greater the likelihood of a deep fade. Figures 5.17-5.19 show typical observed returns seen at the receiver. Again we observe no significant multipath returns in excess of 1 μsec.

One may argue, what about places where there are multipath returns in excess of one microsecond?. For this reason, another set of delay spread measurements were performed at site-F. Figures 5.20-5.22 illustrate the typical delay power spectrum at site F, for chip rates of 1 Mchips/s, 8 Mchips/s and 24 Mchips/s DS-BPSK spread spectrum signal, respectively. The main reason for this experiment was to intentionally set the receiver up for receiving multipath returns in excess of 1 μs. We also wanted to see how the channel appears to a spread spectrum system when its chip rate is varied. Indeed, at many locations, multipath returns were observed which were in excess of 1μs. However, not all of these rays carry significant power

at all locations. As a result, we took the delay spread measurements to learn how many paths can the receiver resolve as the chip rate is varied. We observed that in down town Manhattan, for example, the excess delays with significant power are less than 1 μsec. This implies that a narrower band system could resolve only (depending on its chip rate) one ray whereas a wider band system could resolve more than one ray. When we repeated the delay spread measurements in site F, we observed the following:

1. Excess delays more than 1 μsec are possible.
2. The multipath returns arrive in clusters of rays consisting of one specular component and several other components closely spaced in time. This latter case is explained by the fact that the specular component can bounce back and forth between the side streets around the mobile, causing the increased number of returns to arrive at the mobile in a very short time with respect to one another. Because of this repetitive bouncing these rays do not have significant power, however their sum may cause the receiver to see them as one individual component; this of course depends on the chip duration.
3. Clusters with excess delays greater than 1 microsecond arrive with low probability of occurrence in an urban setting like Manhattan. A suboptimal RAKE receiver for higher chip rate with a 400 nsec span would be a good choice. The lower chip

rates systems will not gain considerably by use of RAKE. In a suburban-like environment such as site F, since the probability of having two clusters with their powers differing by a few dB is low, a switchable RAKE receiver with a 400 nsec span which could detect and switch to the largest clusters would be a good choice.

It is clear from these figures that as the chip rate is decreased, the ability of the spread spectrum receiver to resolve the "far out" multipaths is also decreases, hence one can expect to see fewer "far out" multipaths with a narrower band CDMA system.

Figures 5.23-5.27 present the typical delay power spectrum observed at site A. where omni-directional antennae were used. For example, in Figure 5.23, we see that four returns are within 10 dB of the strongest return. It should be noted that each point on this figure is 42 nsec apart. A 24 Mchips/s B-CDMA system can resolve these multipath returns and further use a coherent RAKE receiver with five fingers to improve its fade margin by 9 dB. As the chip duration of the system increases, the chance of using a RAKE decreases. Therefore, a narrower band system cannot use a RAKE to collect this available signal energy. The improvement for outdoor can be as high as 14 dB when a coherent RAKE is used (See Figure 5.28).

## Conclusion

In this work, we considered the most important parameter in a Personal Communication System; Multipath Fading, and its impact on system performance.

It is shown that the received power loss due to fading (the fade margin before despreader) increases dramatically as the signalling bandwidth decreases below 11 MHz. In particular, comparing the fade margins of 1 MHz and 15 MHz bandwidth signal reveals a difference in fade margin of approximately 10 dB.

Comparing the results of suburban areas with urban areas (in microcellular and low antenna height), we observed that the fade margins are lower for urban than suburban areas. This is explained by canyon like structure of urban areas which accounts for the reception of multipaths from one direction rather than every direction. Subsequently, less multipaths arrive at the mobile antenna. On the other hand, in the suburban area under study (a residential neighborhood of Port Washington, NY), where the average building height is approximately the same as the transmitting antenna height and there are many open fields such as backyards and spaces between houses which account for multipath arrival from every direction at the receiver. Nakagami-4.5 and Nakagami-7 approximate the fade statistics for

suburban and urban environment.

The suburban experiments performed for evaluation of fade margins after despreader reveal an increase in fade margin of 15 dB with probability 0.001, for an one finger receiver. We believe that the reason behind this is that components scattered by the houses arrive at the mobile within a very short delay with respect to the system's chip duration. Because of this small delay, and the fact that the returns have power comparable to that of the shortest return, the variations become very large. The variations tend to decrease less when the chip rate is increased. Since, a wider band SS system can resolve most of the multipath returns, therefore, it can use a coherent RAKE receiver to lower its fade margin by up to 14 dB. This improvement cannot be achieved by narrowband CDMA systems having bandwidths less than 10 MHz. Further, it was shown that the multipath observed in practice had almost all of its energy concentrated in a time interval of less than 1μsec (for high antenna heights) with main signal component about 100-200 nsec apart. Therefore, the narrower the bandwidth of the spread spectrum signal the larger the number of rays which can occur within a chip duration. Hence the greater the probability of a deep fade. For low antenna heights the excess delay is concentrated in a time interval of less than 500 nsec with main signal components 40 nsec apart.

It was also shown that in a particular environment if a distant multipath signal was present and if this reflection was delayed more than 1μsec away from the main lobe, then a narrowband spread spectrum system can use RAKE to collect this added power. It should be noted, however, that narrowband system must collect this extra energy since its main signal rays suffer from severe multipath fading independent of the other delayed signals. However, these locations were found to be confined to a very low probability of existence within a prescribed cell.

Indoor measurements reveal that there are 5 dominant returns when a 24 Mchips/s system is used. The typical excess delay was 350 nsec and individual components were often 40 nsec apart. It was shown that a RAKE with five fingers could improve the fade margin by approximately 9 dB. Again this improvement cannot be achieved by a narrowband system since such a system could not distinguish between the multipath returns.

## Future Work

Although measurements presented in this dissertation give an insight to what to expect in the channel as the chip rate is varied, one can extend this work such that to characterize the channel fully as a function of the system chip rate.

This characterization would involve building a channel sounder which can resolve all the multipaths (5 nsec resolution) and performing extensive measurements in various environments. Only then we can really know how the channel is behaving given a specific chip rate used in the system. A more elaborate and more complex variable rate, variable m-code channel sounder is under design by the author.

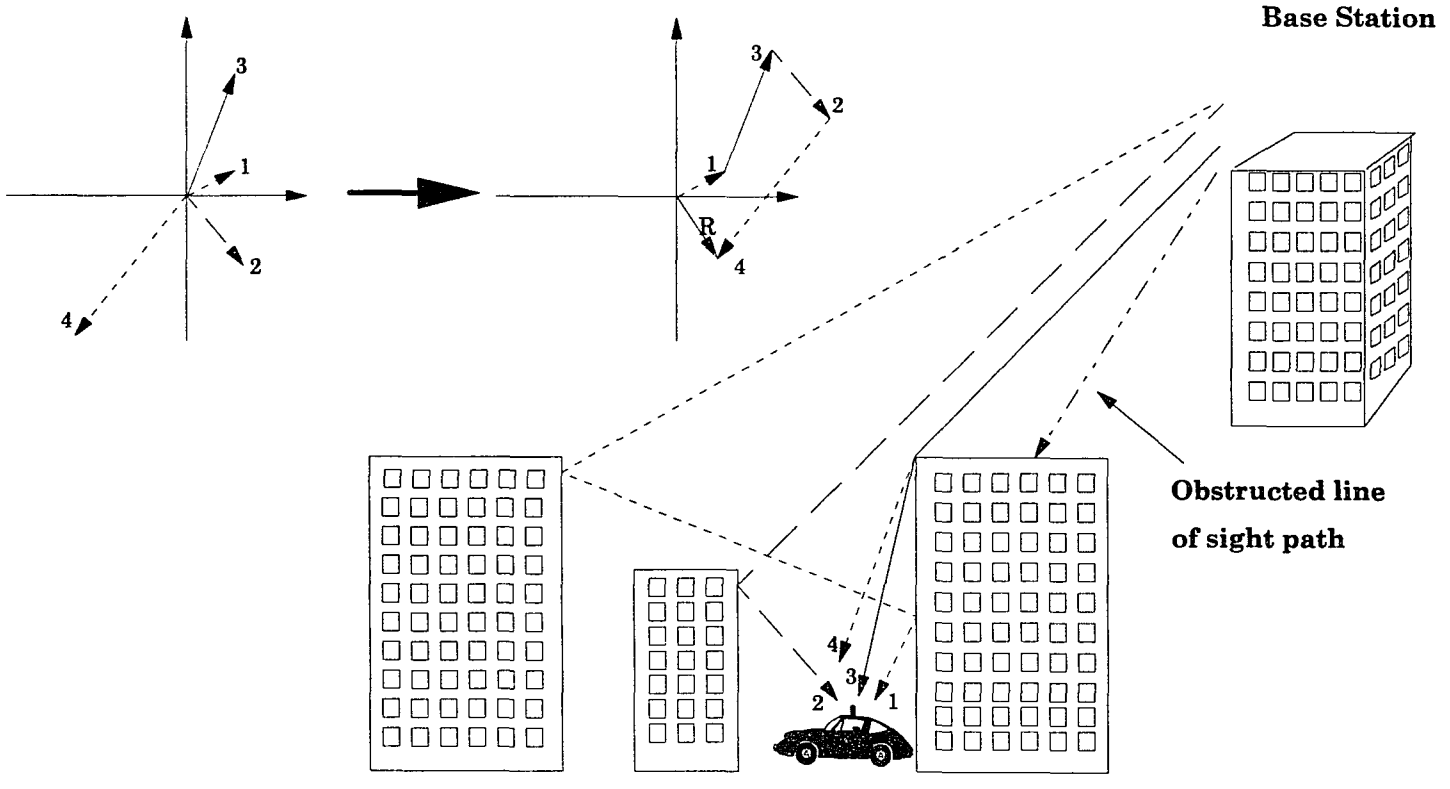


**Figure 1.1: Multipath Propagation Phenomena**

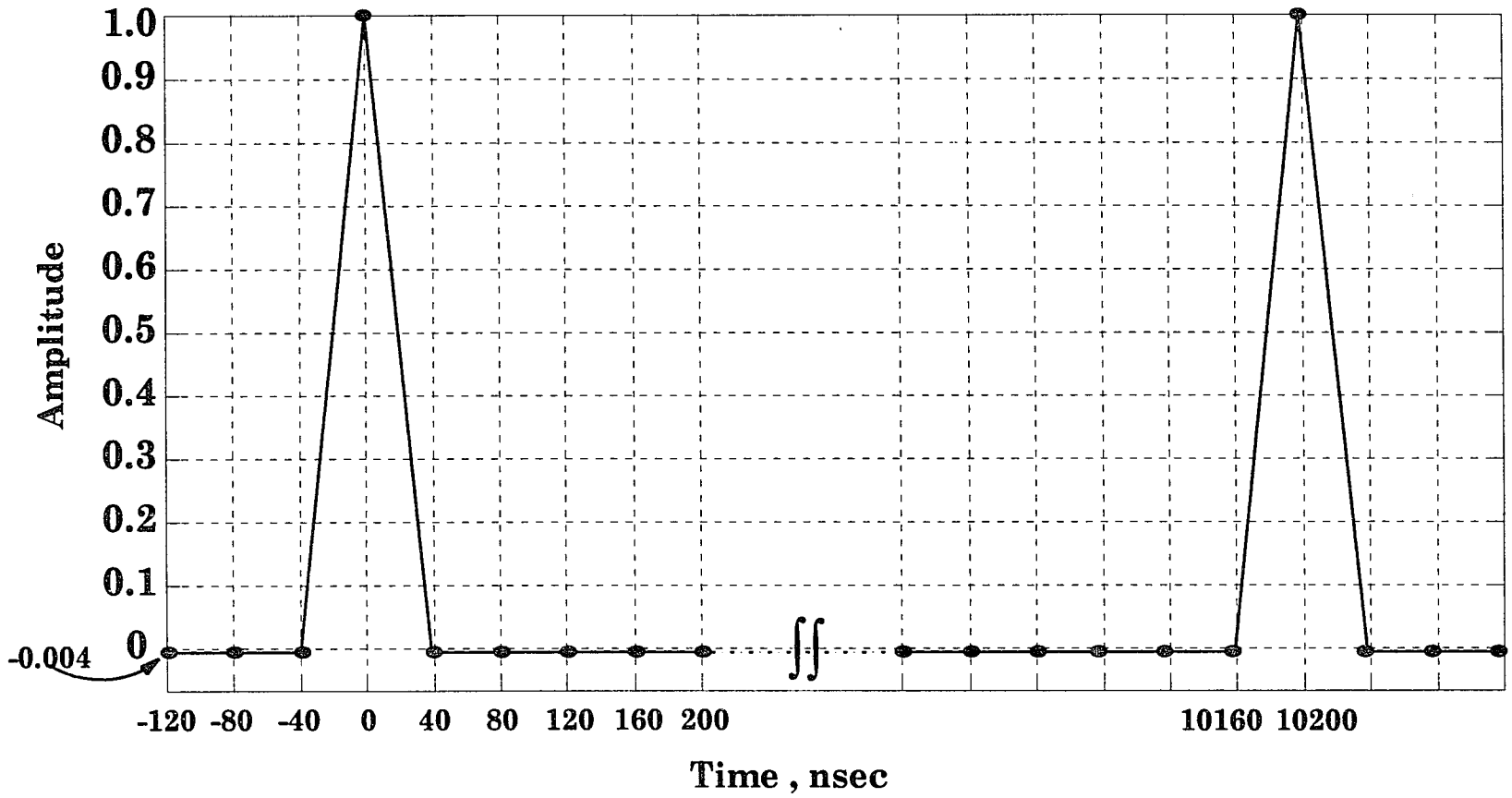


**Figure 2.1: Autocorrelation Function of a 255 PN-sequence, Chip rate = 25 MHz**

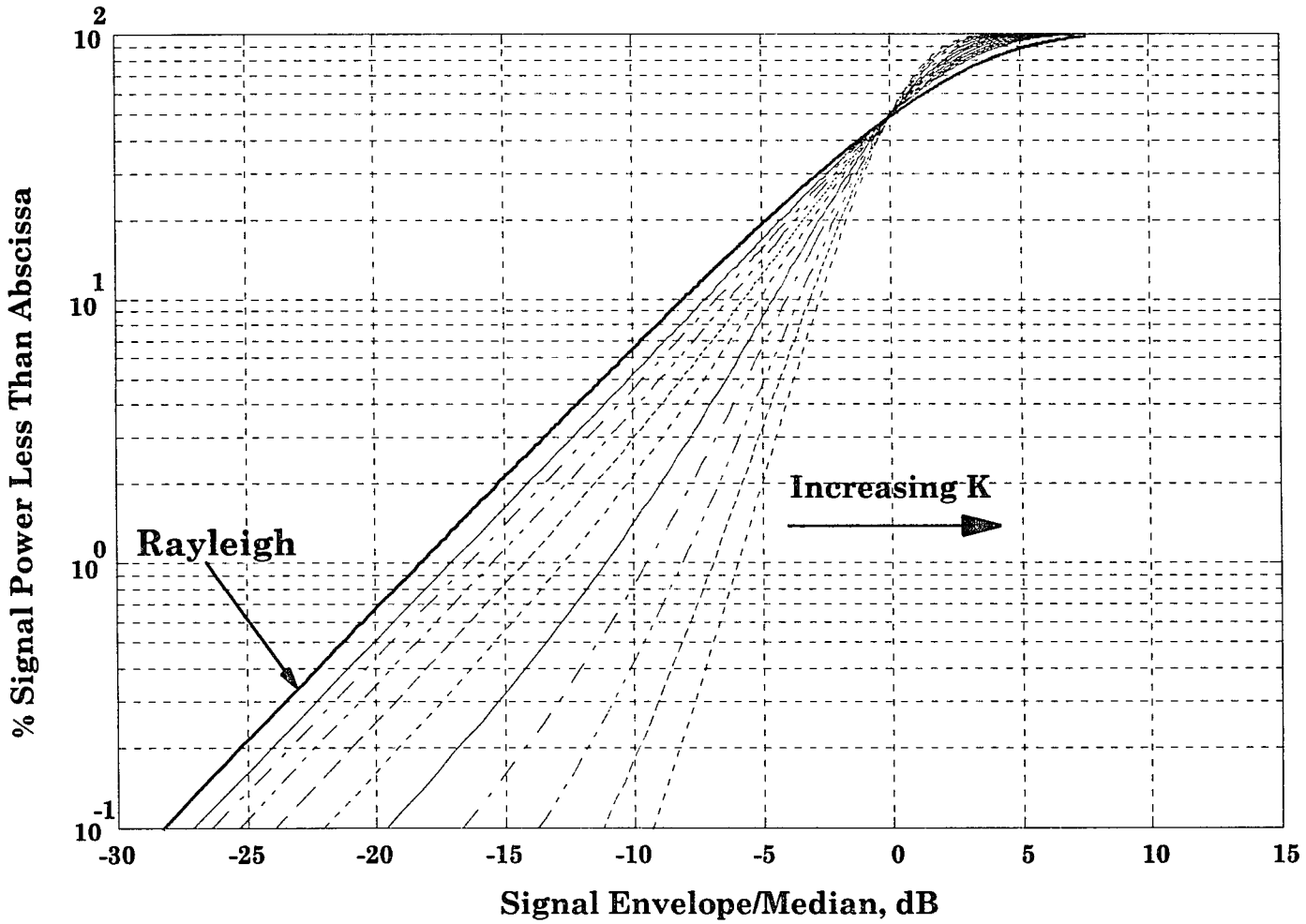


**Figure 2.2.: CDF of Rician Distributed Random Process as a function of K**

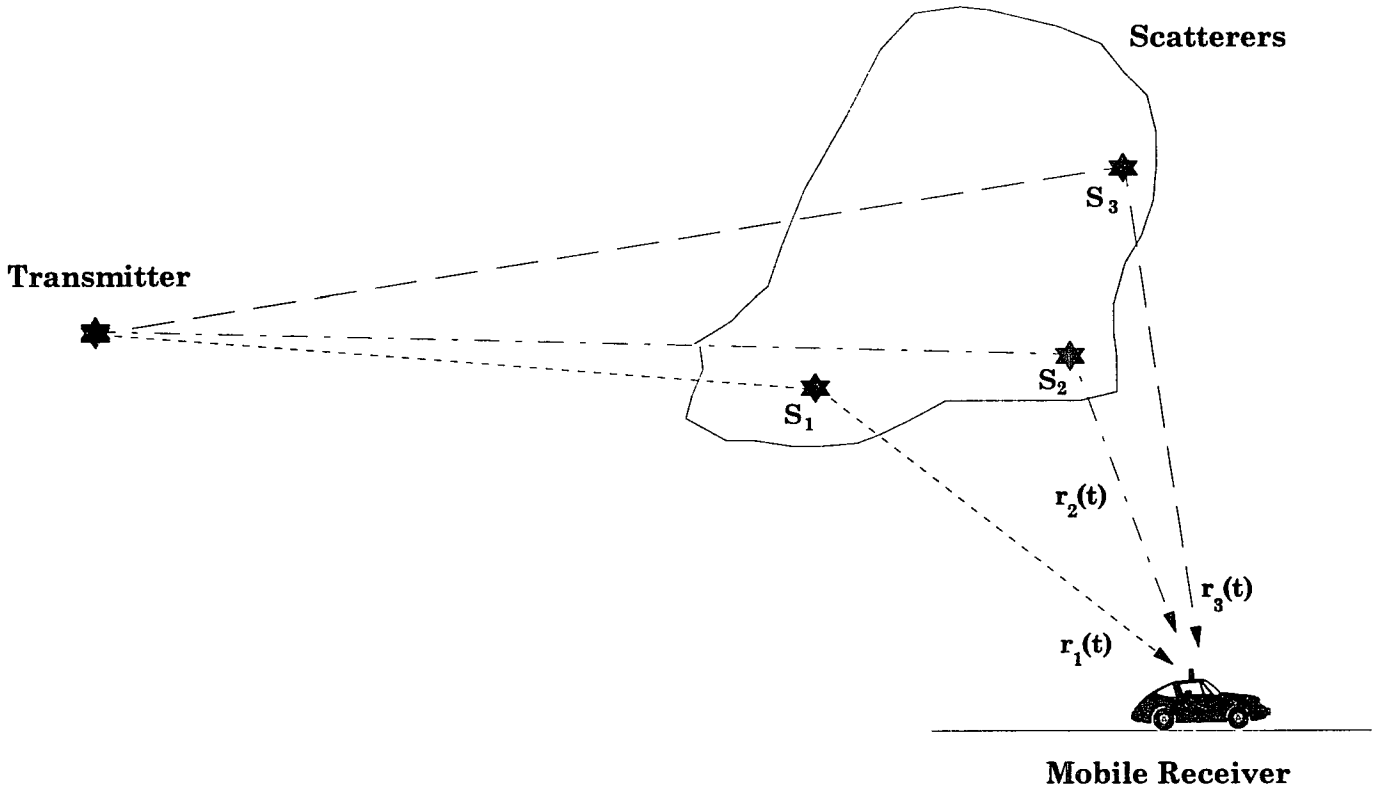


**Figure 2.3: Multipath Scattering Phenomena**

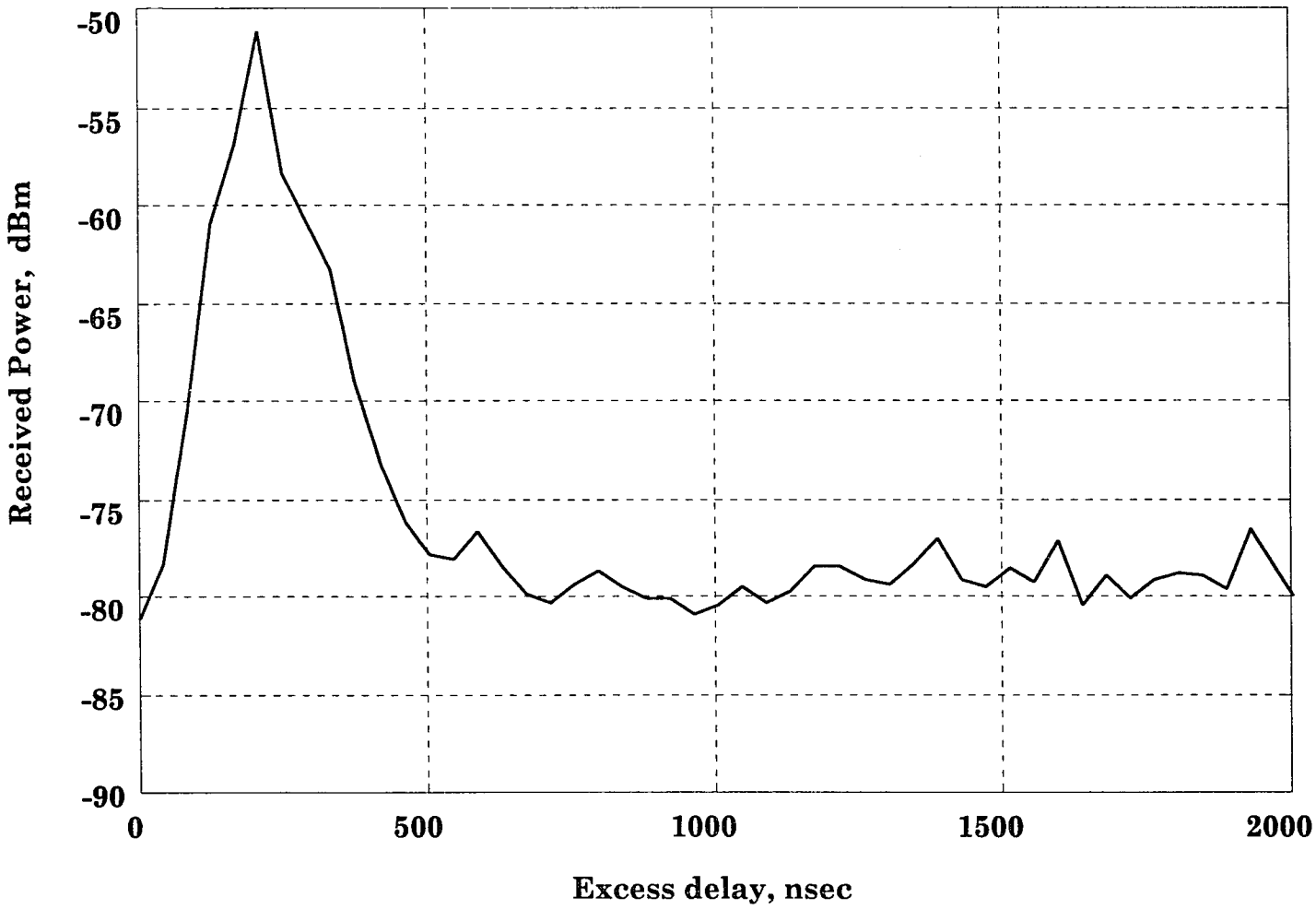


**Figure 2.4: Delay Power Spectrum**

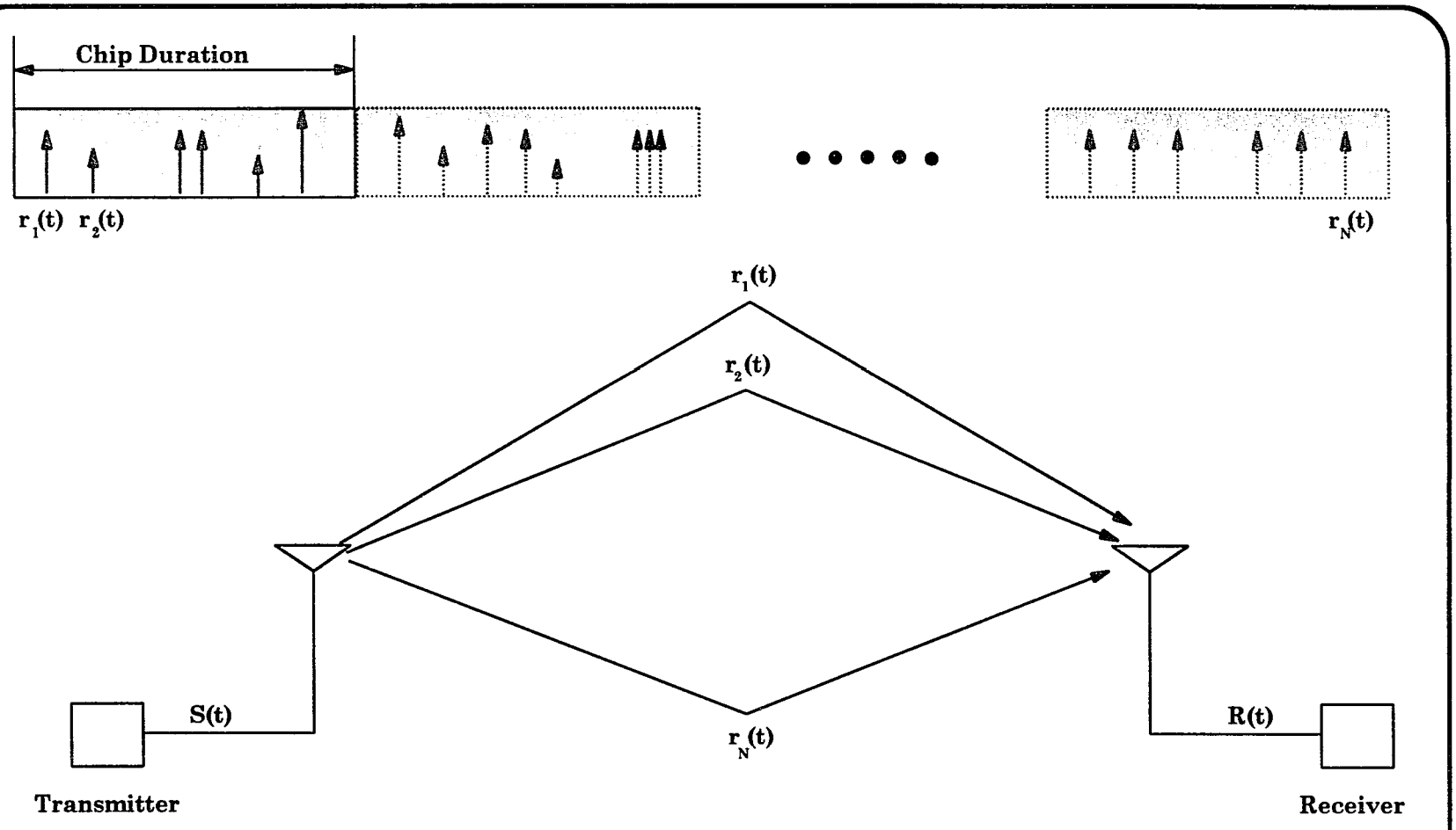


**Figure 2.5: Illustration of the Close-in and Far-out Multipaths**

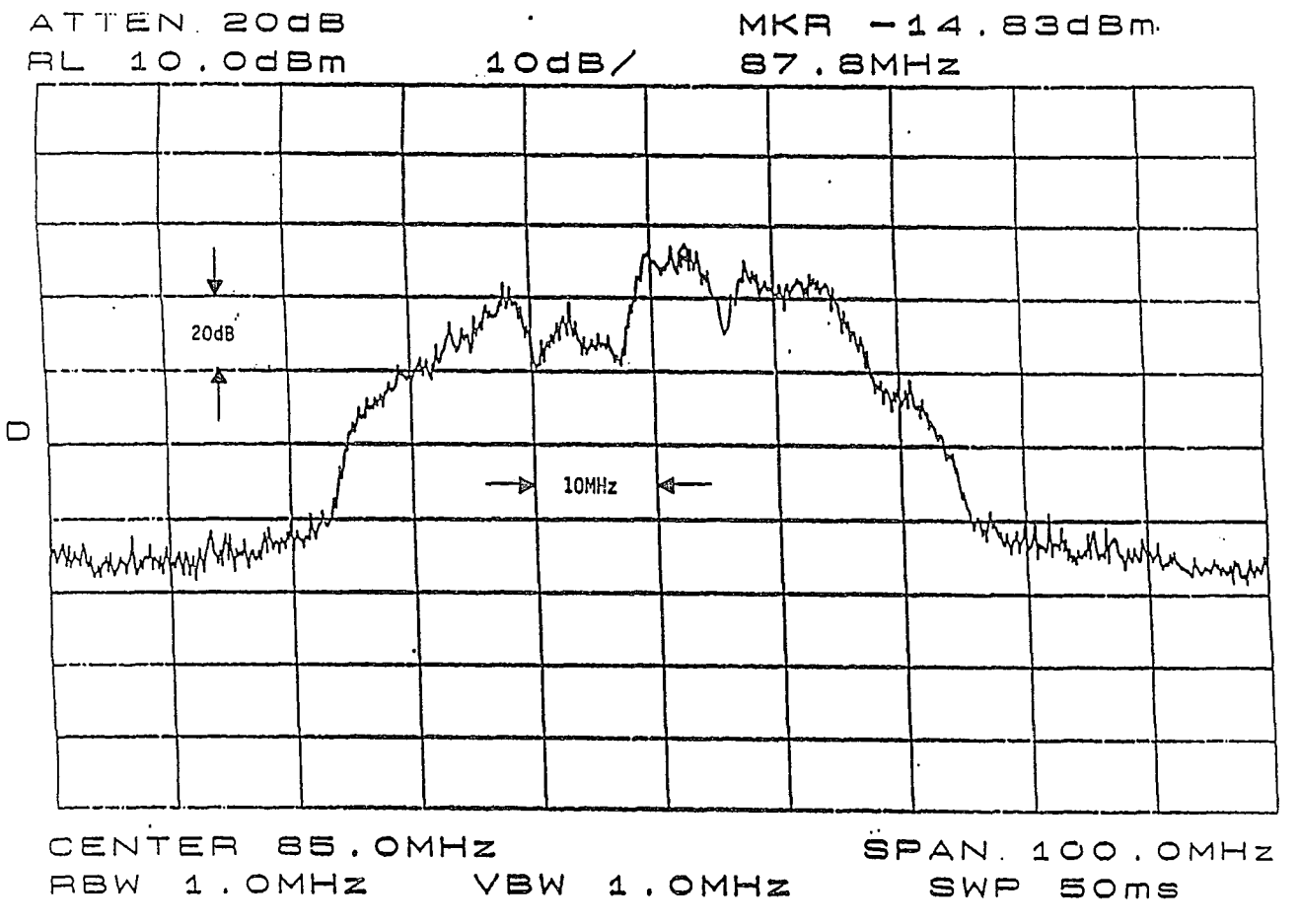


**Figure 2.6: Variation of the Power Spectral Density of the received signal under severe fading condition. (NAC Building, City College)**

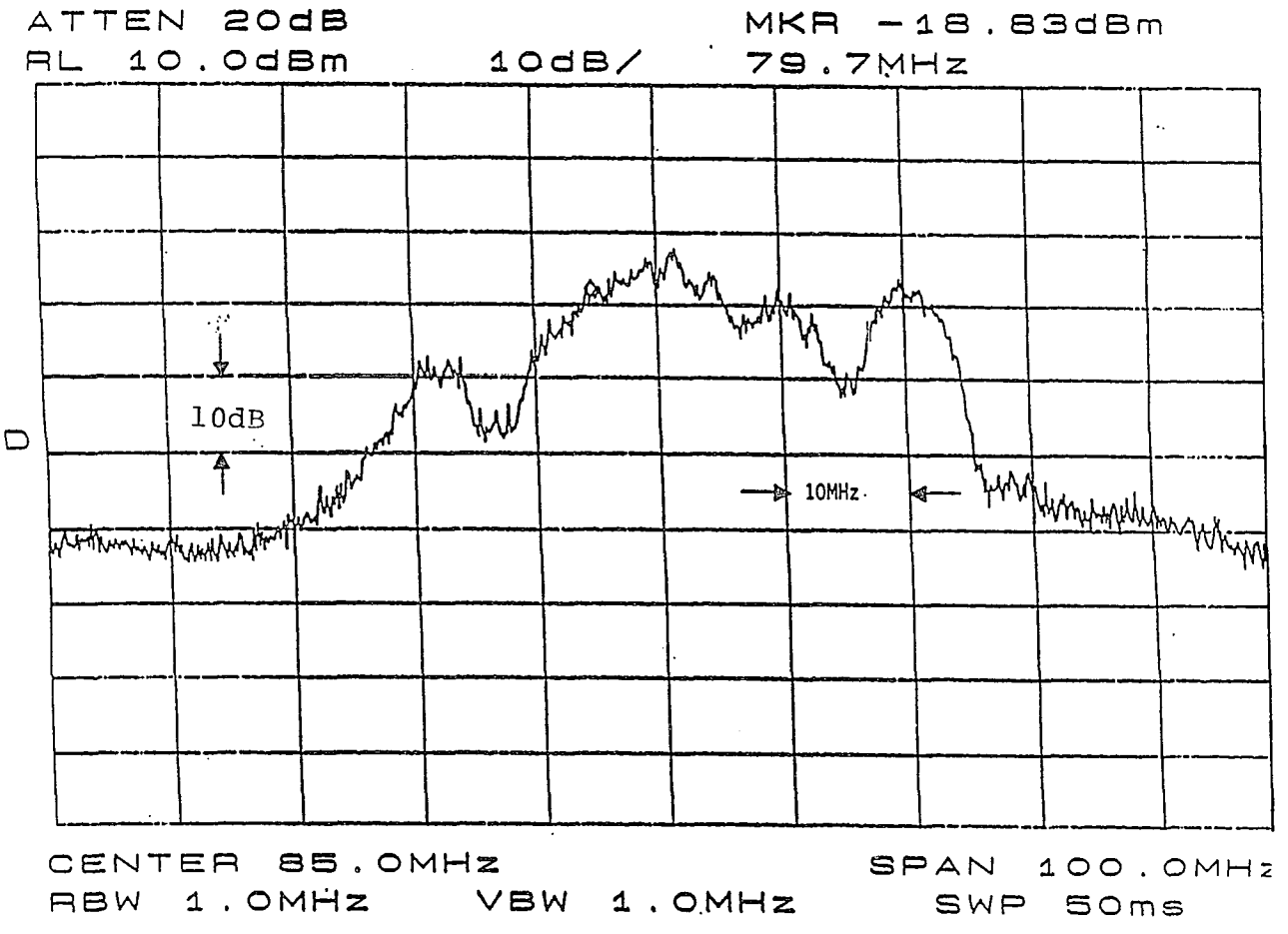


**Figure 2.7: Variation of the Power Spectral Density of the received signal under severe fading condition. (InterDigital Building)**

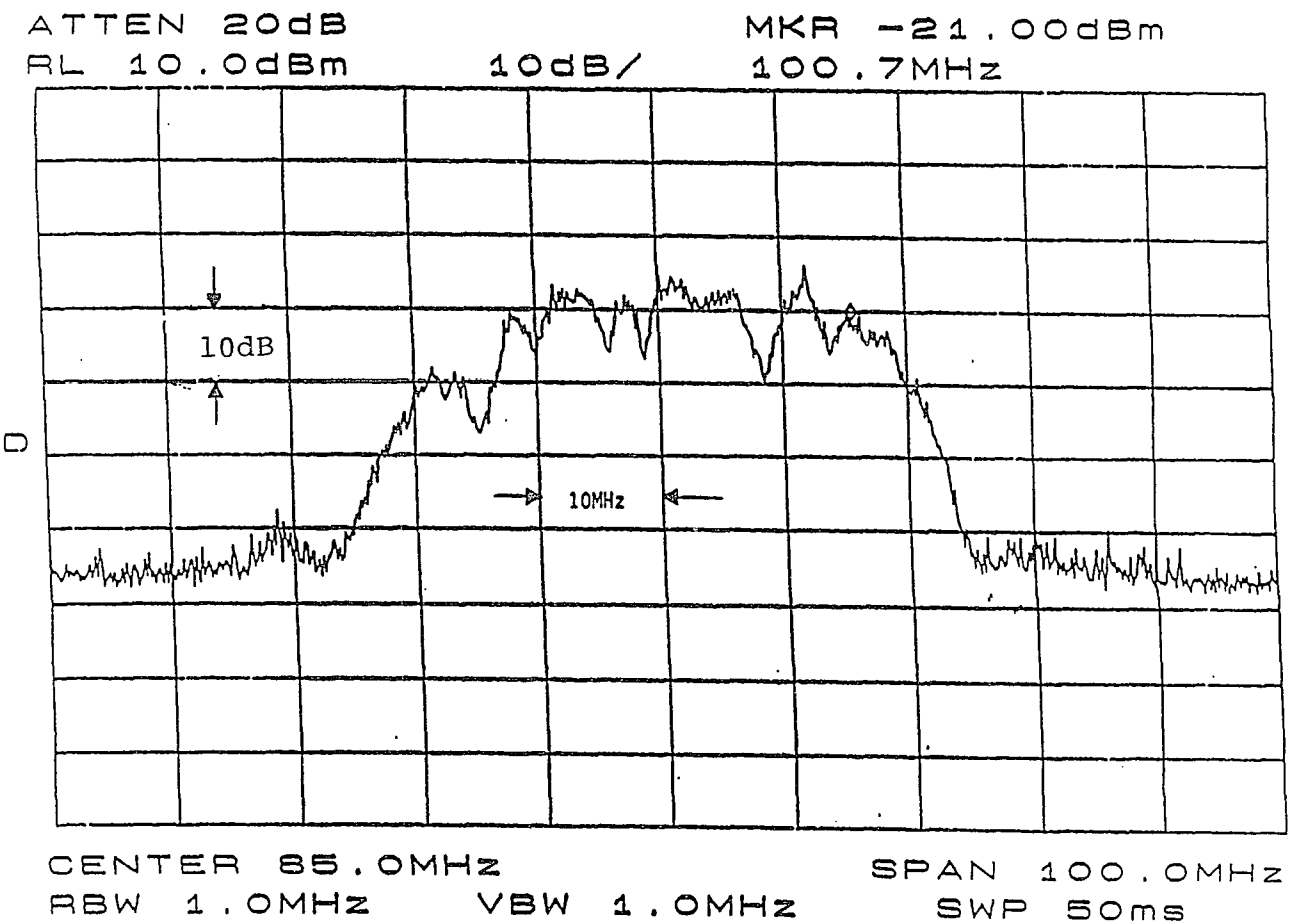


**Figure 2.8: Variation of the Power Spectral Density of the received signal under severe fading condition. (Haven Ave., Port Washington)**

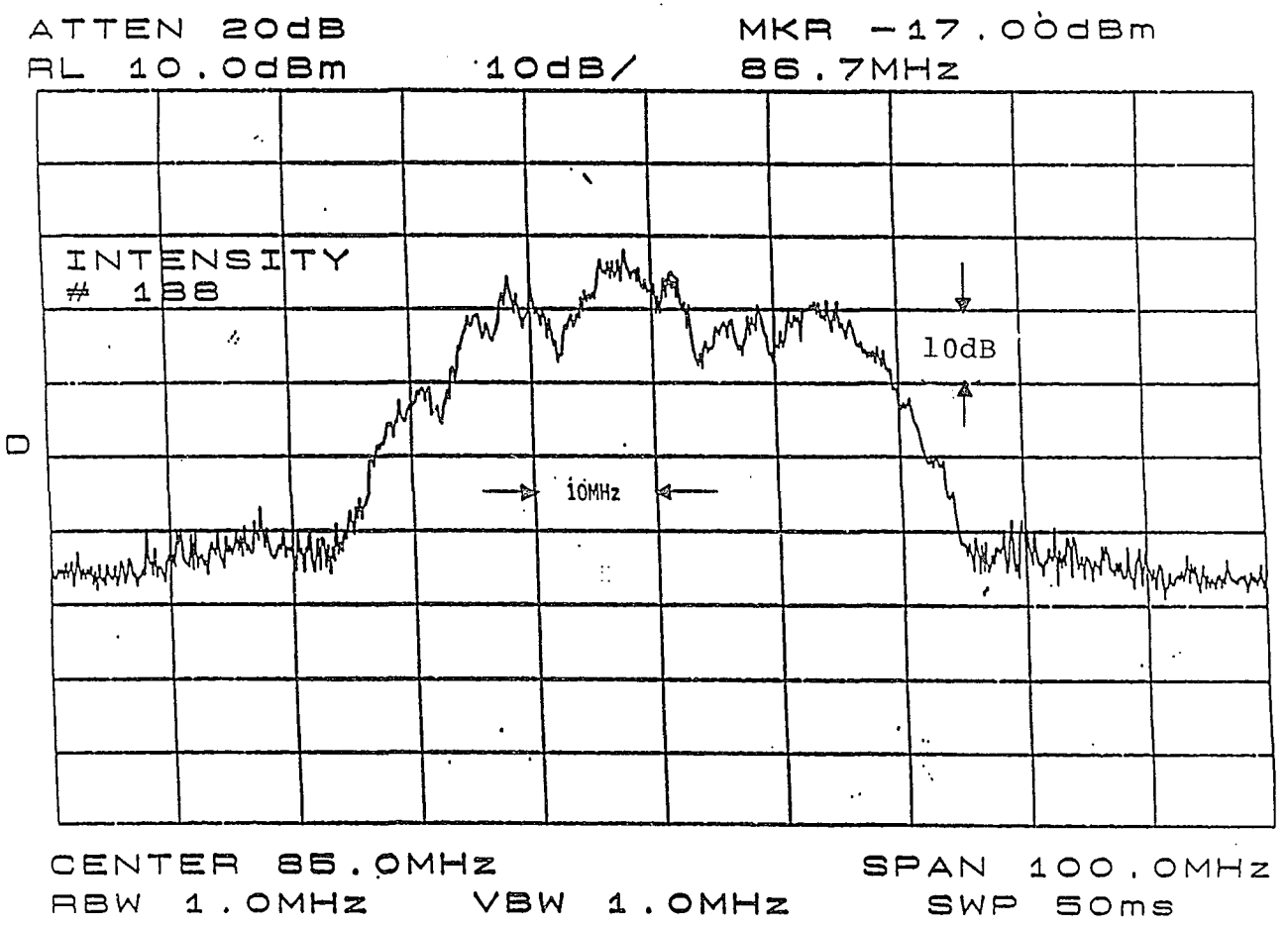


**Figure 2.9: Variation of the Power Spectral Density of the received signal under severe fading condition. (Second Ave. and 18th st., Manhattan)**

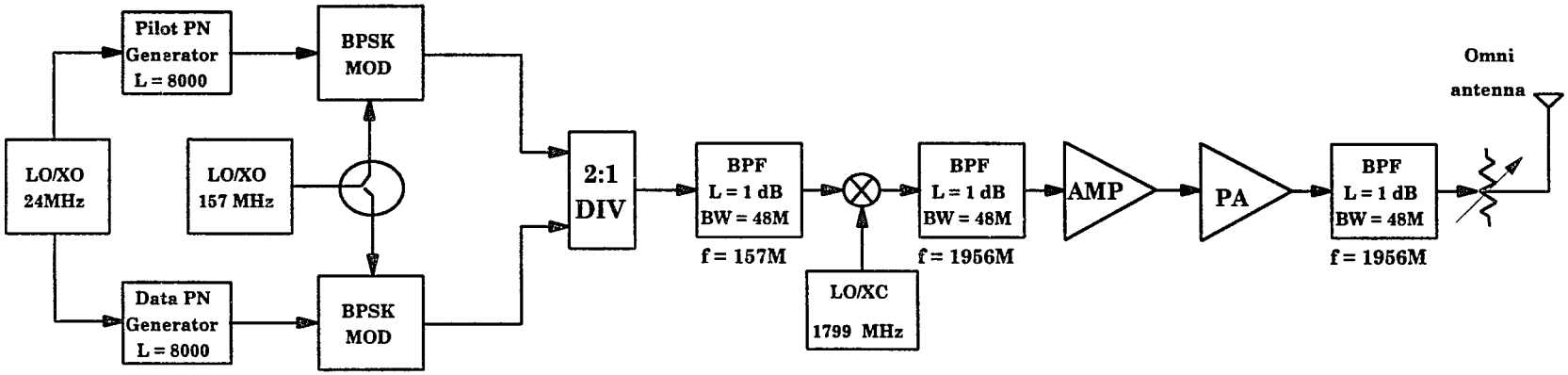


**Figure 4.1: The DS-BPSK Transmitter Configuration.**

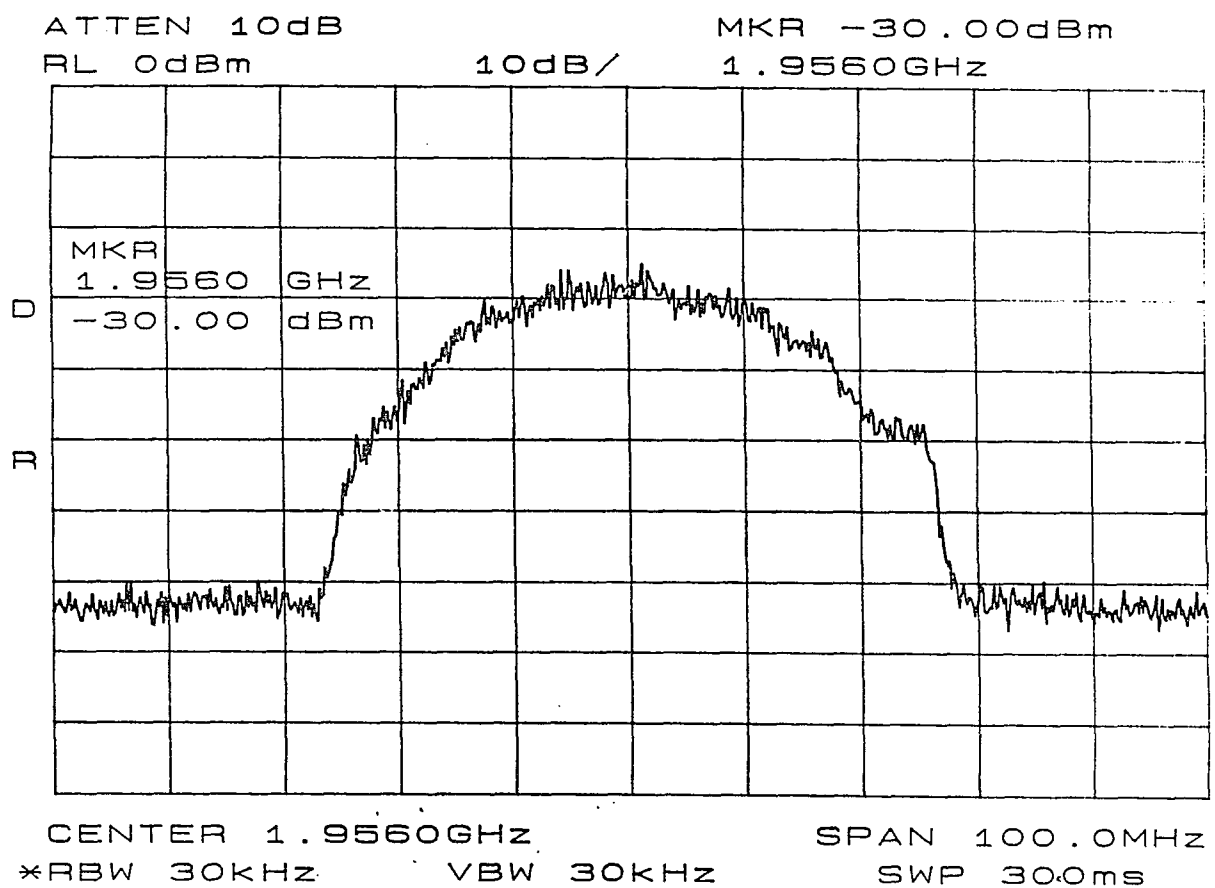


**Figure 4.2: Power Spectral Density of a 24 Mchips/s spread spectrum signal in presence of no fading.**

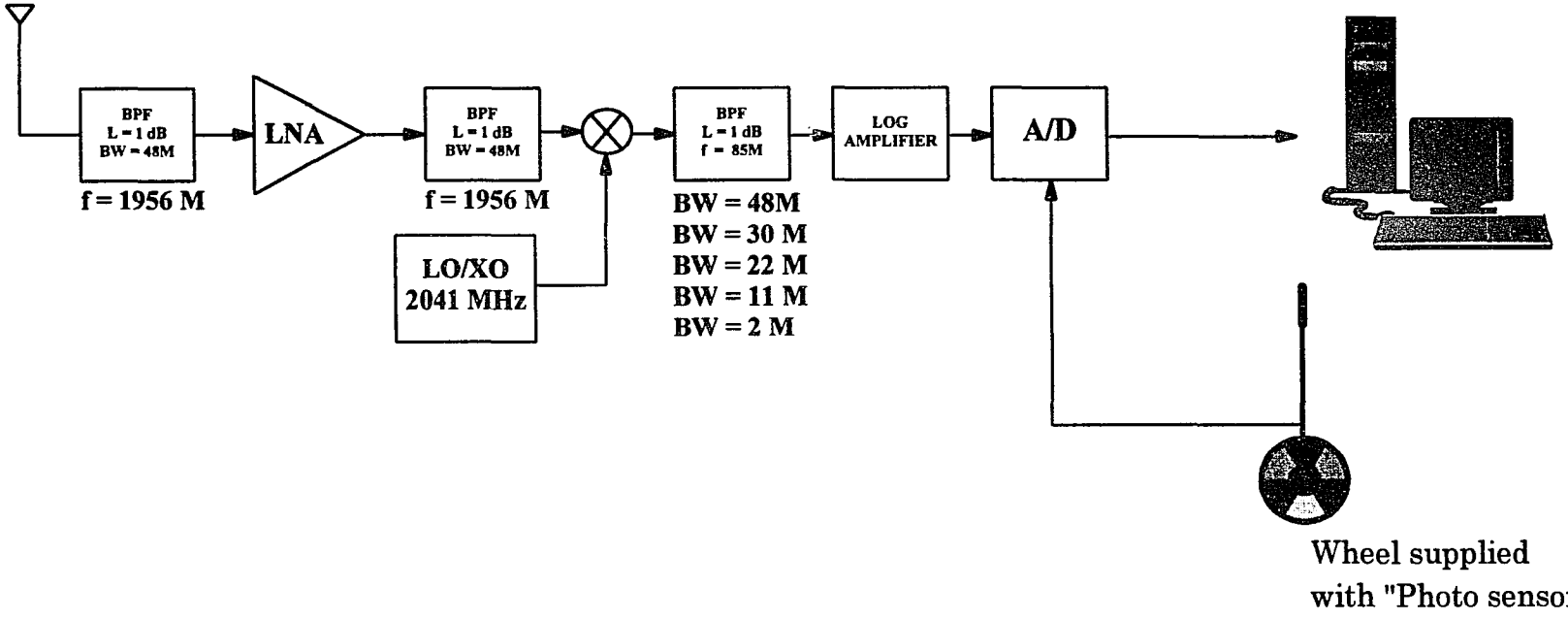


**Figure 4.3: The DS-BPSK Receiver Configuration before despreader.**

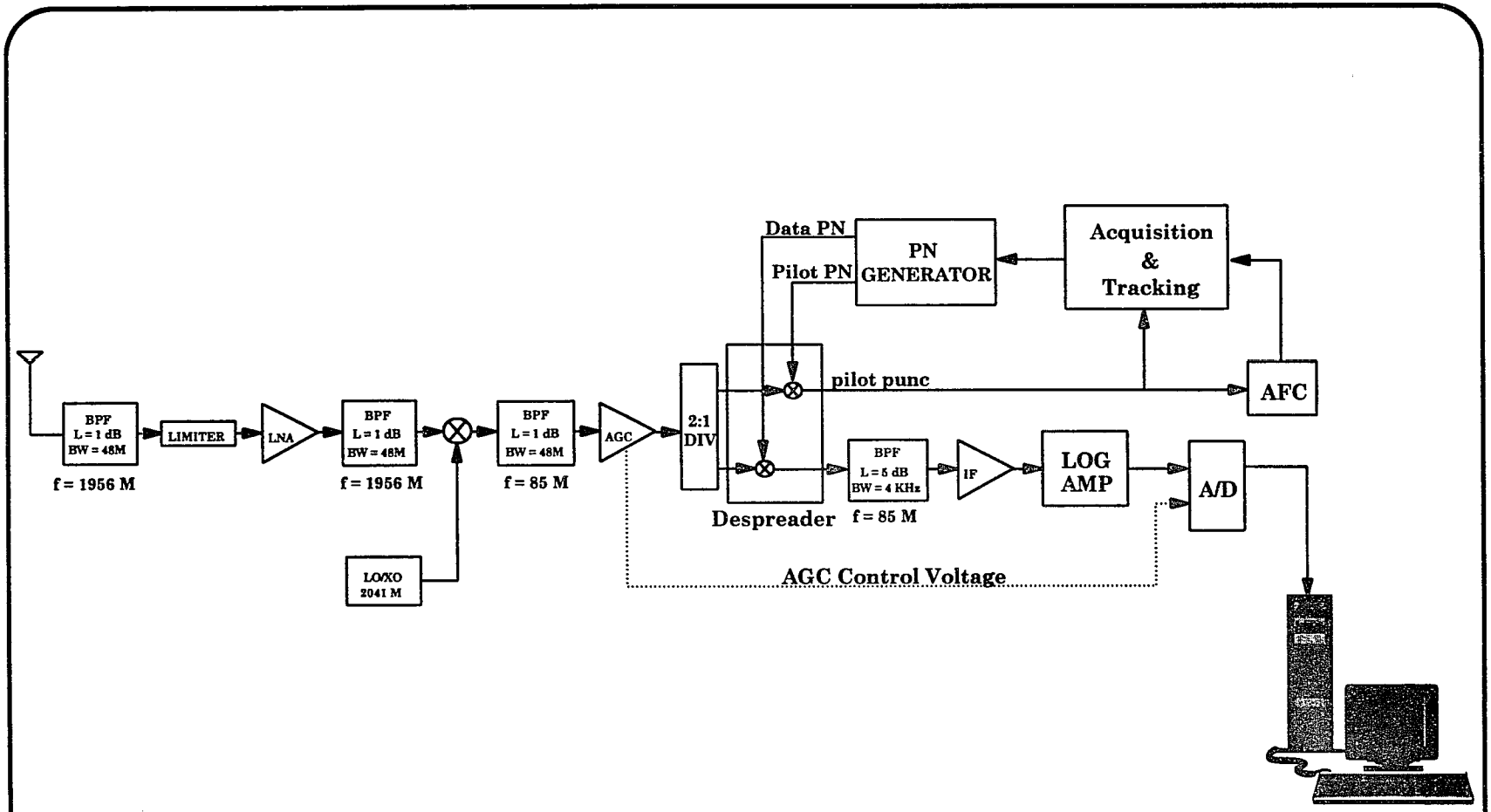


**Figure 4.4: The DS-BPSK Receiver Configuration after despreader.**

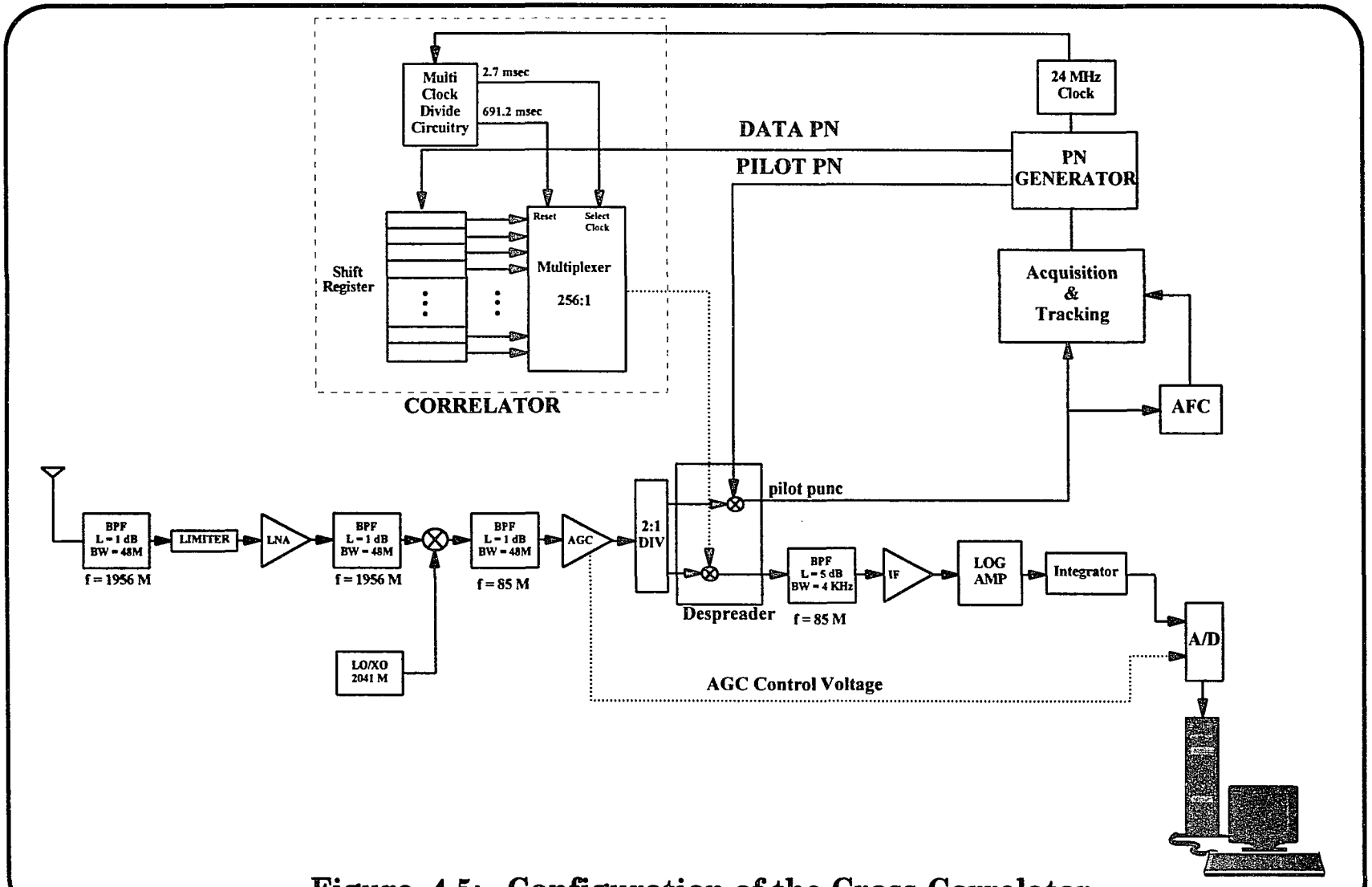


**Figure 4.5: Configuration of the Cross-Correlator**

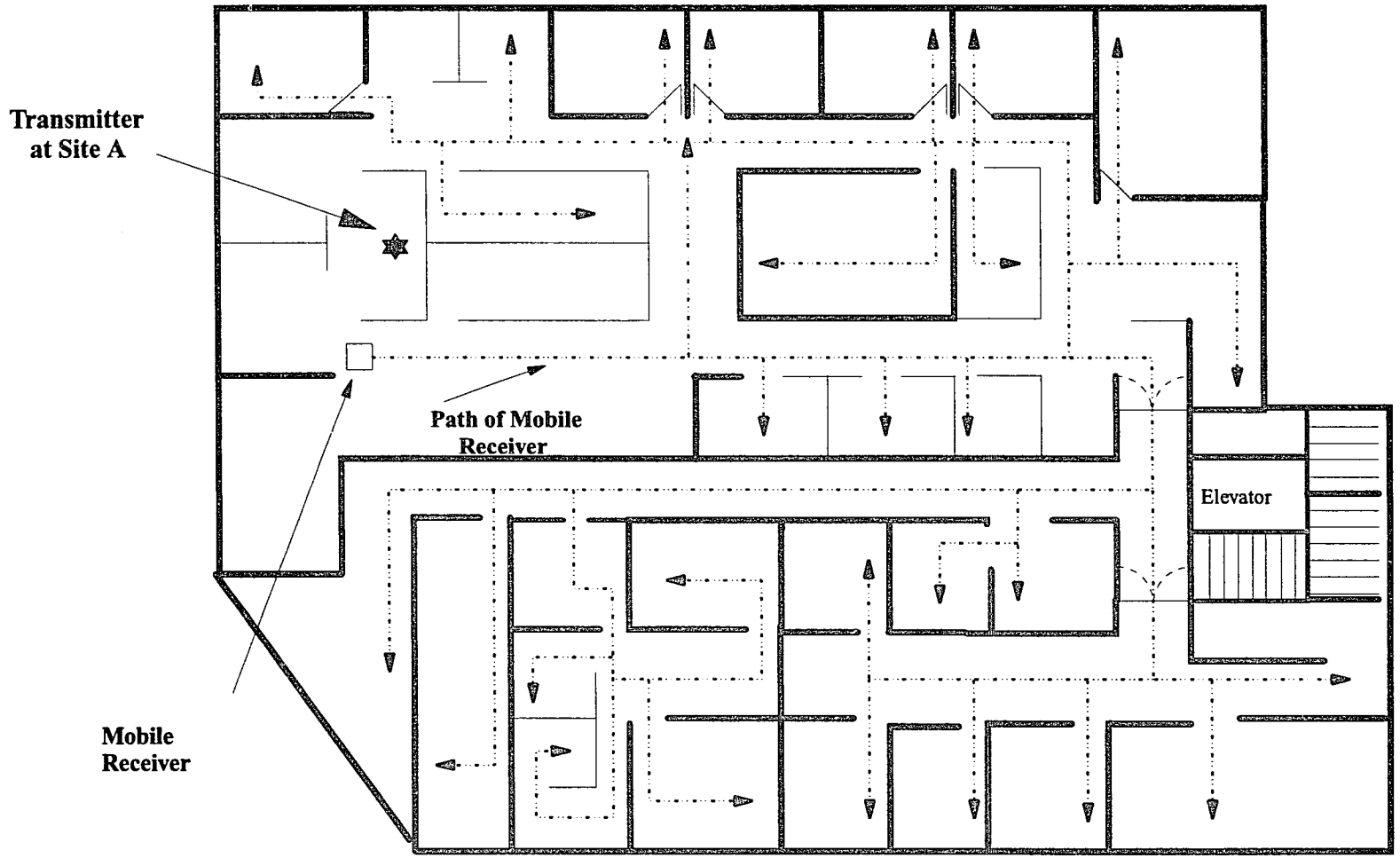


**Figure 4.6: Floor Plan of InterDigital Building, showing the path of mobile receiver.**

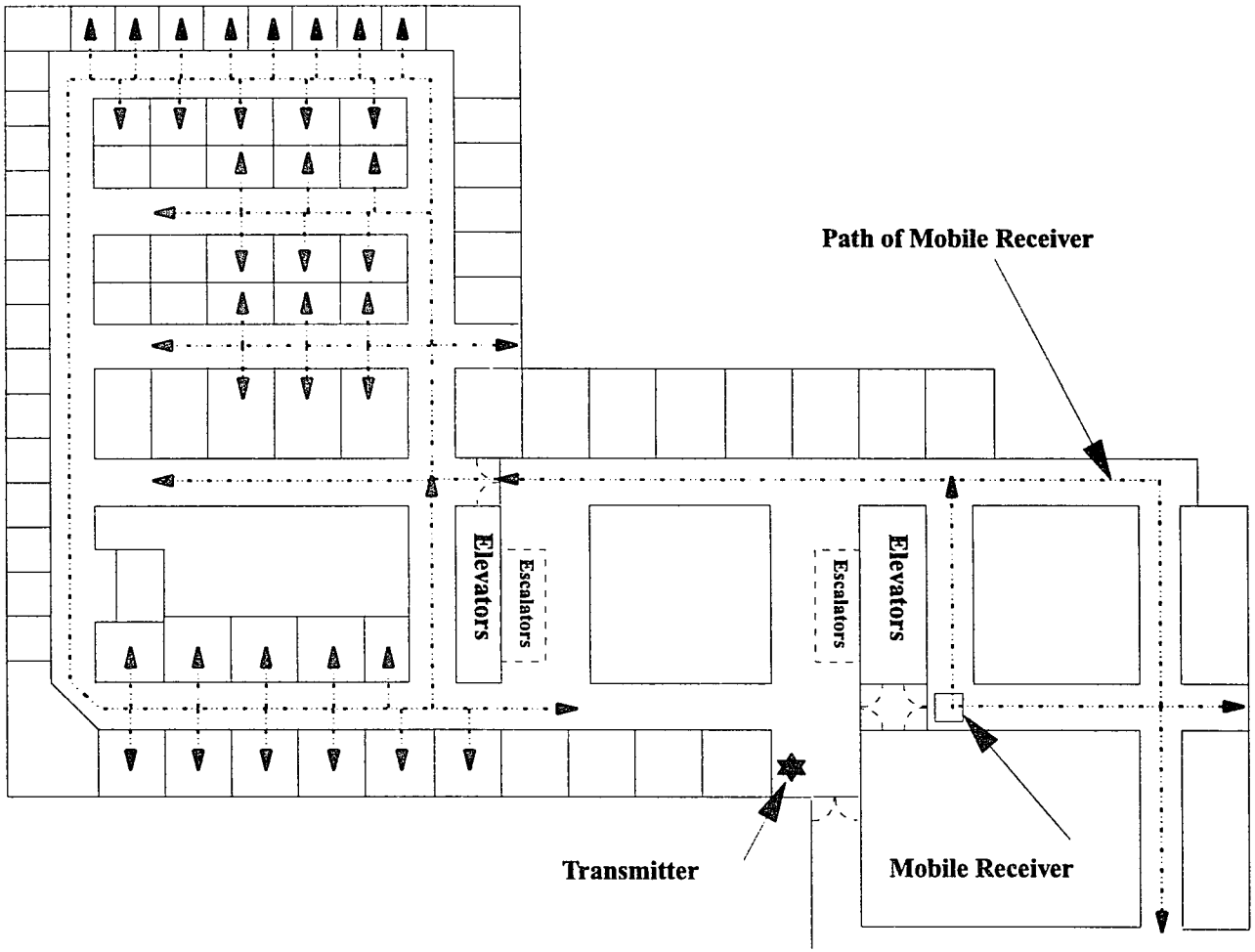


**Figure 4.7: Floor plan of the 6th floor of NAC Building (site B), showing the transmitter and receiver locations.**

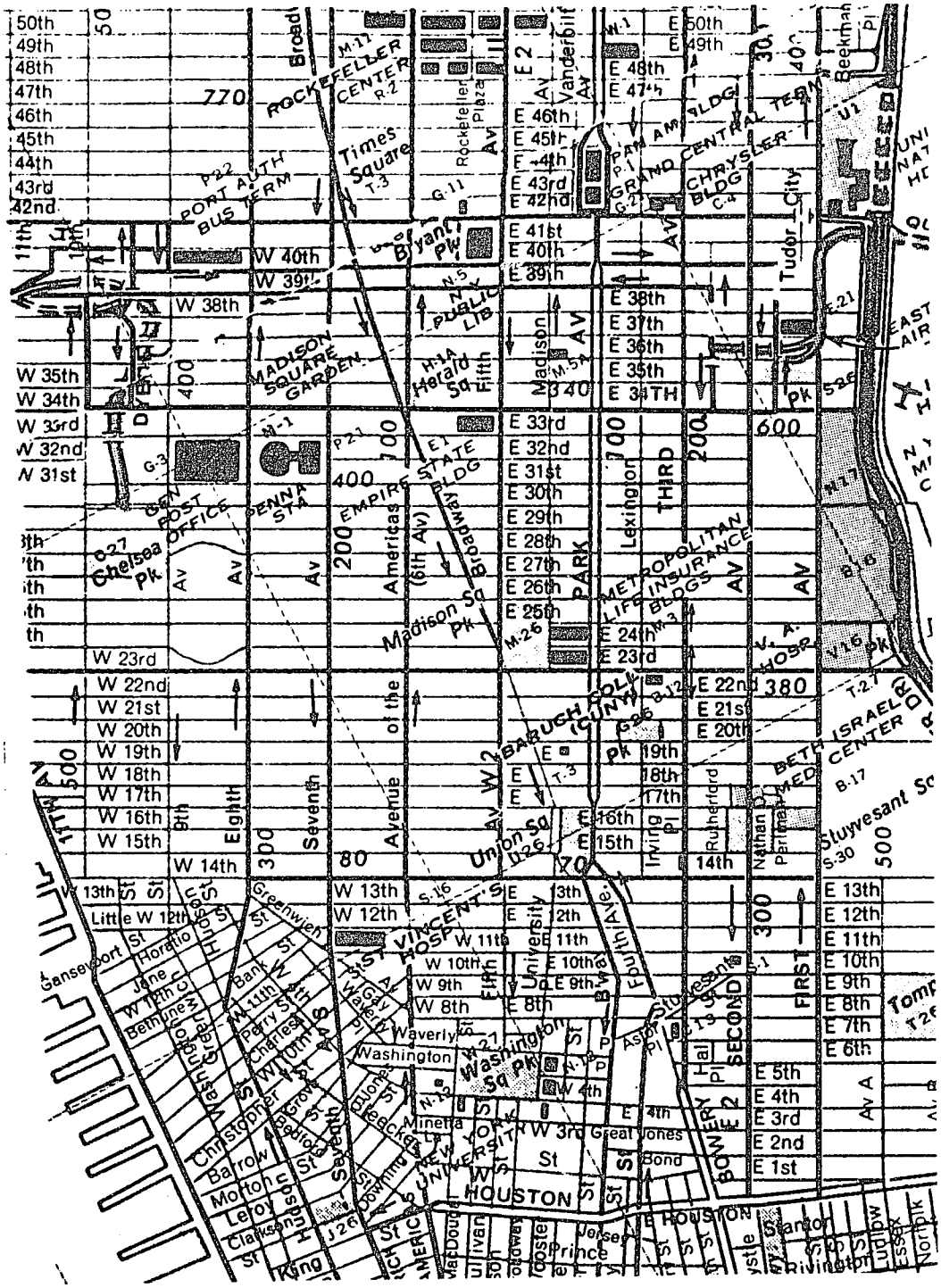


**Figure 4.8: Showing the map of Down-Town New York City ( Sites C & E).**

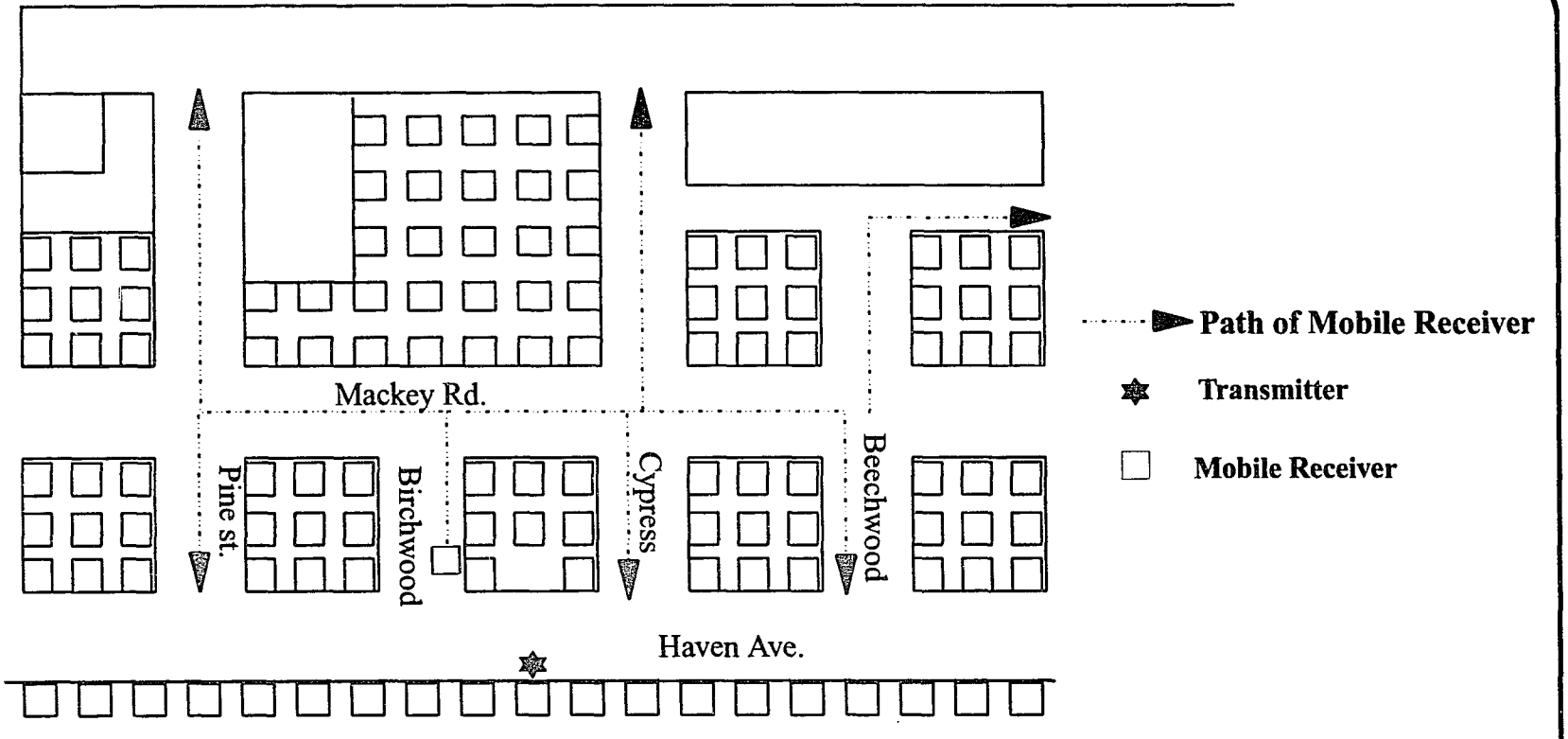


**Figure 4.9: Street Layout in Port Washington, Site D**

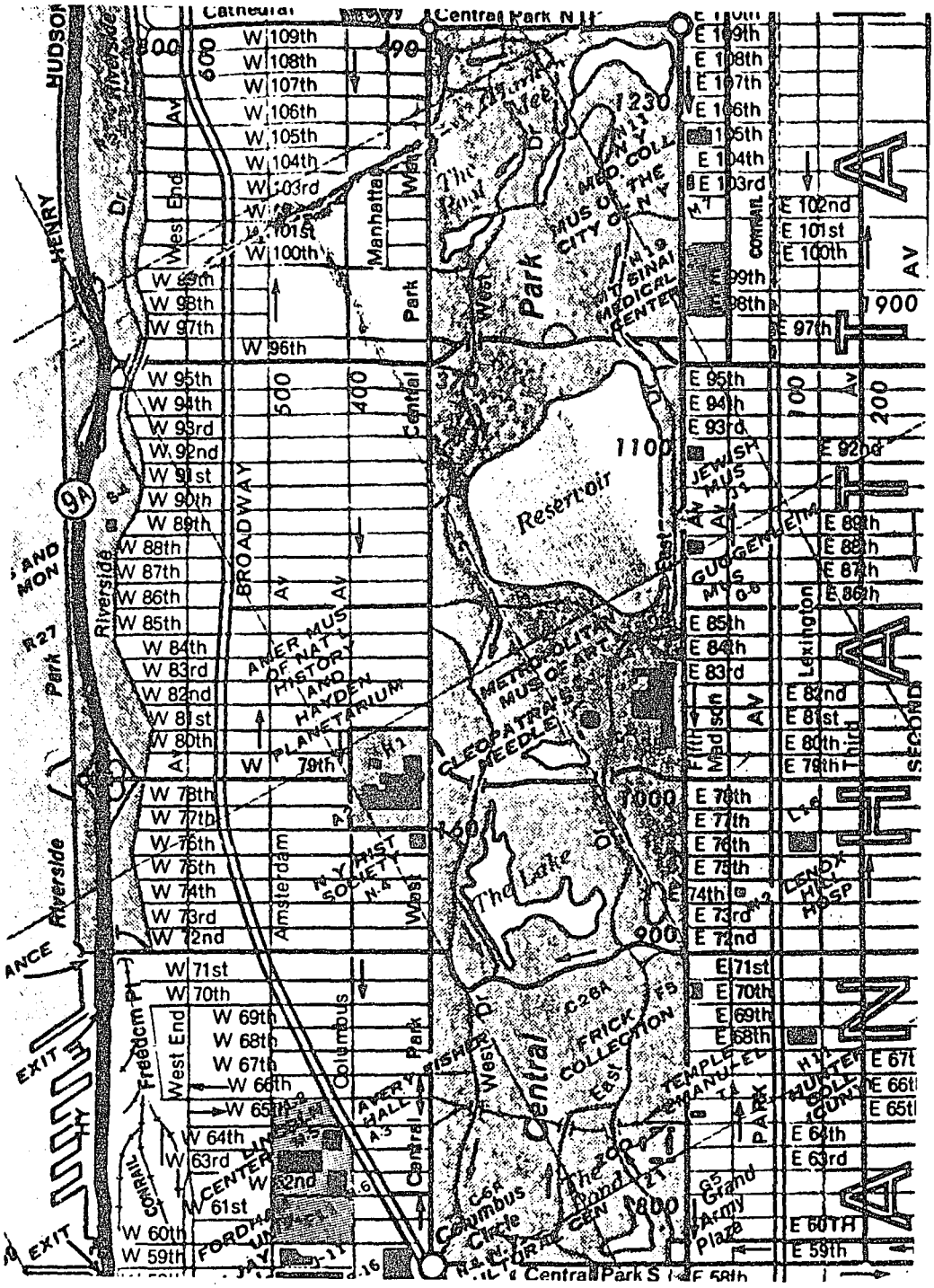


**Figure 4.10: Showing the map of Central Park in New York City ( Site F).**

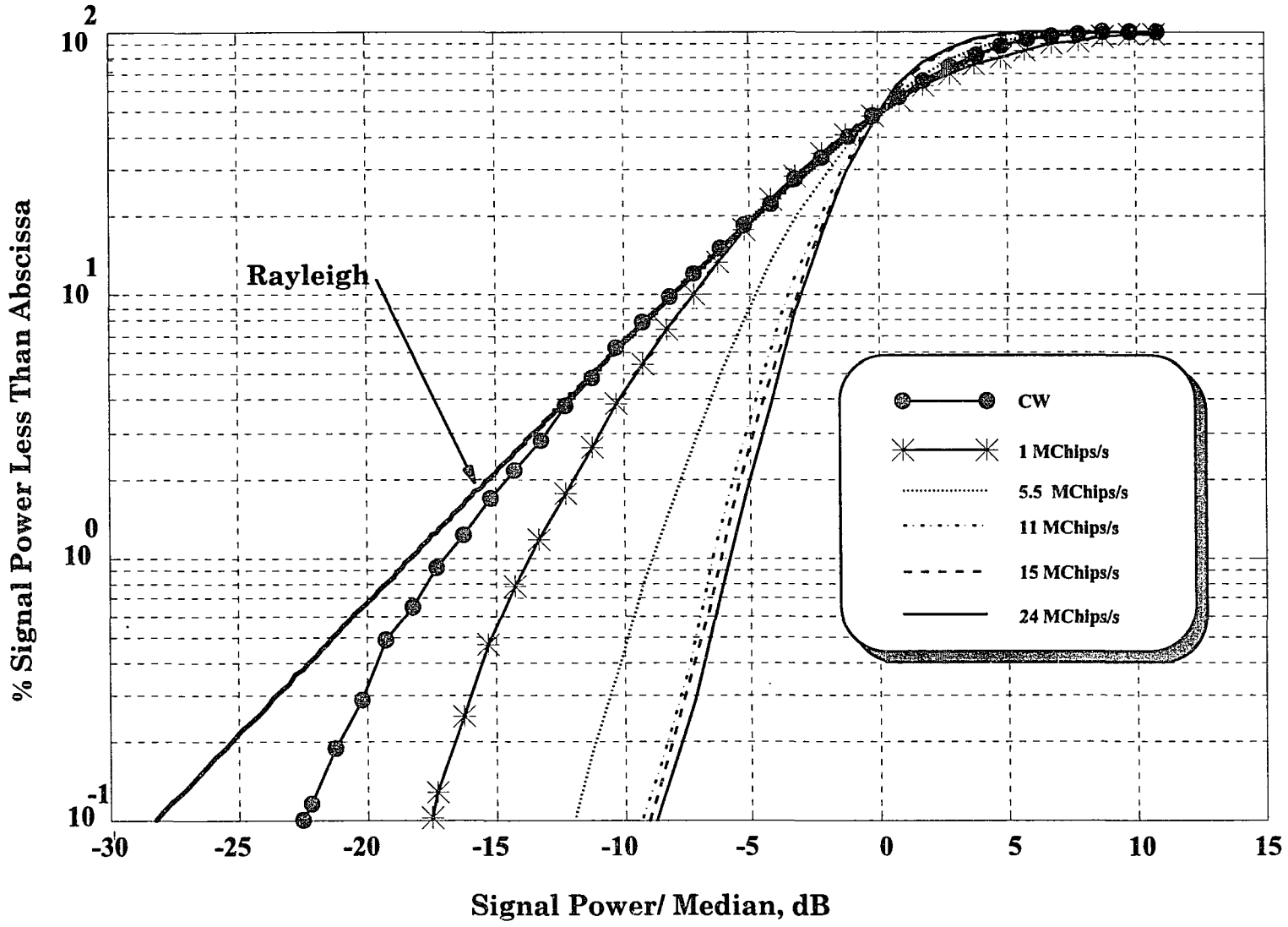


**Figure 5.1: Fade Margin before despreader in suburban areas.**

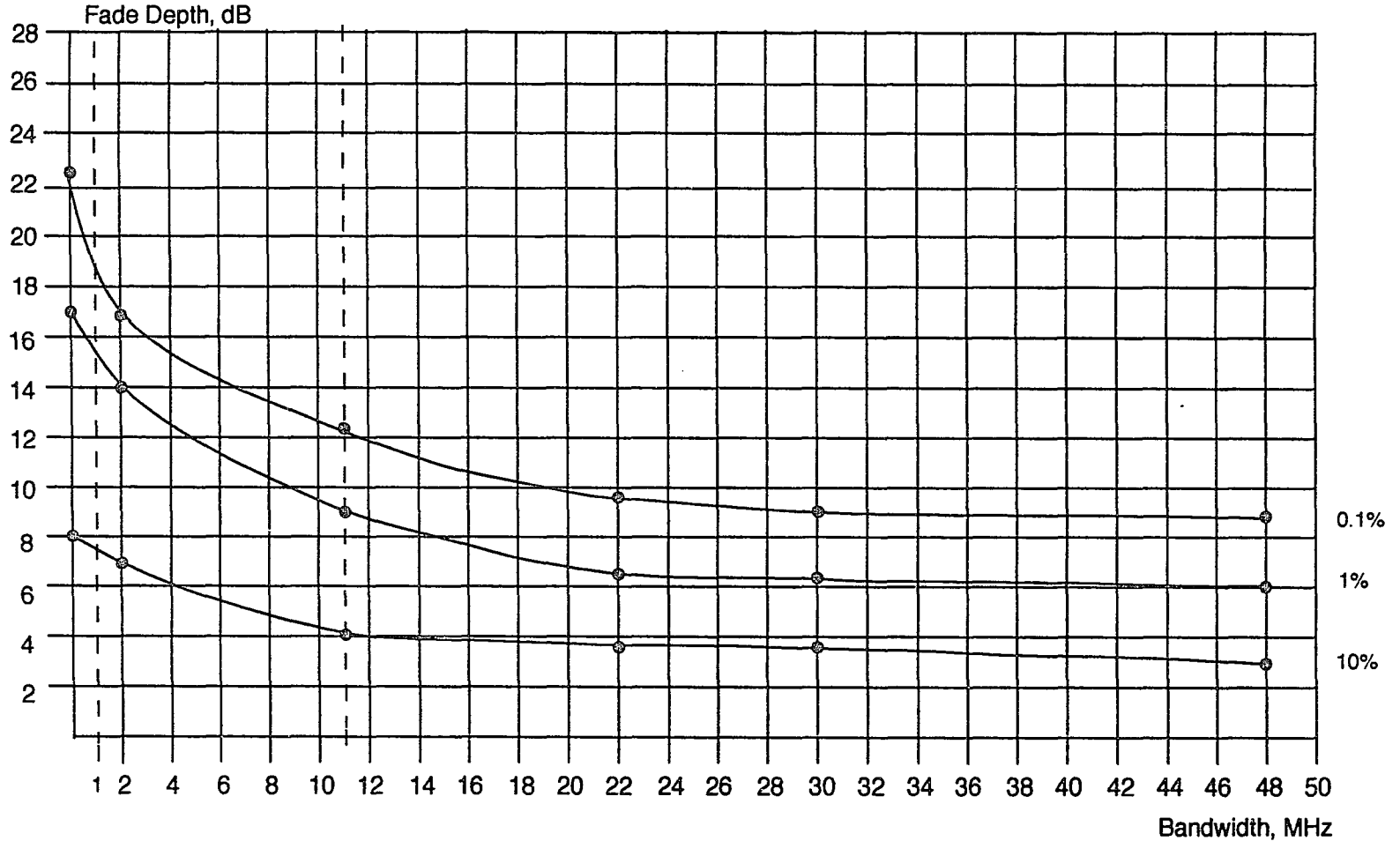


**Figure 5.2: Fade Depth in Suburban.**

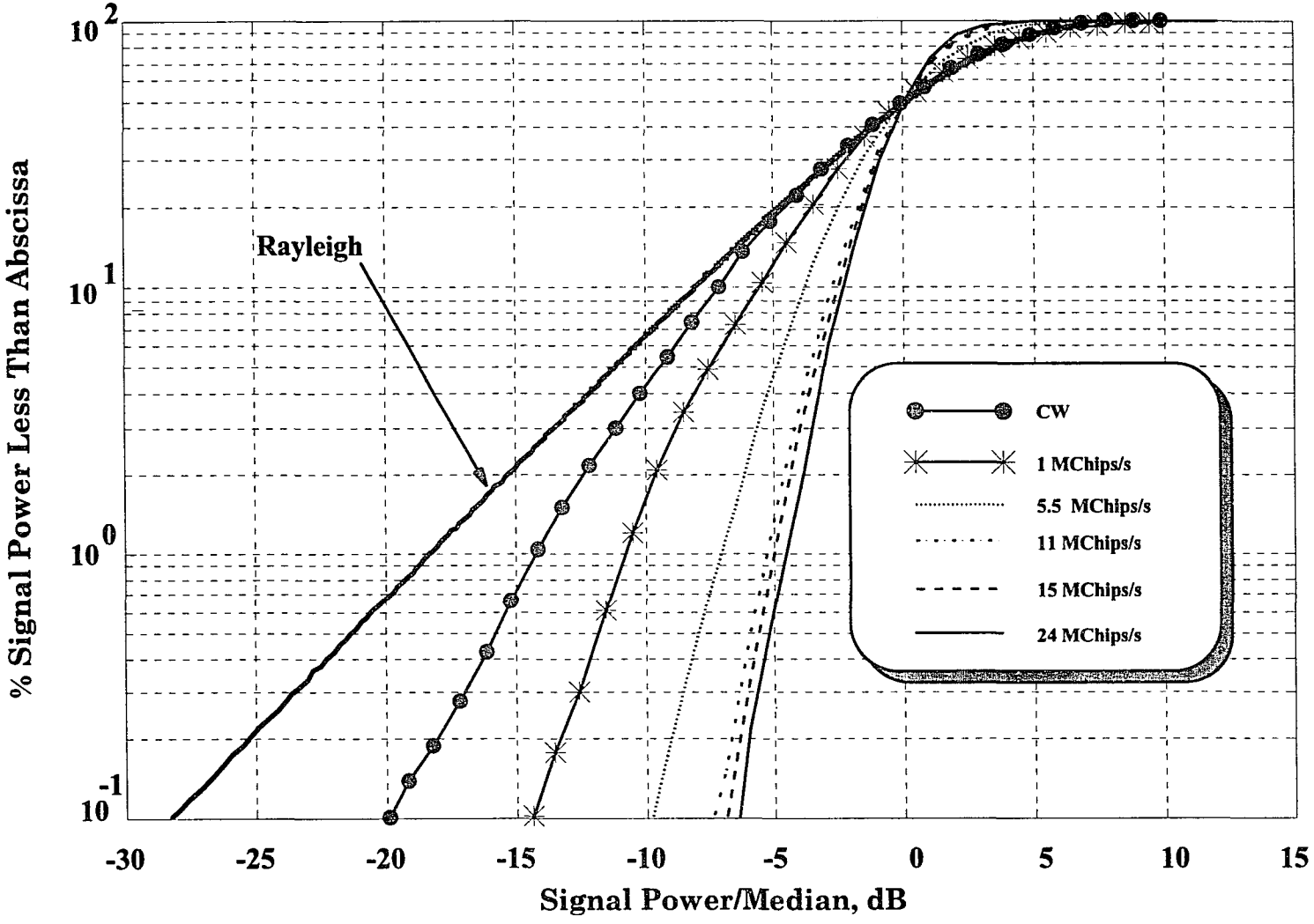


**Figure 5.3: Fade Margin before despreader in urban areas.**

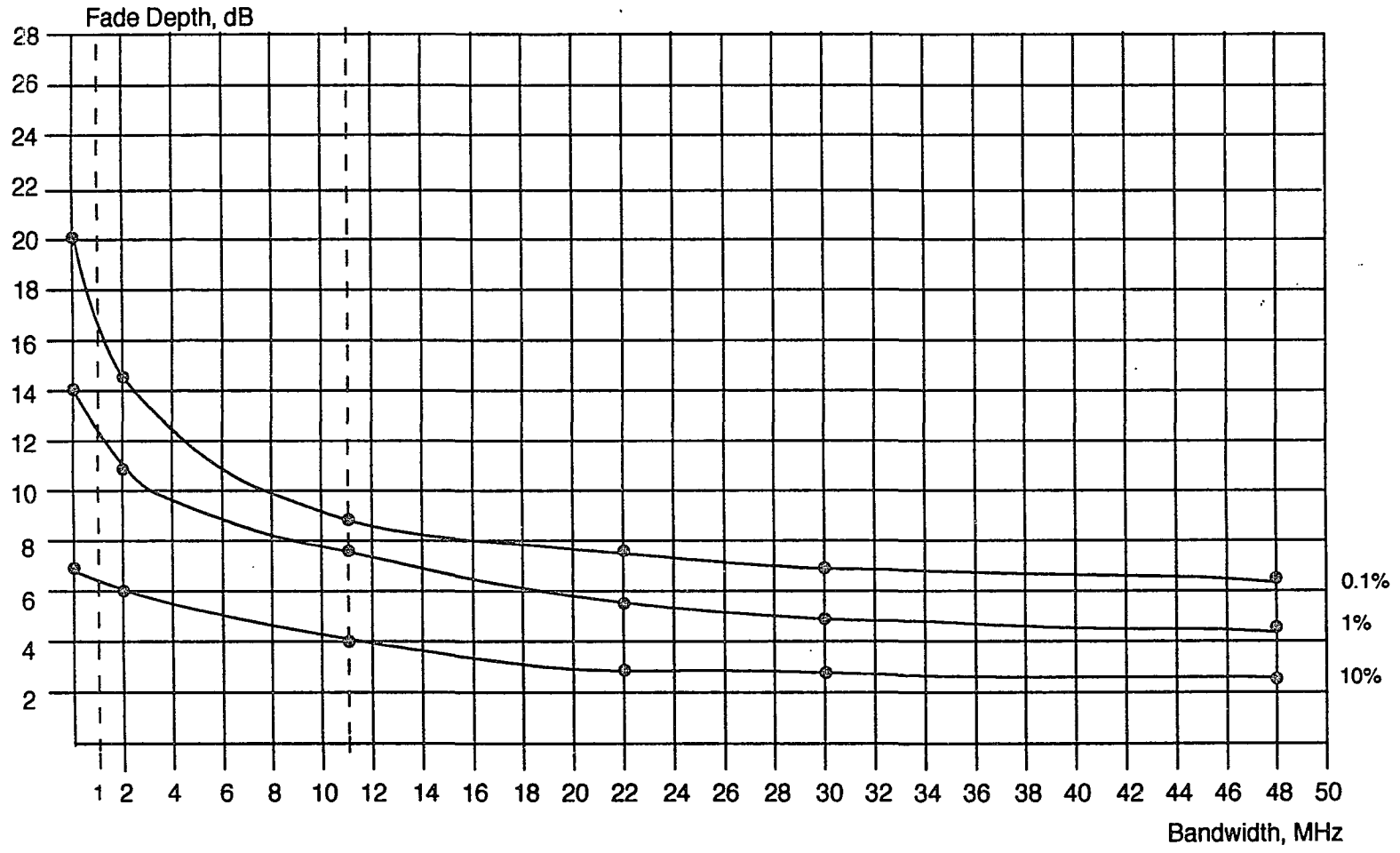


**Figure 5.4: Fade Depth in Urban Areas.**

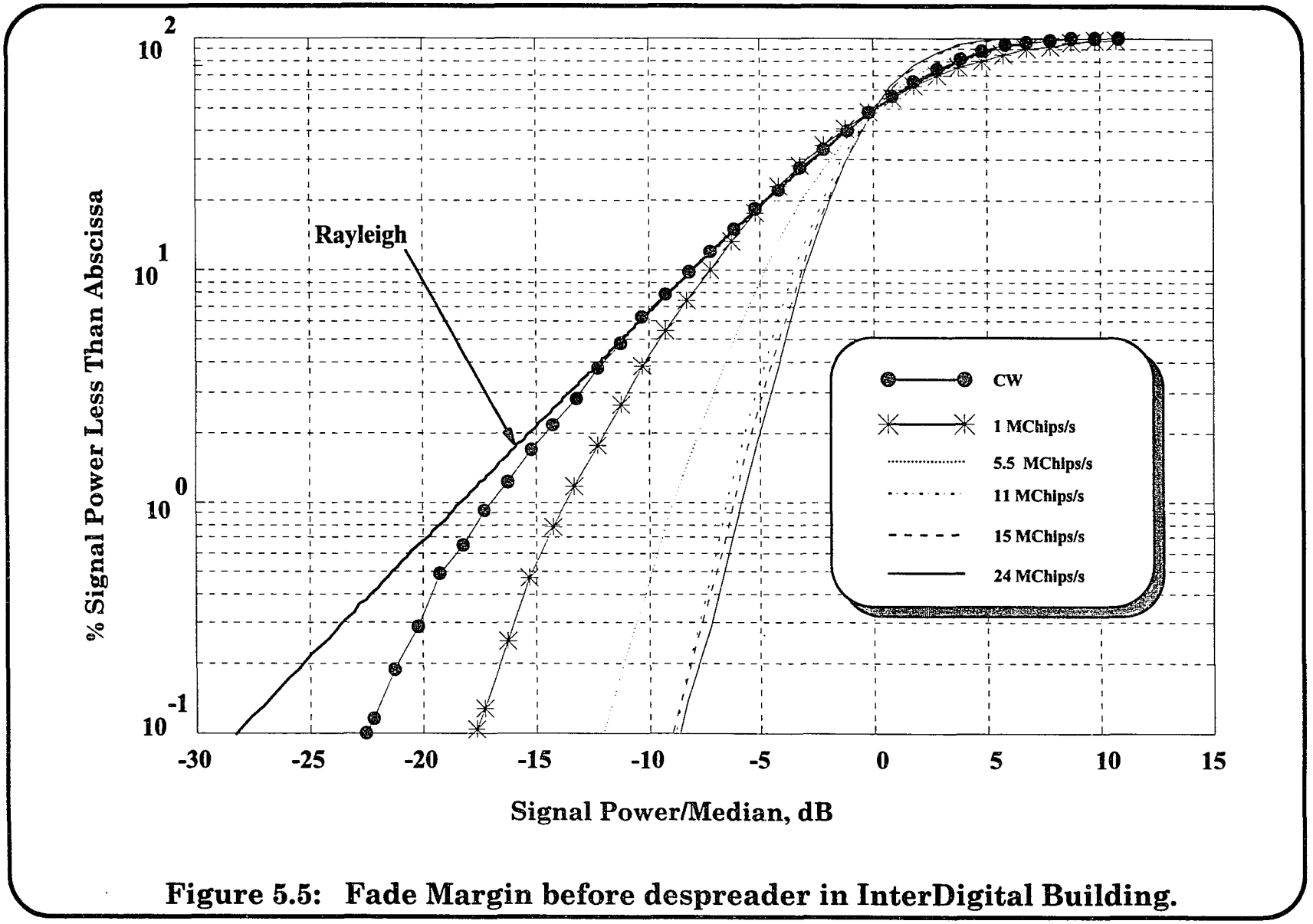


**Figure 5.5: Fade Margin before despreader in InterDigital Building.**

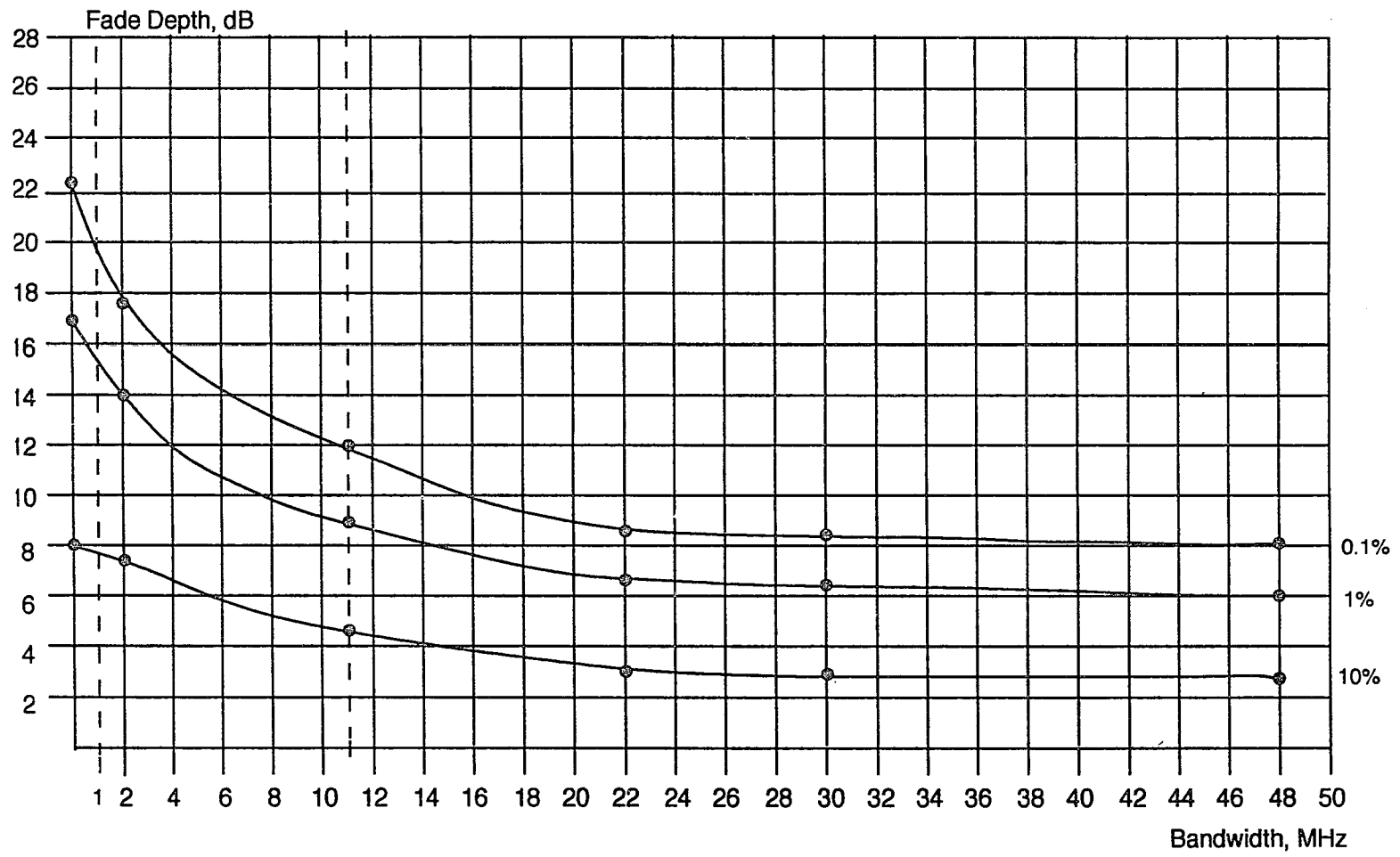


**Figure 5.6: Fade Depth before despreader in InterDigital Building.**

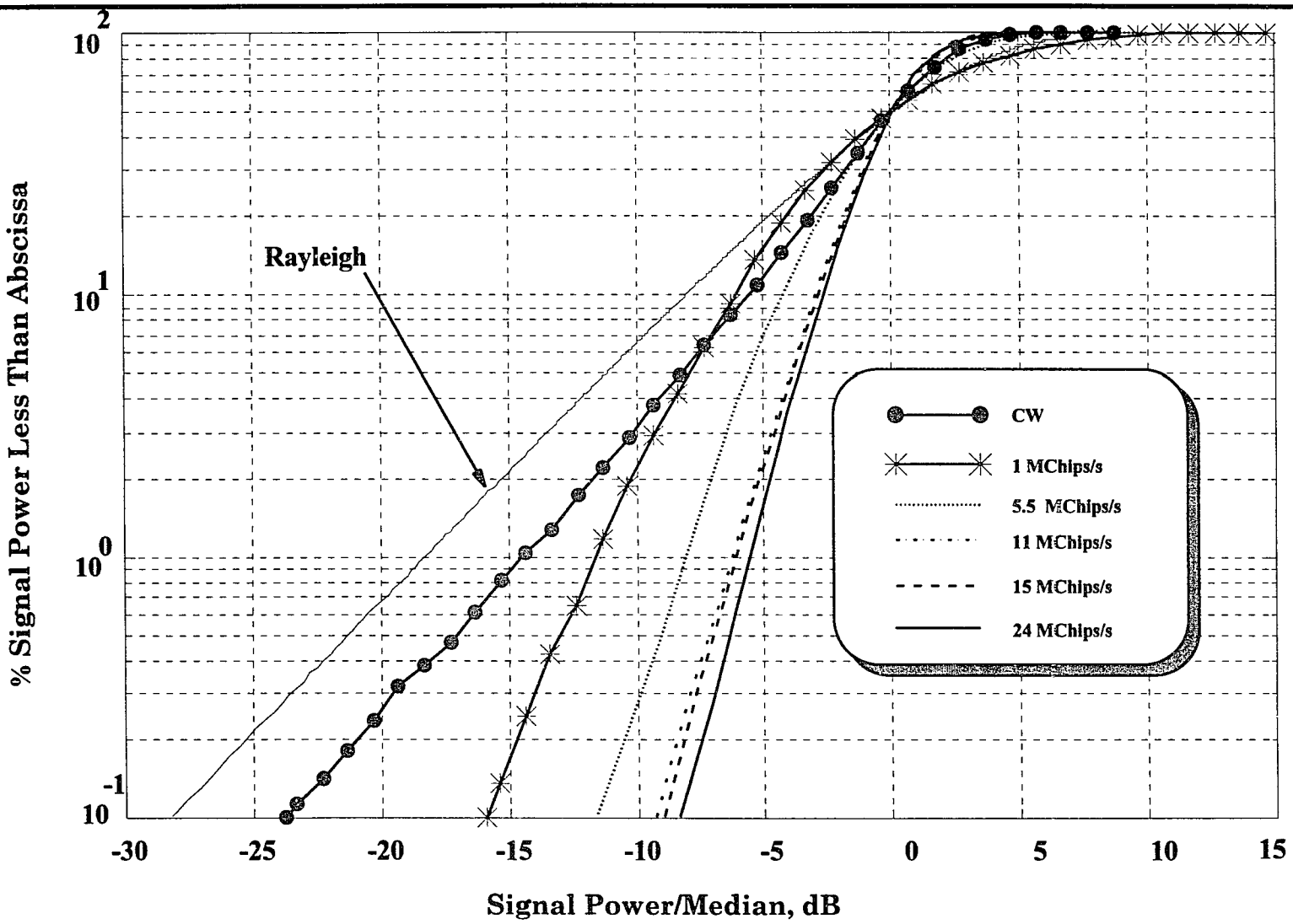


**Figure 5.7: Fade Margin before despreader in NAC Building.**

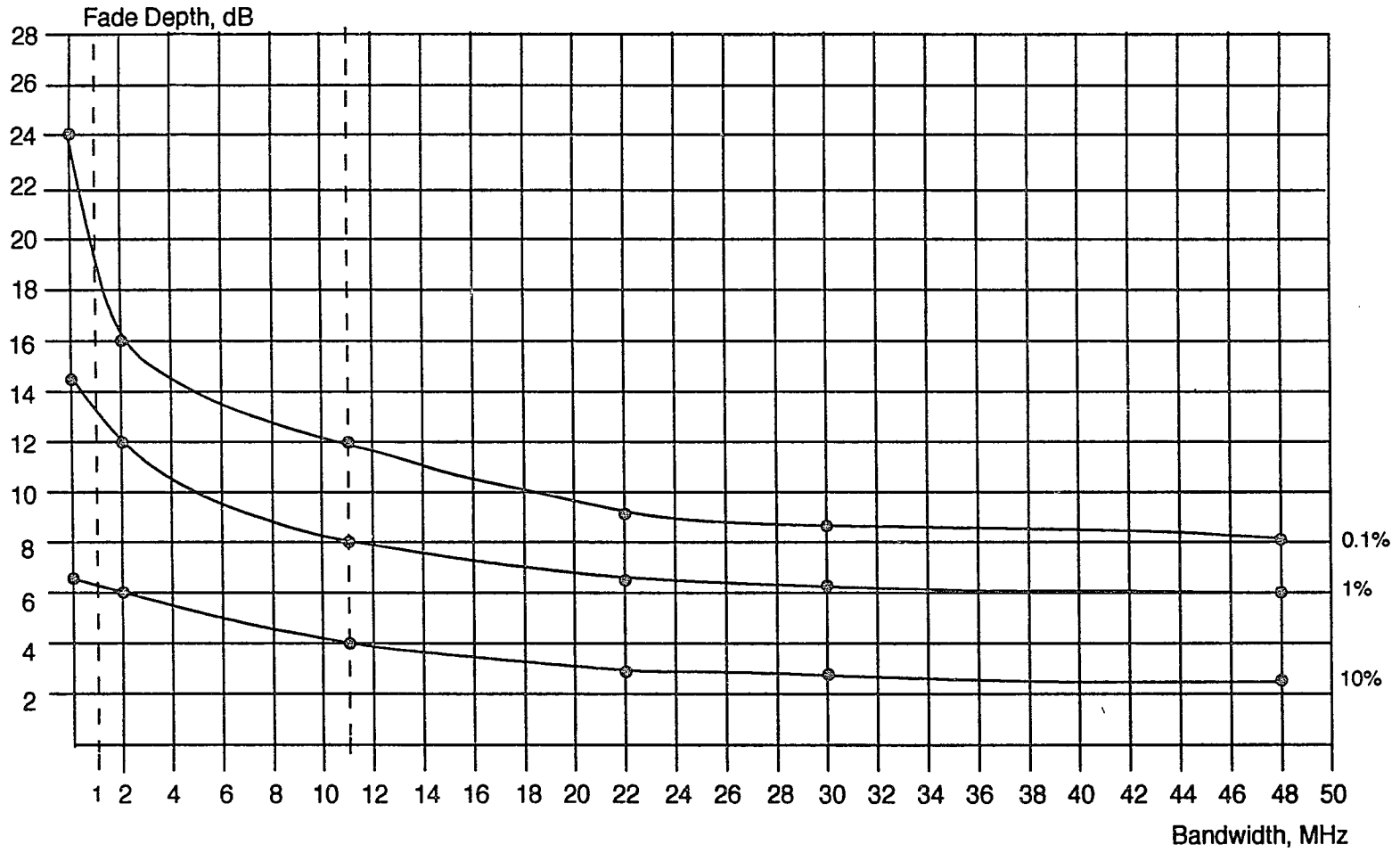


**Figure 5.8: Fade Depth before despreader in NAC Building.**

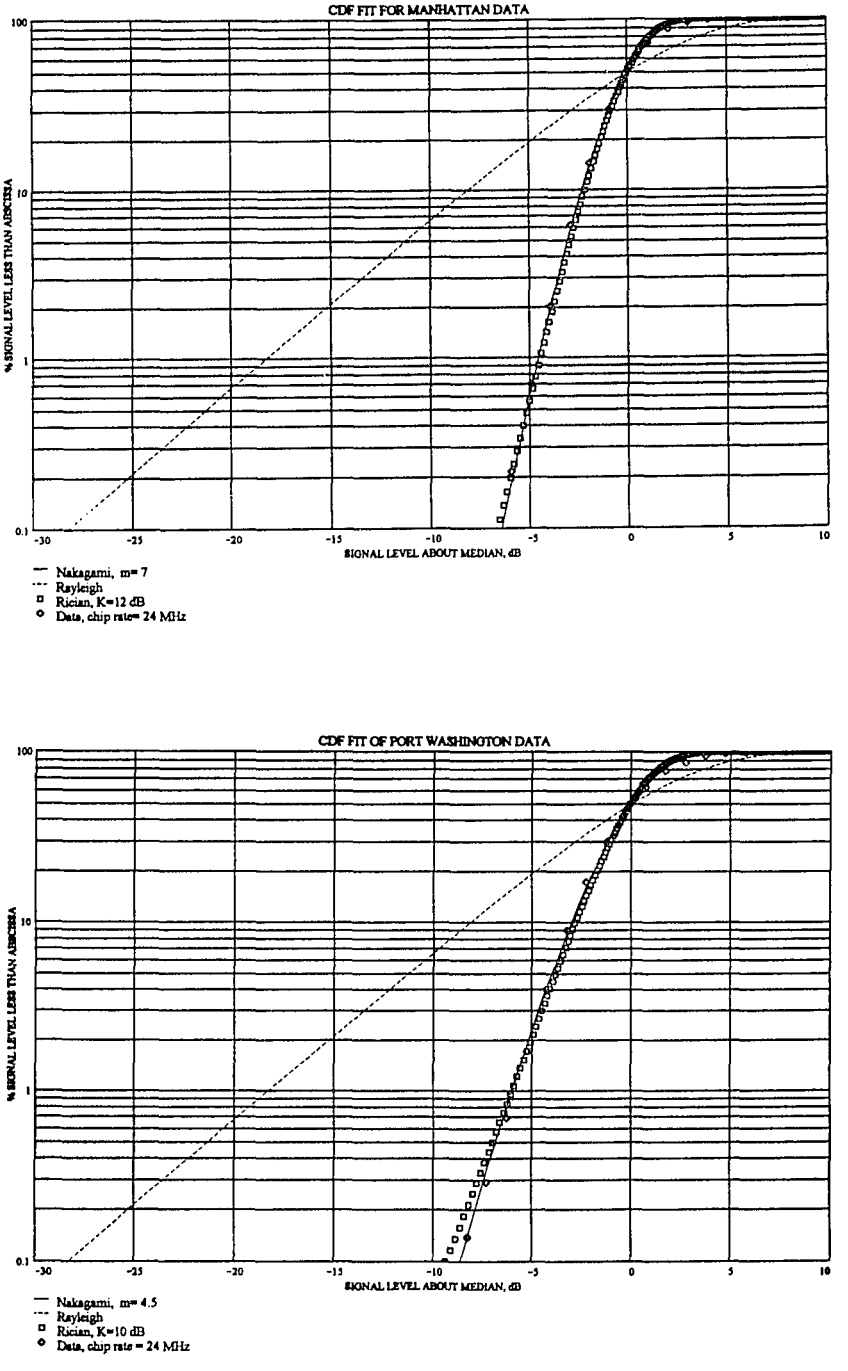


**Figure 5.9: Various distribution fit to outdoor data.**

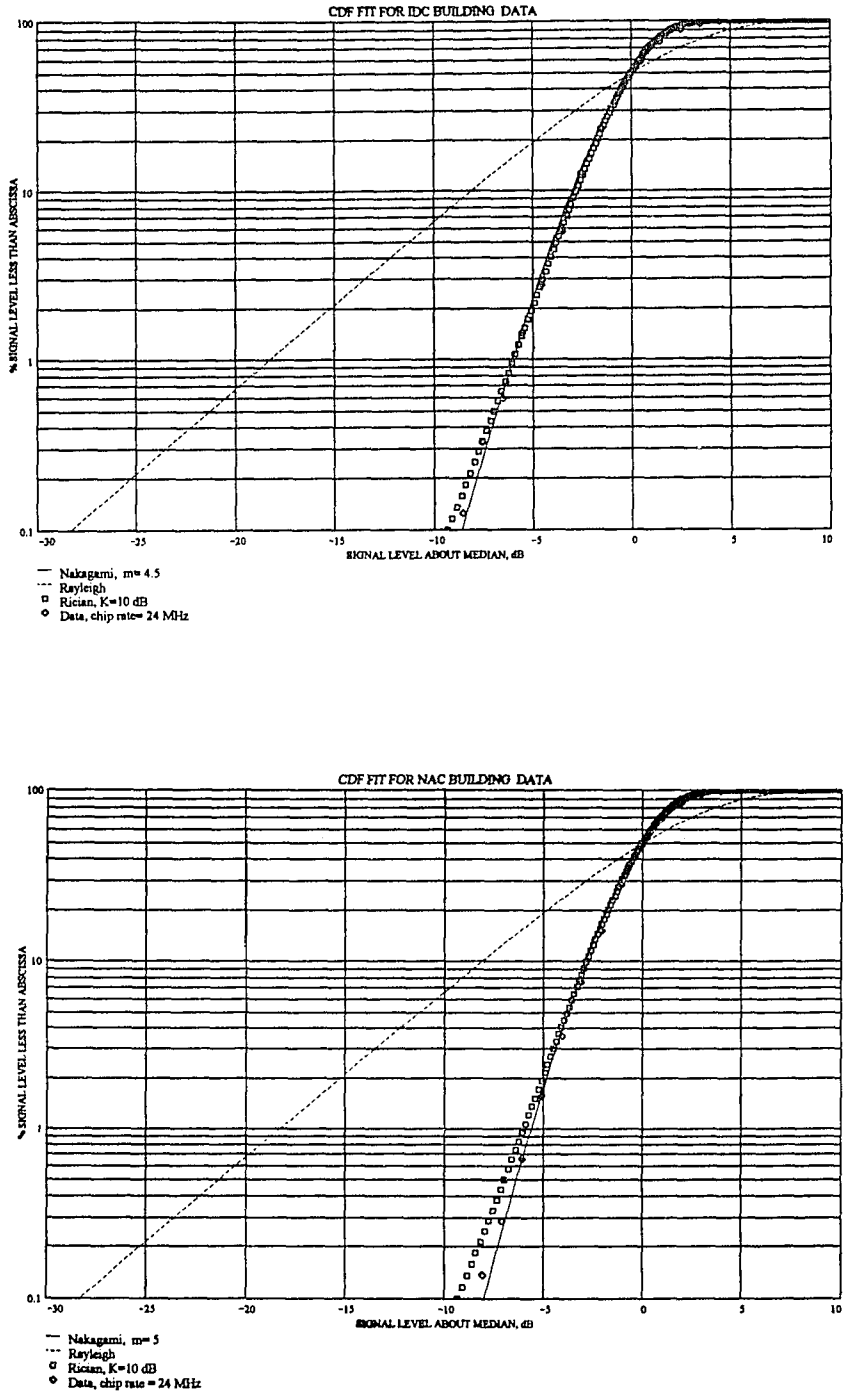


**Figure 5.10: Various distribution fit to indoor data.**

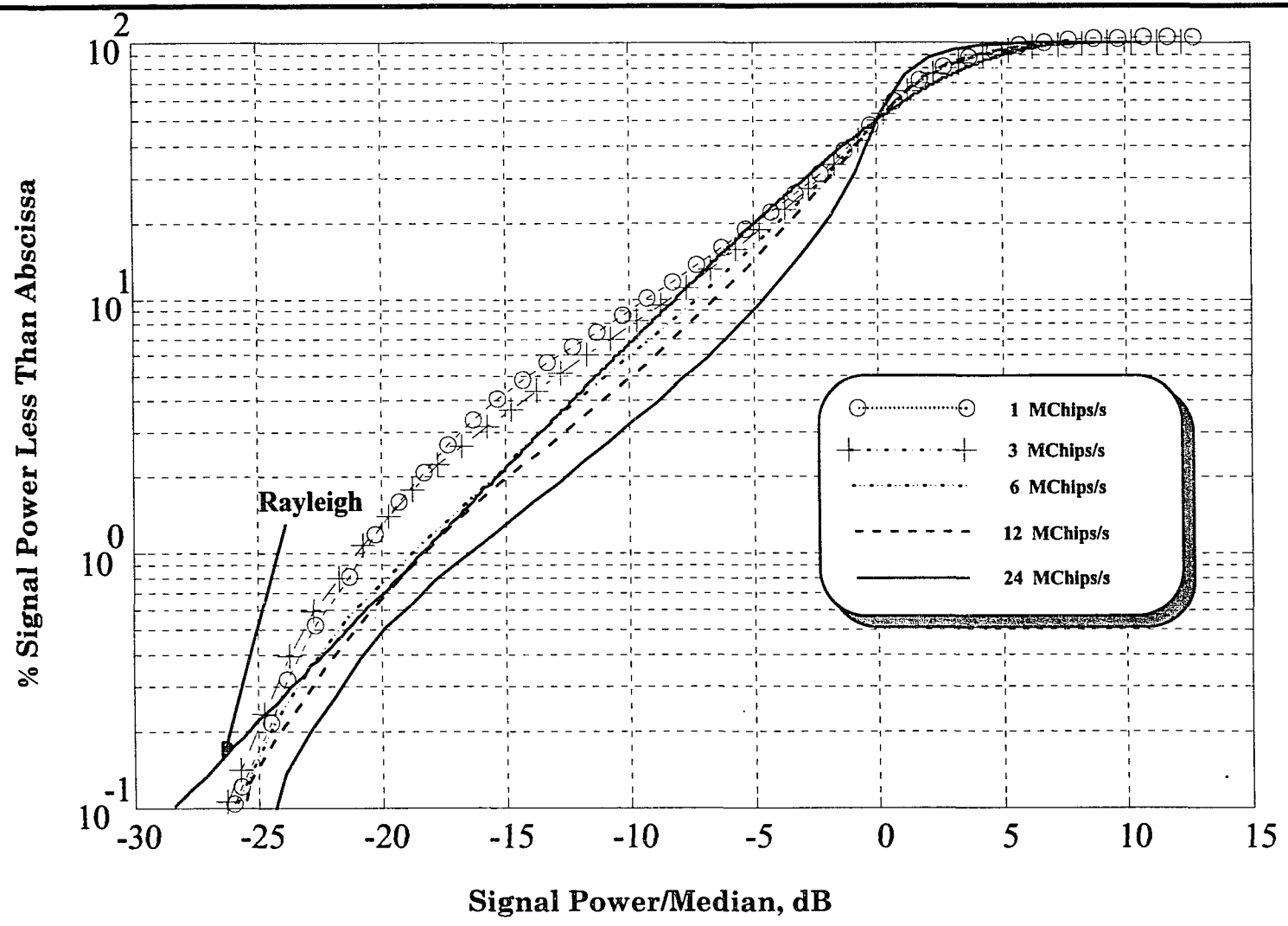


**Figure 5.11: Fade Margin after despreader in Port Washington.**

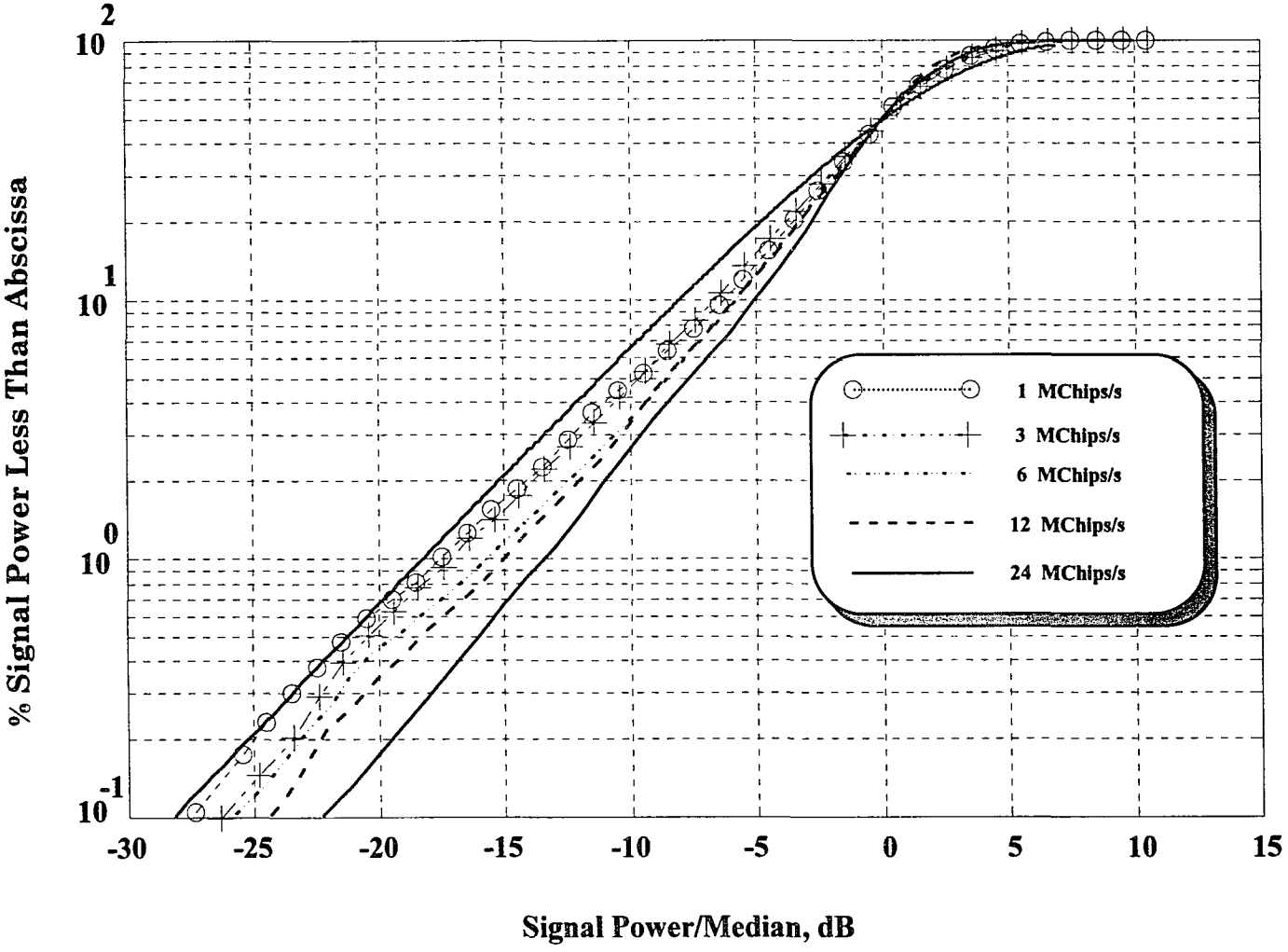


**Figure 5.12: Fade Margin after despreader in InterDigital Building.**

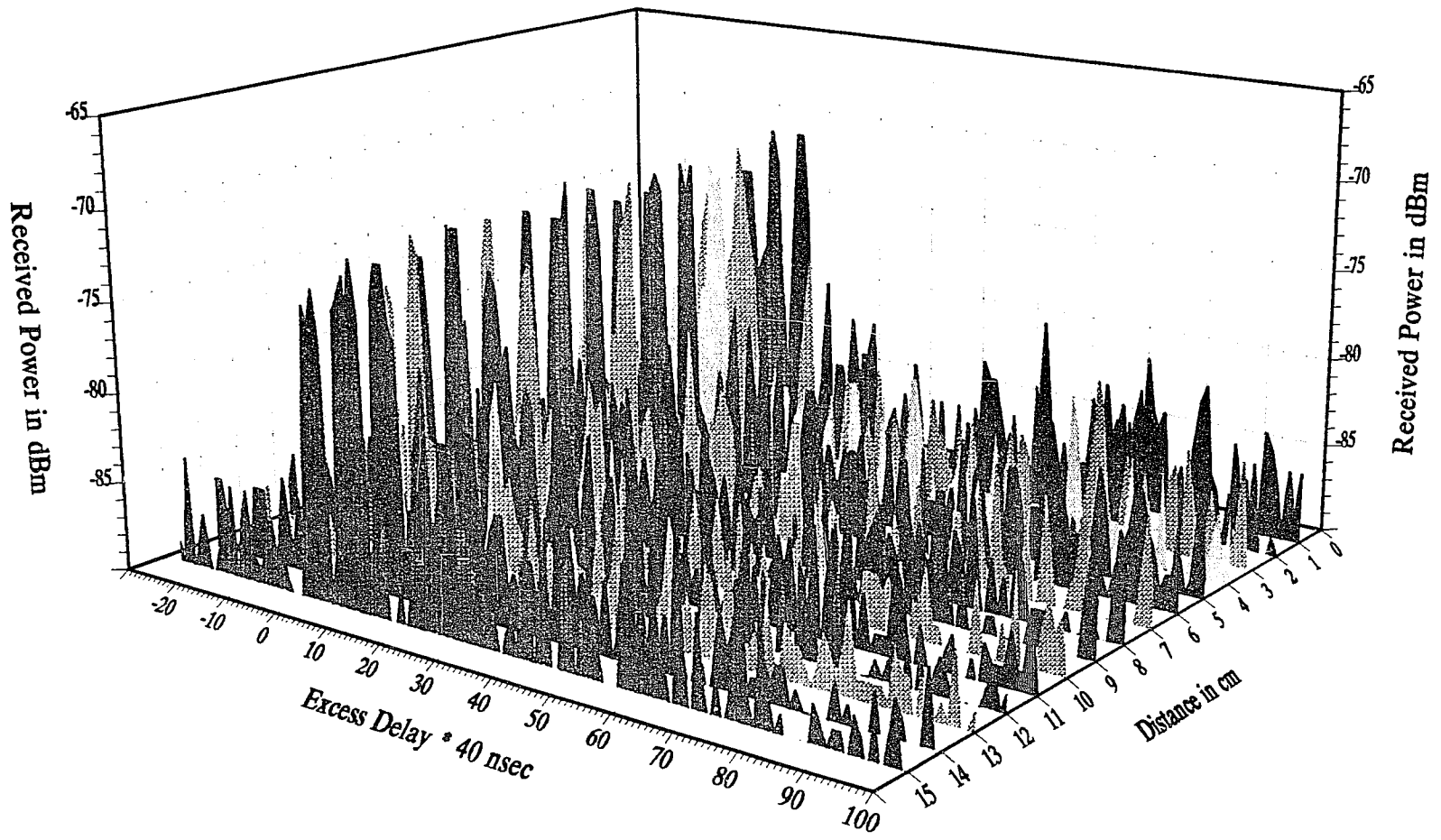


**Figure 5.13: Average Delay Power Spectrum seen at 6th ave. and 23rd st. (omni-antenna).**

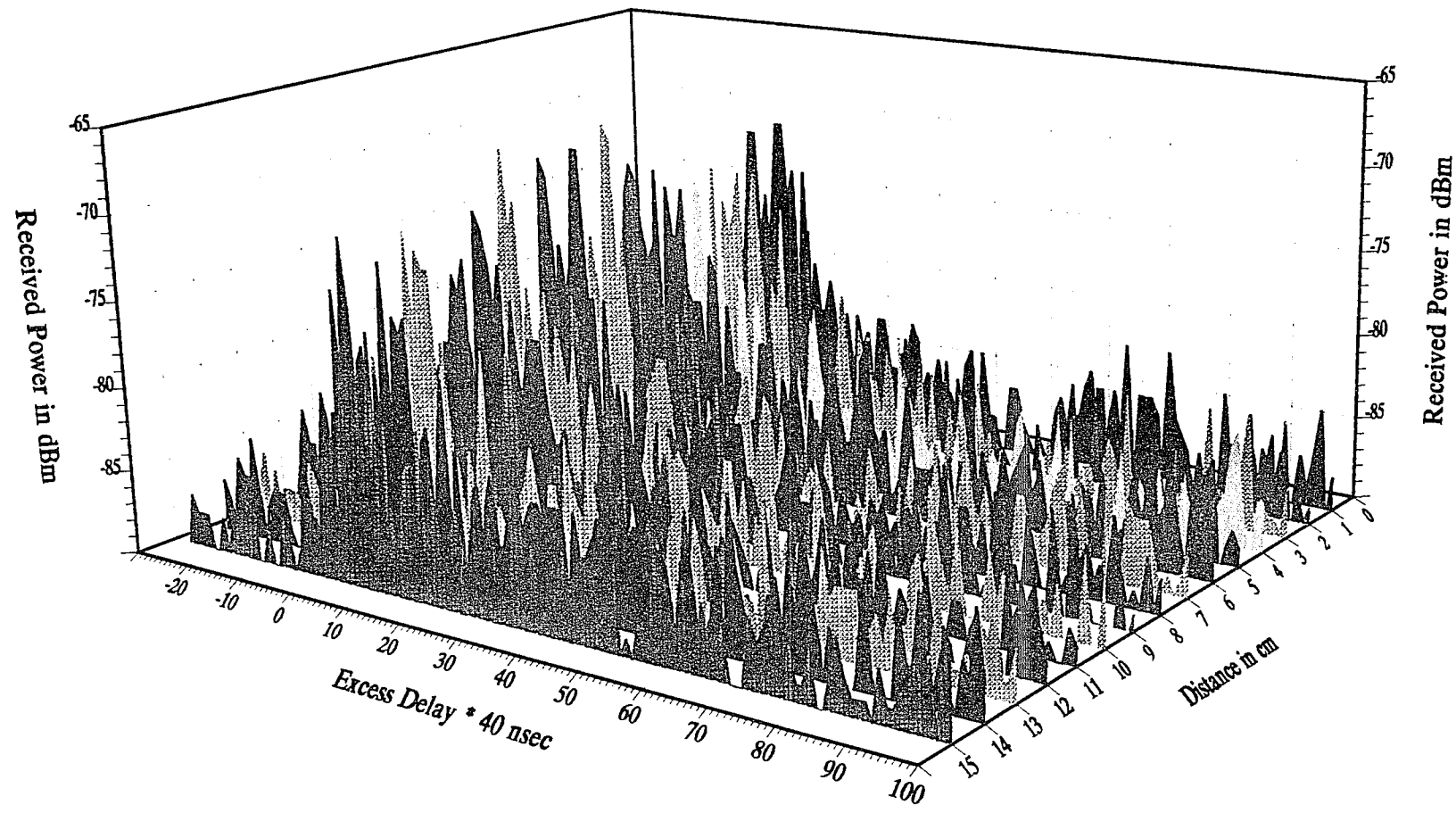


**Figure 5.14: Average Delay Power Spectrum seen at 23rd st between 6th and 7th ave. (omni-antenna).**

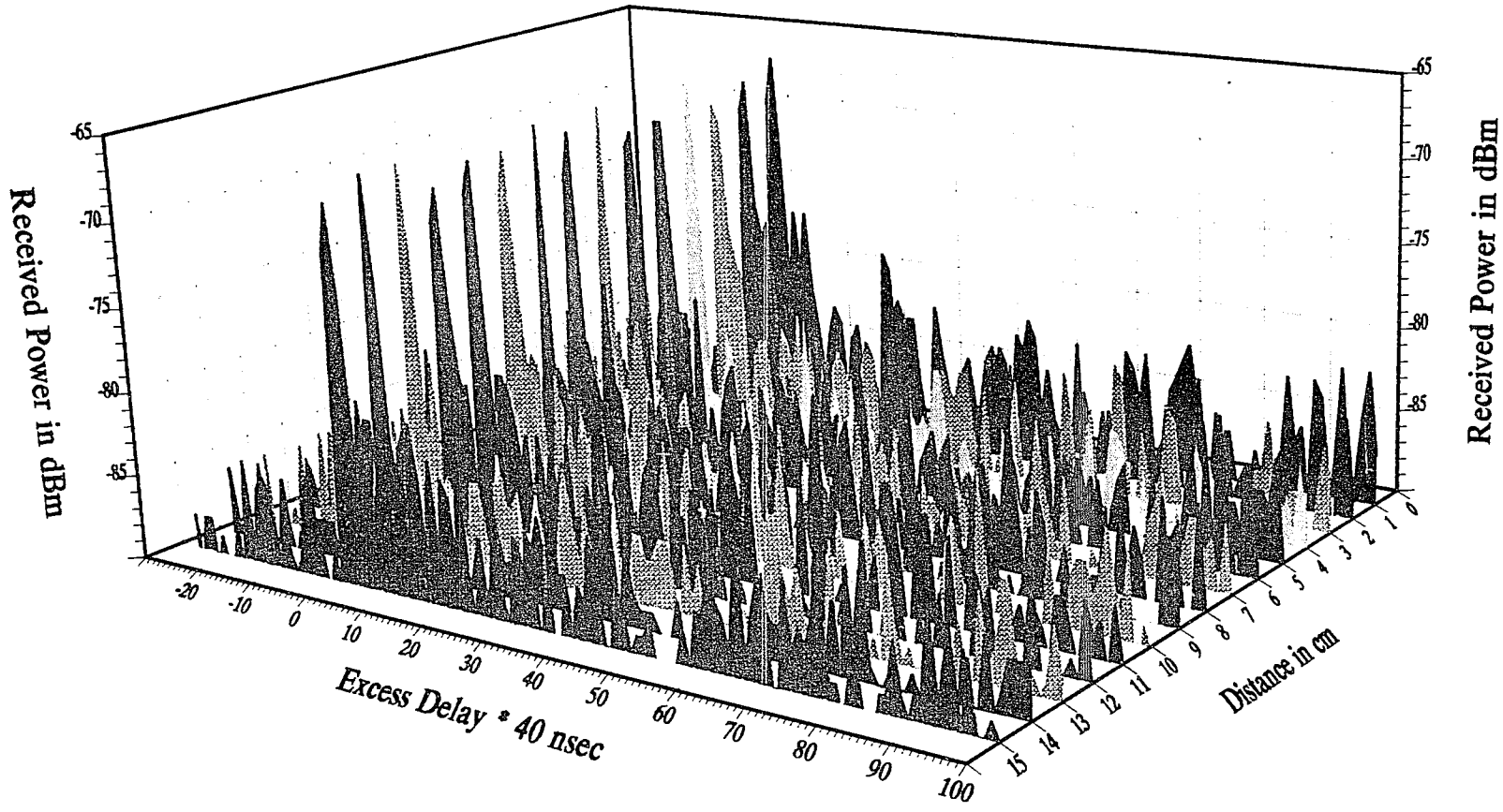


**Figure 5.15: Average Delay Power Spectrum seen at 6th ave. and 23rd st. (Directional -antenna).**

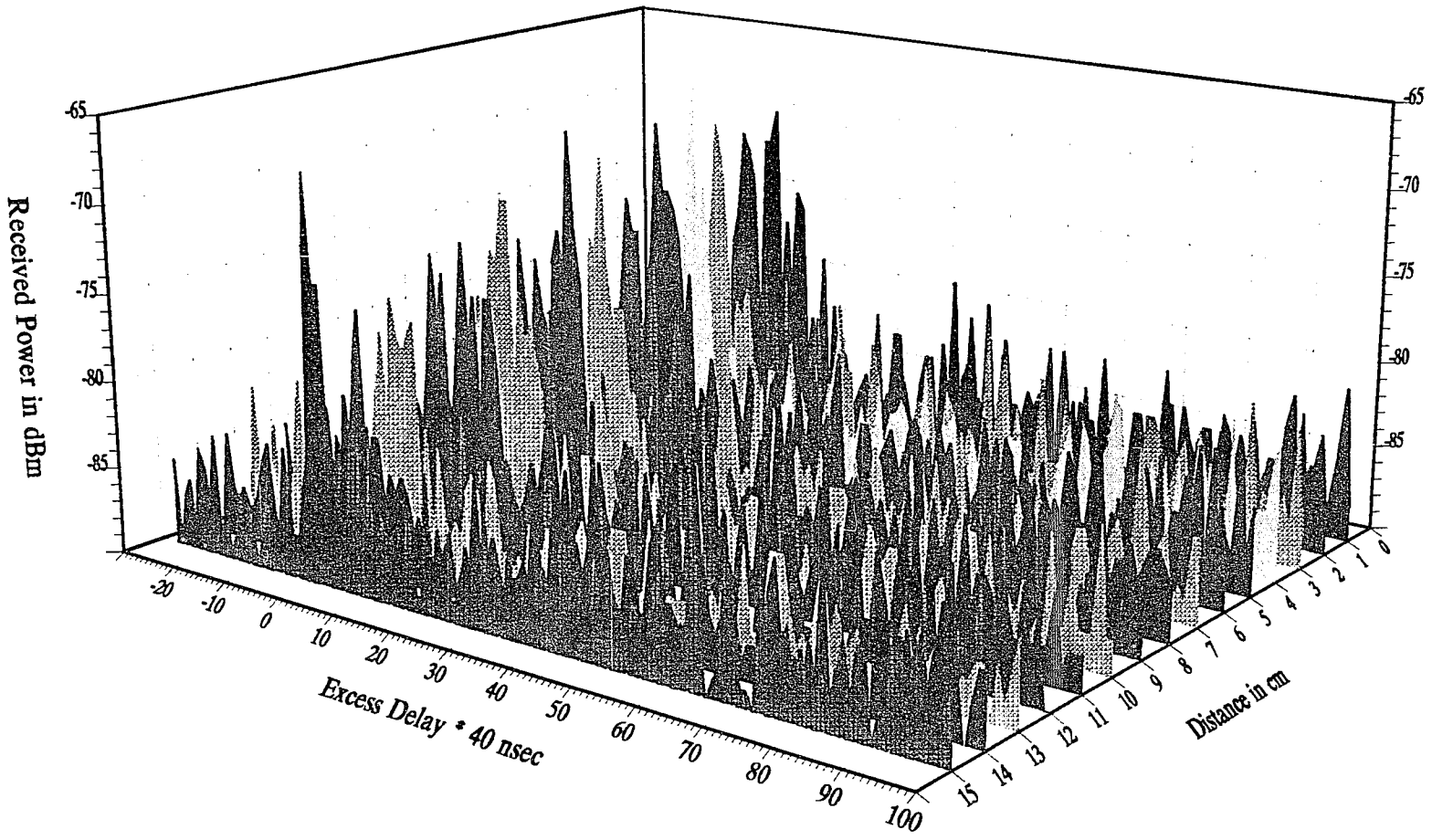


**Figure 5.16: Average Delay Power Spectrum seen at 23rd st between 6th and 7th ave. (Directional-antenna).**

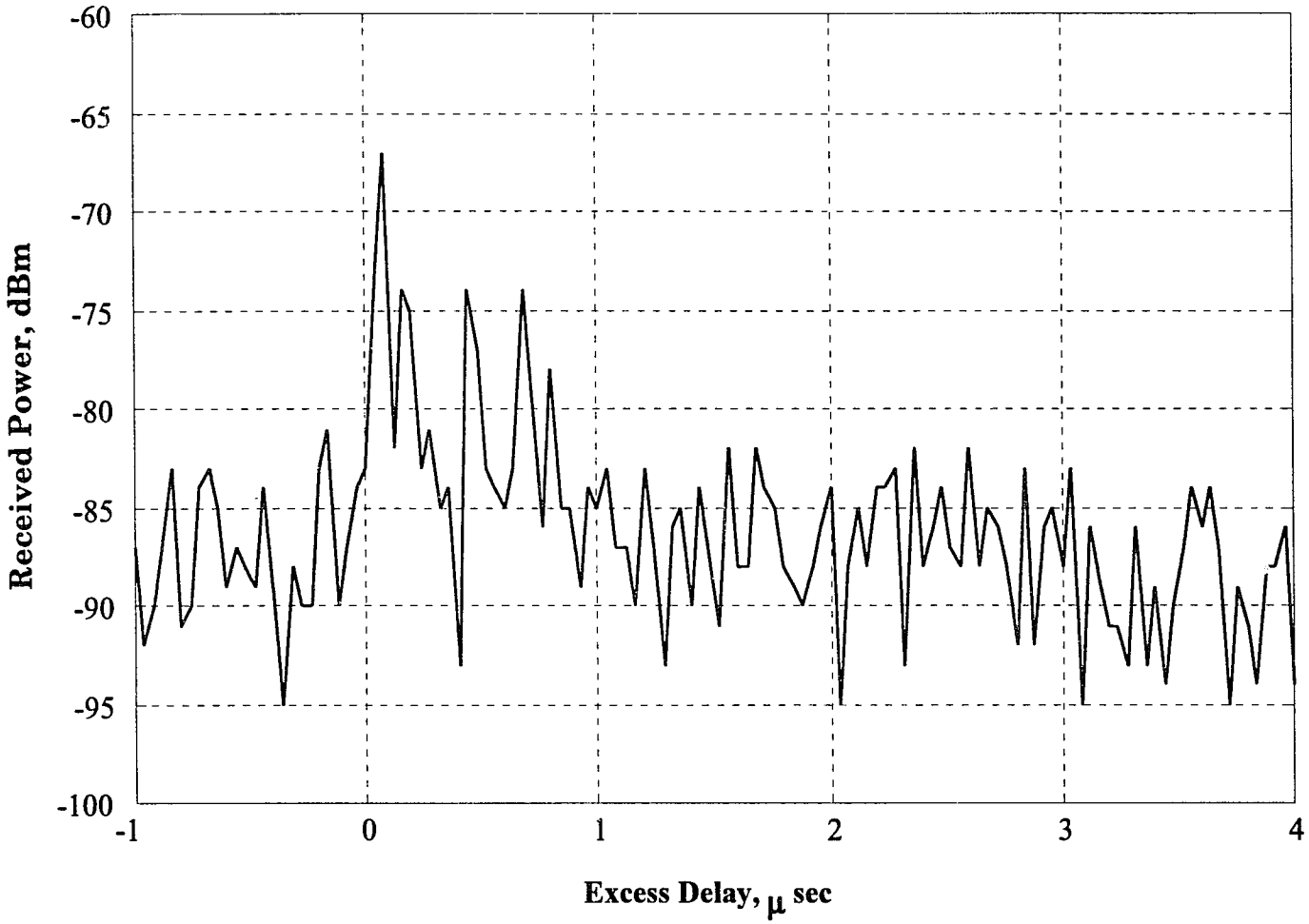


**Figure 5.17: Multipath returns seen at the corner of 7th ave. and 24th st..**

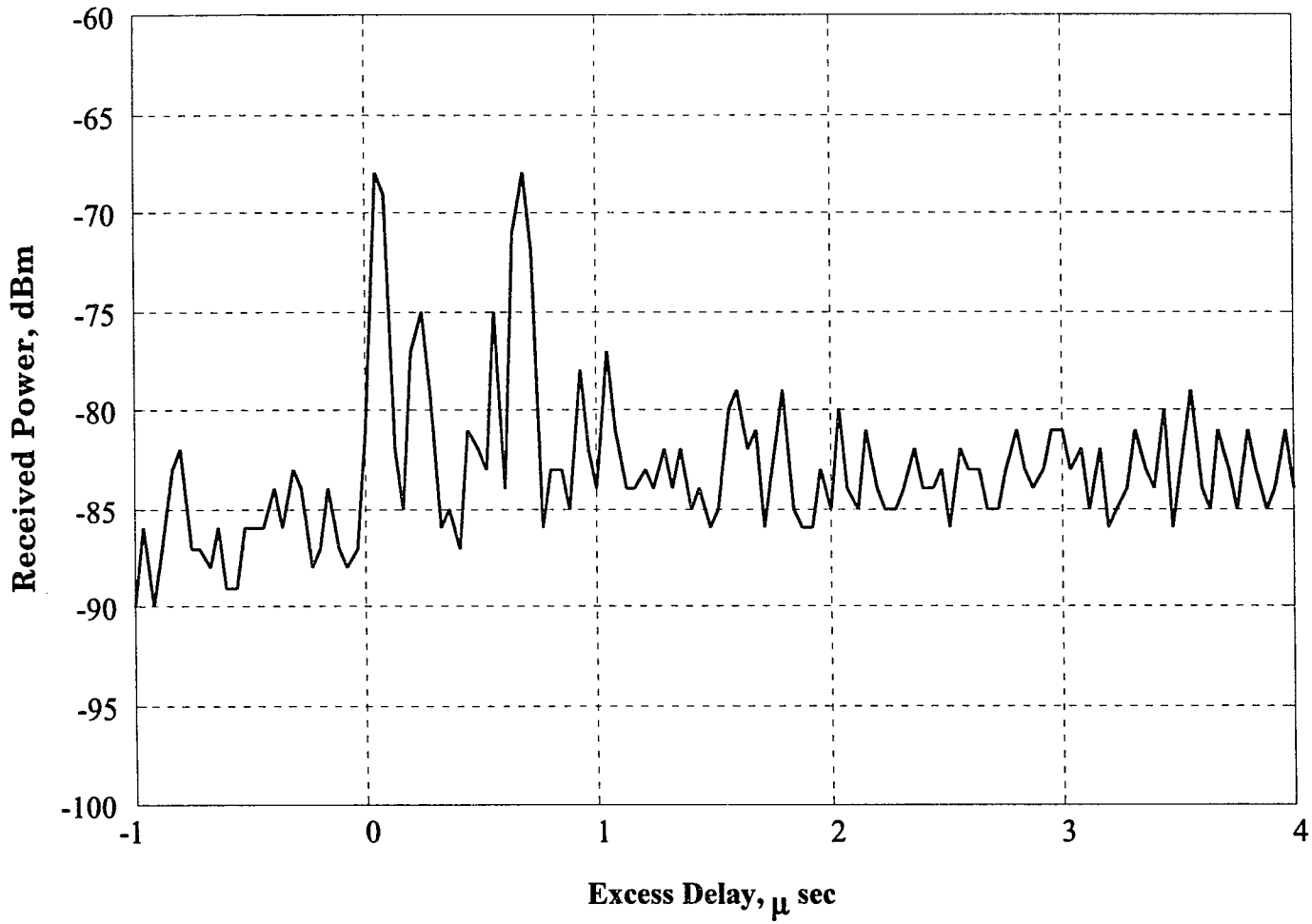


**Figure 5.18: Multipath returns seen at the corner of 8th ave and 26th st.**

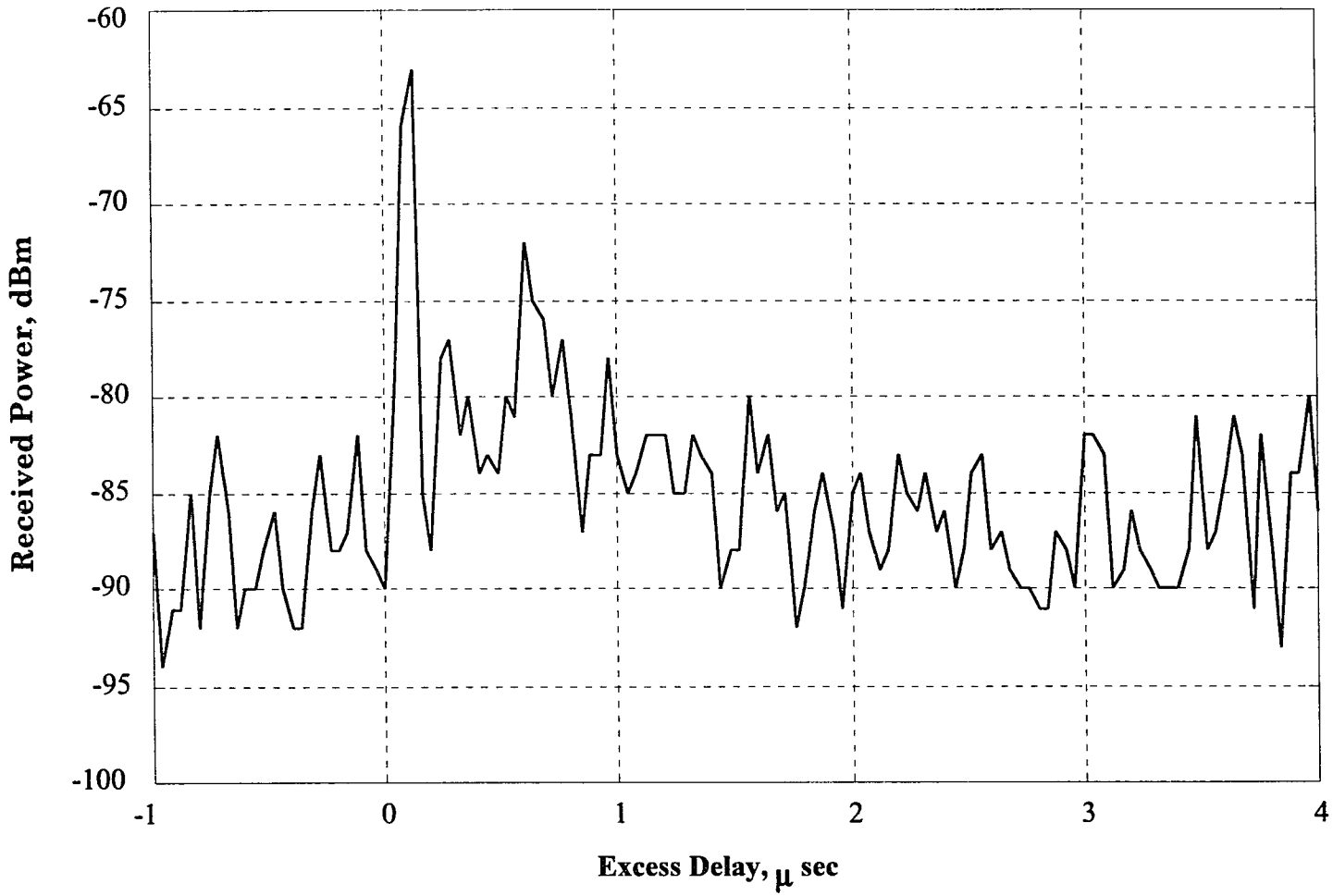


**Figure 5.19: Multipath returns seen at the corner of 7th ave and 25th st.**

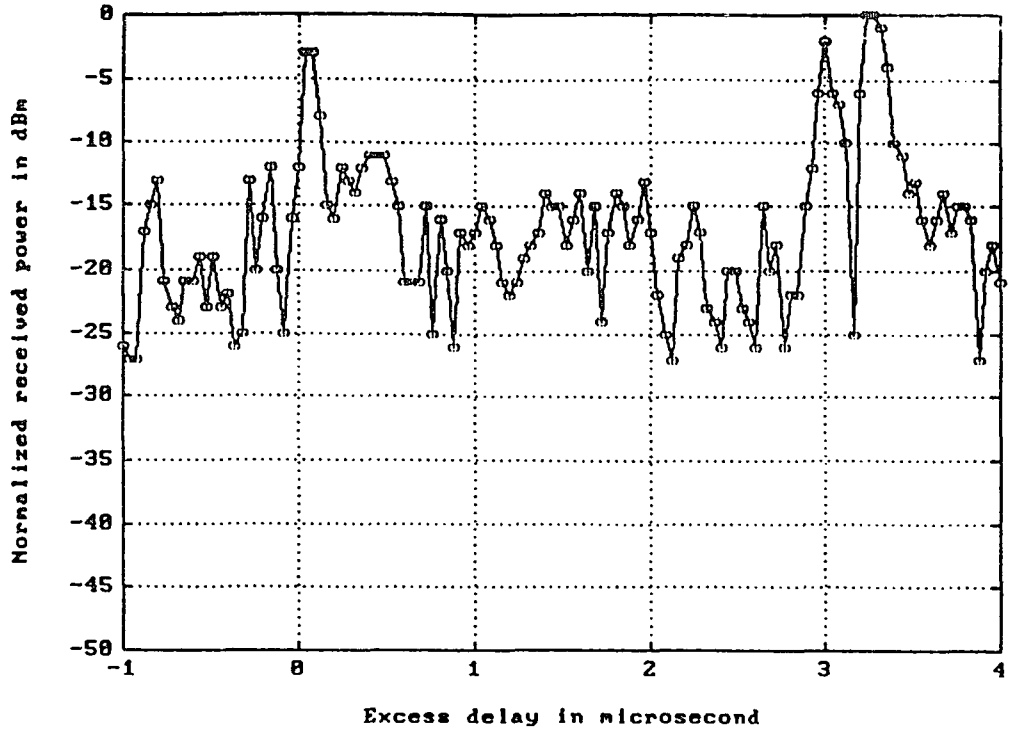


**Figure 5.20: Delay Power Spectrum at site F, Chip rate = 24 Mchips/s.**

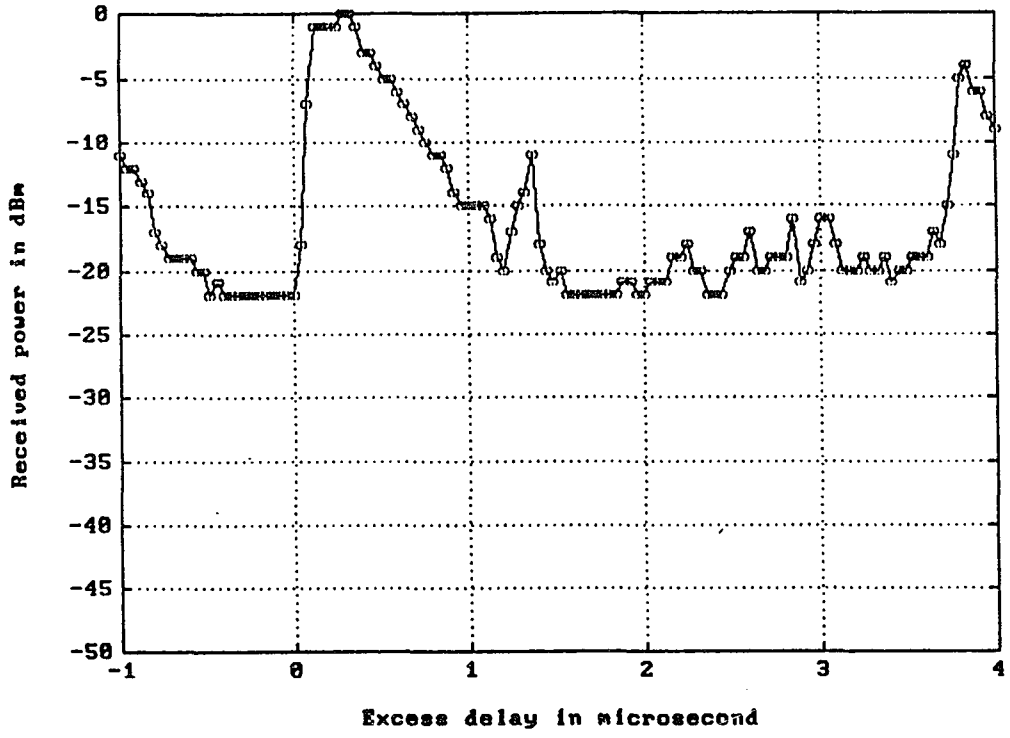


**Figure 5.21: Delay Power Spectrum at site F, Chip rate = 8 Mchips/s.**

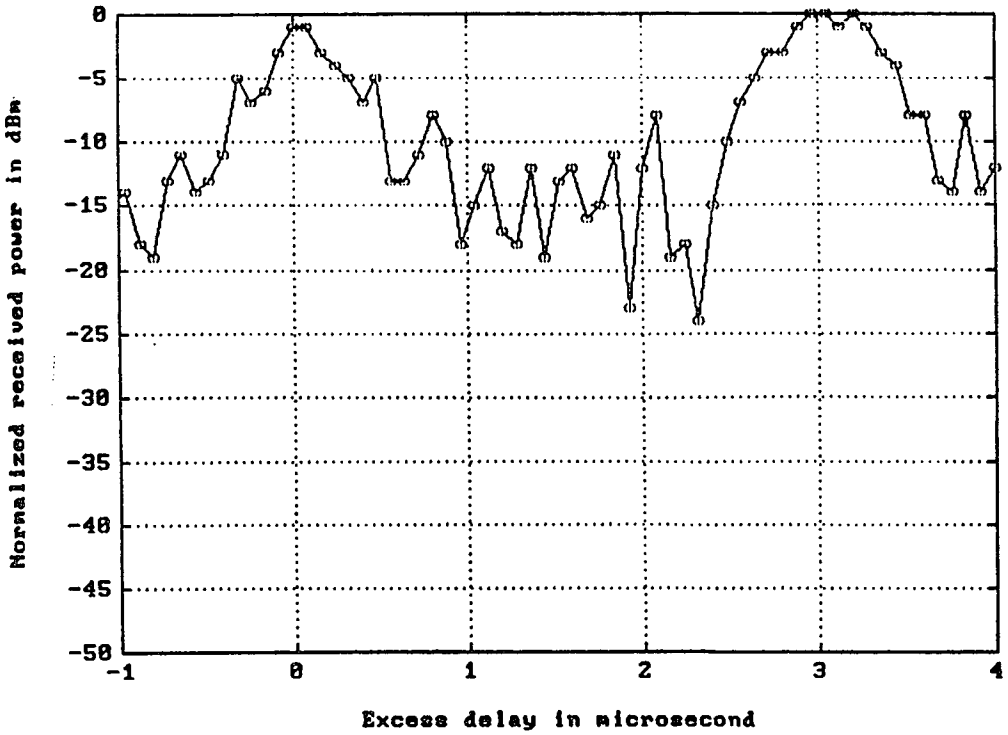


**Figure 5.22: Delay Power Spectrum at site F, Chip rate = 1 Mchips/s.**

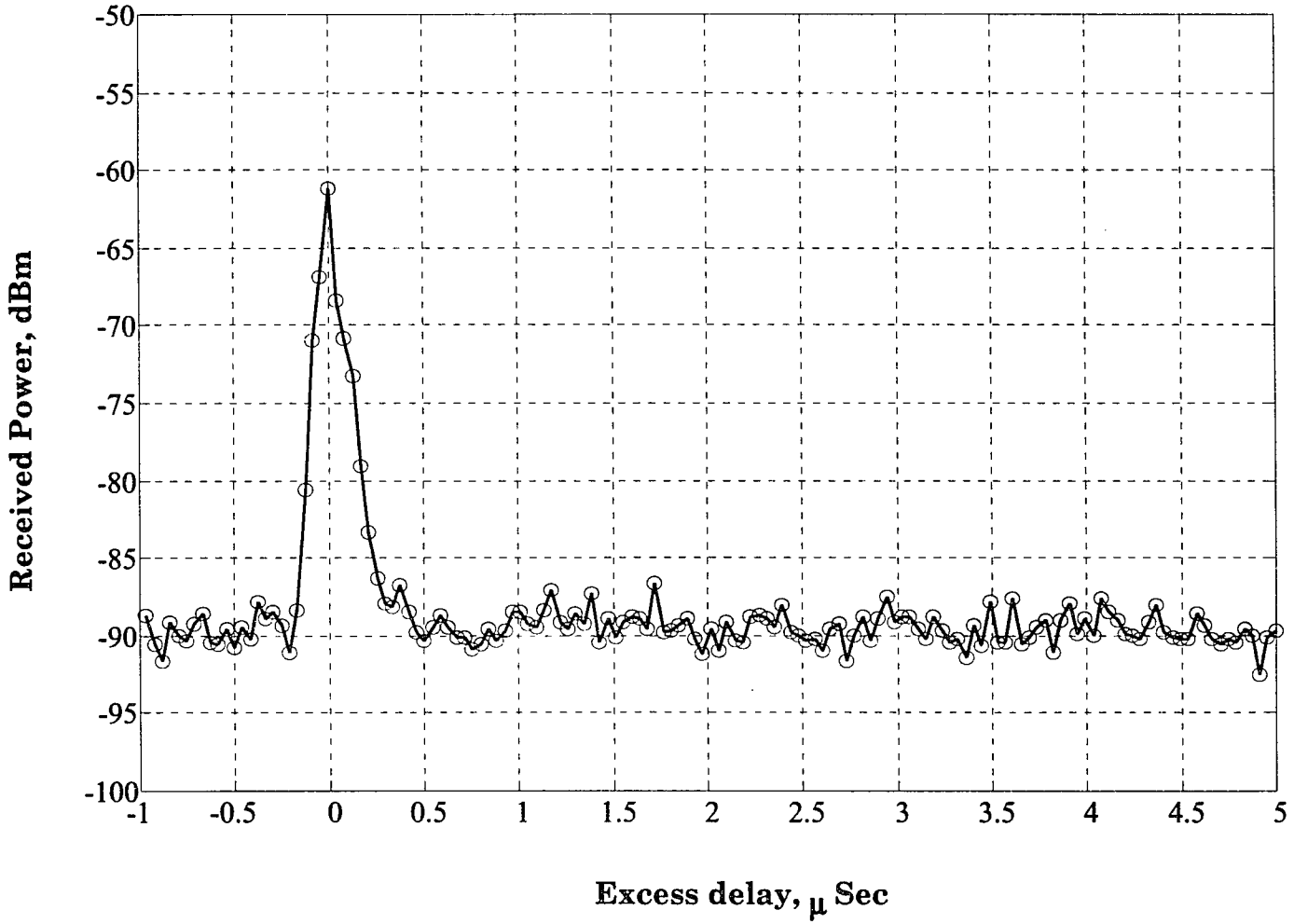


**Figure 5.23: Typical Delay Power Spectrum observed at site A, Chip rate = 24 Mchips/s.**

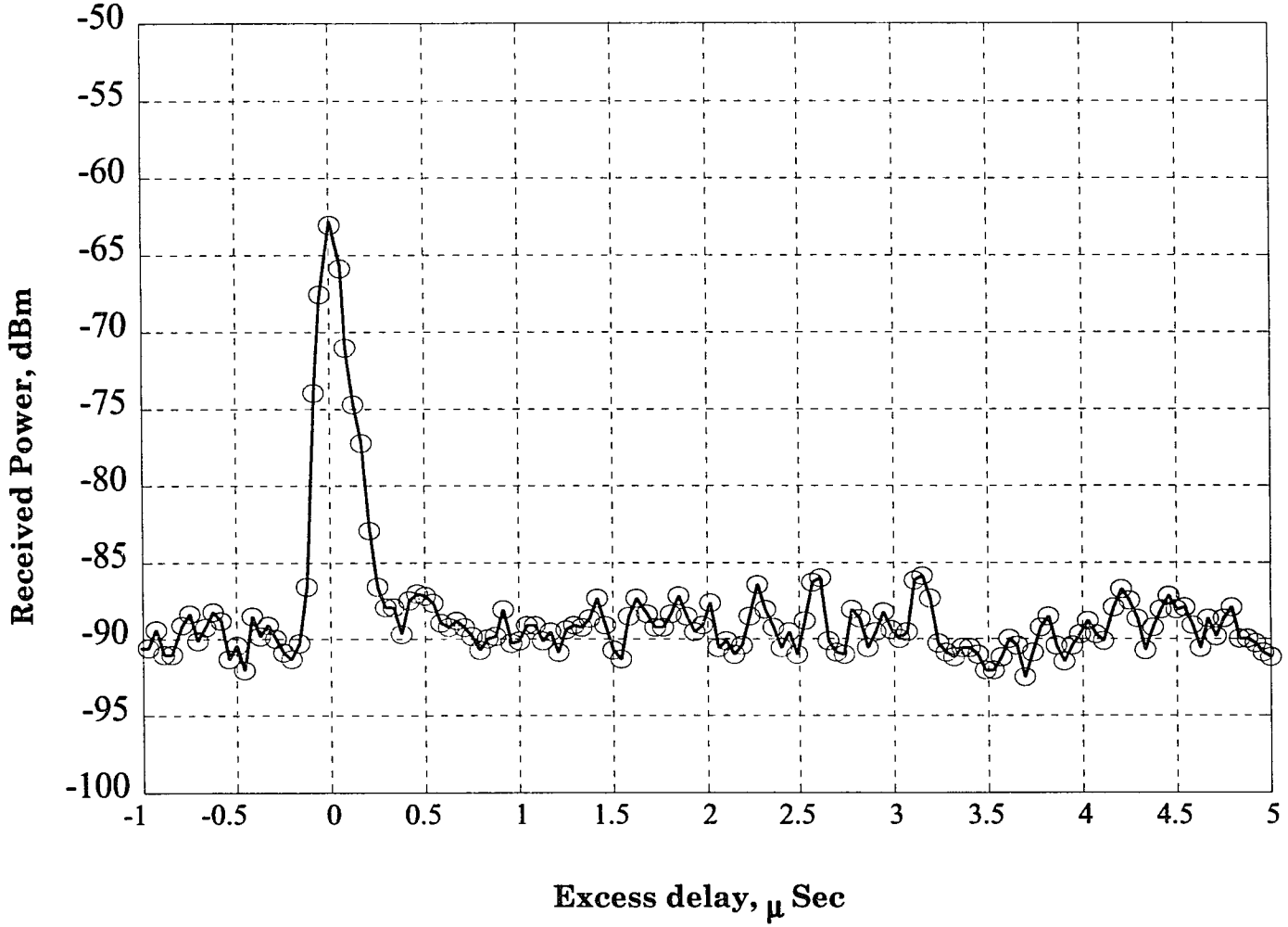


**Figure 5.24: Typical Delay Power Spectrum observed at site A, Chip rate = 12 Mchips/s.**

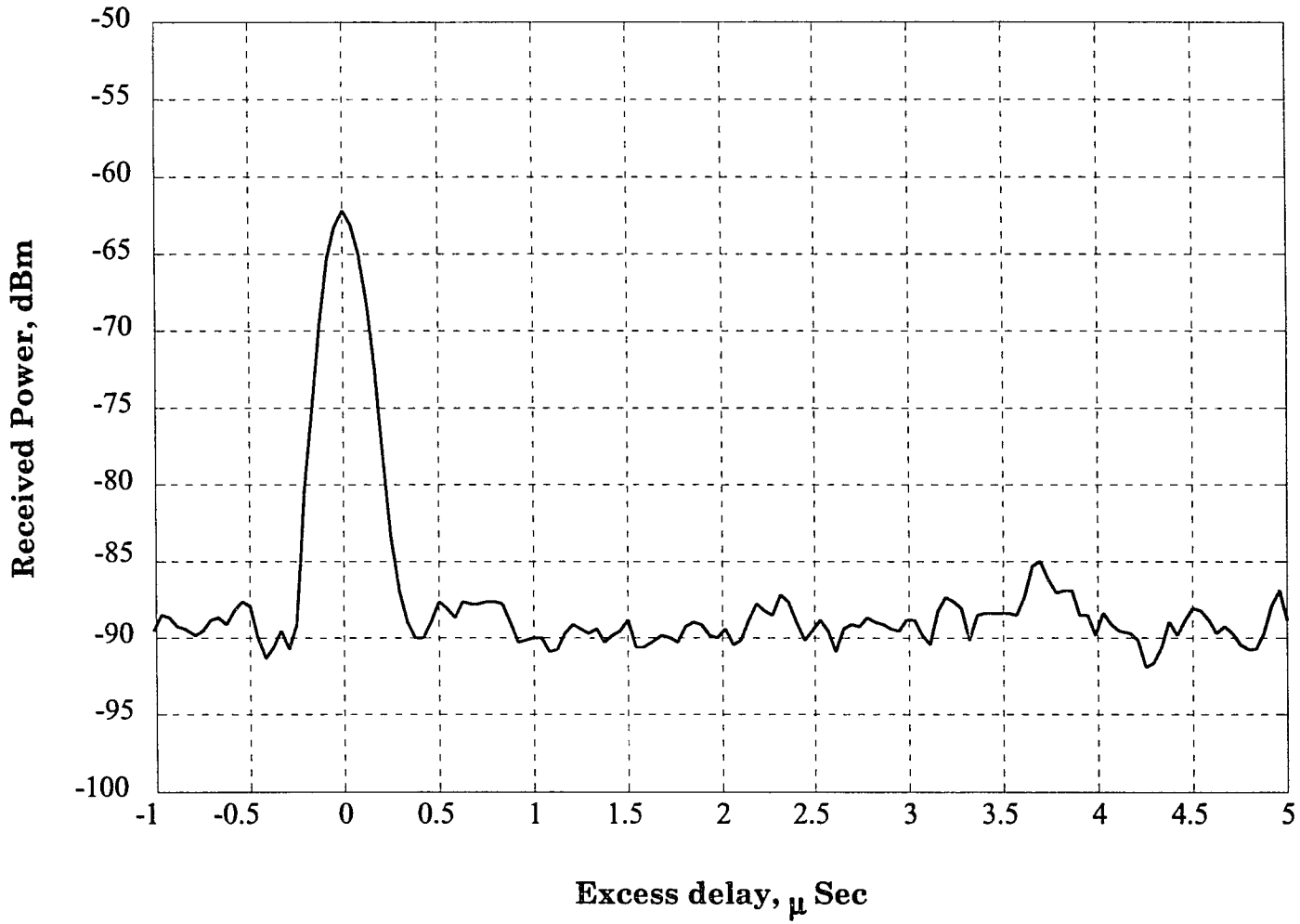


**Figure 5.25: Typical Delay Power Spectrum observed at site A, Chip rate = 6 Mchips/s.**

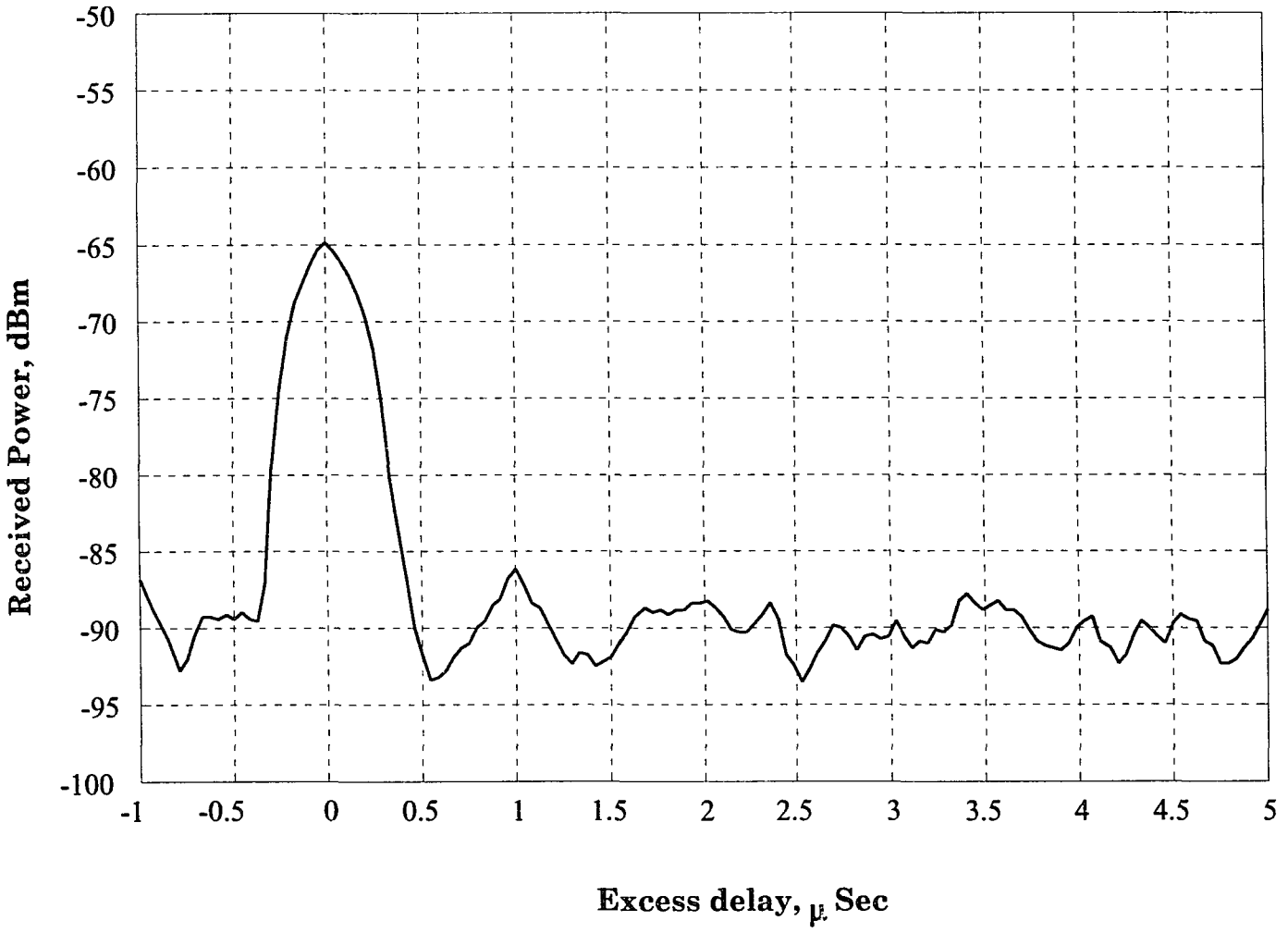


**Figure 5.26: Typical Delay Power Spectrum observed at site A, Chip rate = 3 Mchips/s.**

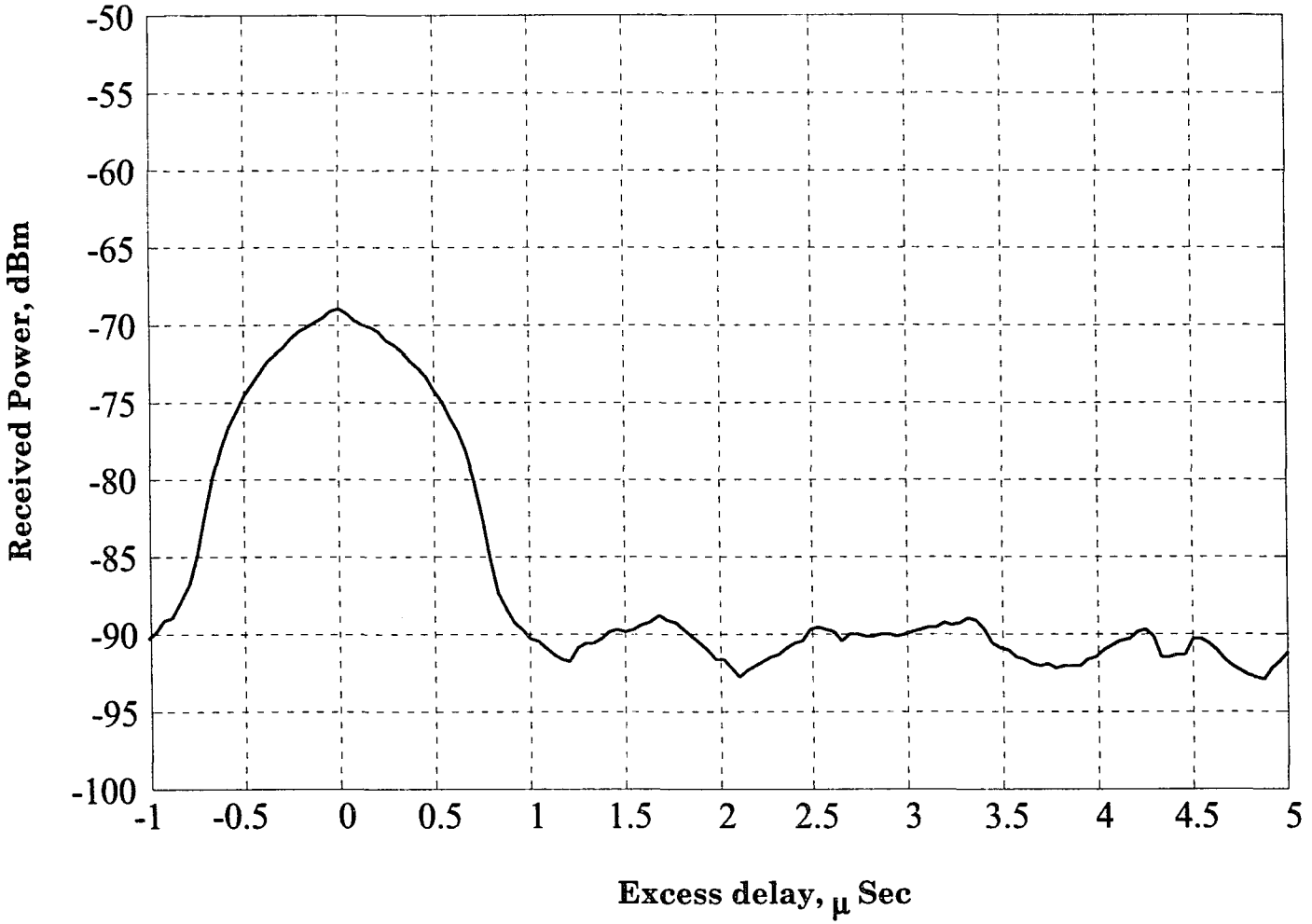


**Figure 5.27: Typical Delay Power Spectrum observed at site A, Chip rate = 1 Mchips/s.**

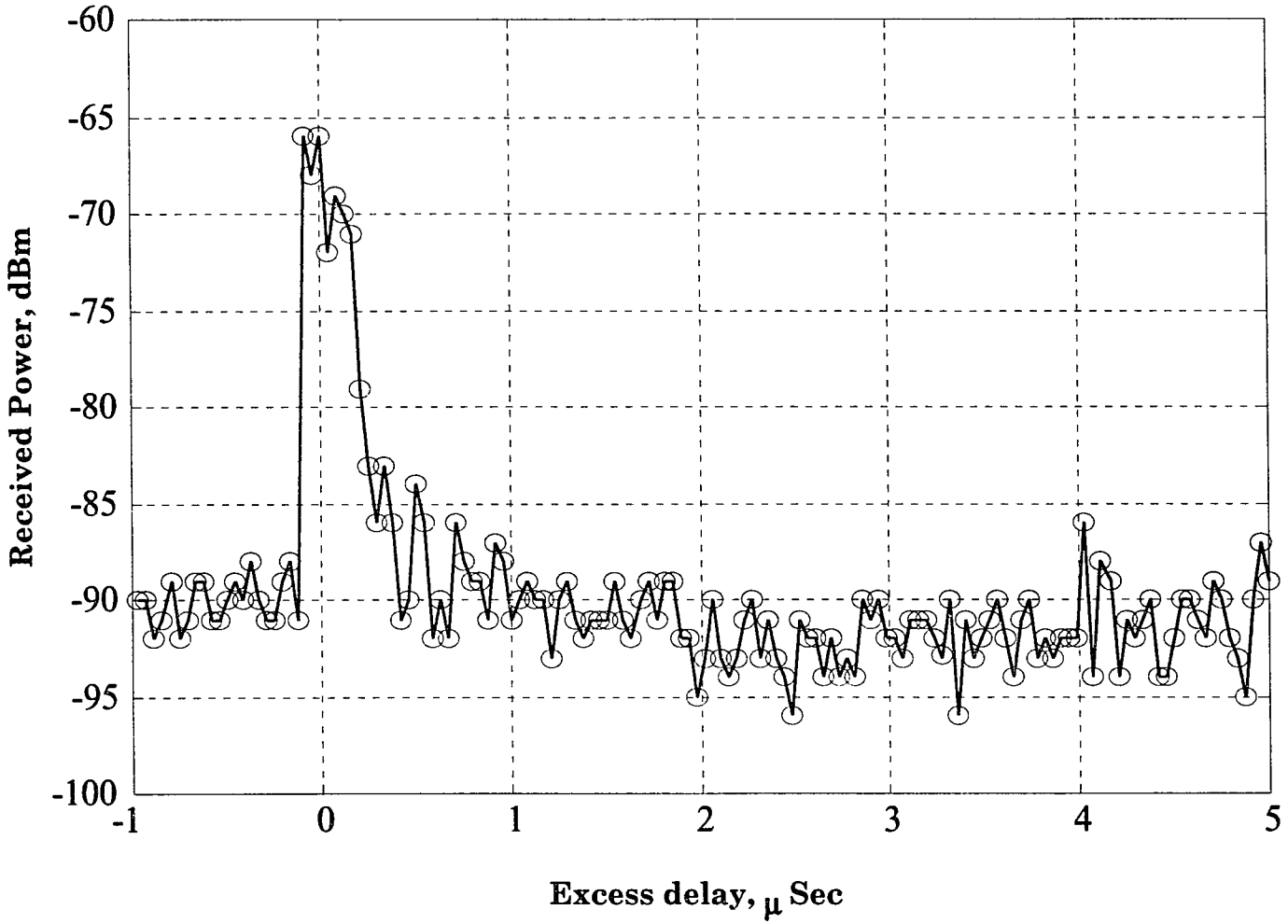


**Figure 5.28: Typical Delay Power Spectrum observed at site D, Chip rate = 24 Mchips/s**

## References

[1] W.Y.C. Lee, "Smaller Cells for Greater Performance," IEEE Comm. Magazine, vol.29, No.11, November 1991.

[2] R. Steele, "The Cellular Environment of Lightweight Handheld Portables," IEEE Comm. Magazine, vol.27, No.7, pp. 20-29, July 1989.

[3] D.C. Cox, "Portable Digital Radio Communications: An Approach to Tetherless access, "IEEE Comm. Magazine, vol. 7, No. 7, pp. 30-40, July 1989.

[4] R.S. Gilhousen, I.M. Jacobs, R. Padovani, A.J. Viterbi, L.A. Weaver Jr., C.E. Weatley III, "On the Capacity of a Cellular CDMA system,"IEEE Veh. Technology, pp. 303-312, May 1991.

[5] G.R. Cooper and R. W. Nettleton, "A Spread Spectrum Technique for High Capacity Mobile Communications, "IEEE Veh. Technology, pp. 98-103, March 1977.

[6] D.L. Schilling, L.B. Milstein, R.L. Pickholtz, F. Bruno, E. Kanterakis, V. Erceg, M. Kullback, W.H. Biederman, D. Fishman, and D. Salreno,"Field Test Experiments using Broadband Code Division Multiple access," IEEE Comm. Magazine, Nov. 1989.

[7] L.B. Milstein, D.L. Schilling, R.L. Pickholtz, V. Erceg, M. Kullback, E. Kanterakis, D. Fishman, W.H. Biederman, and D. Salreno,"On the Feasibility of a CDMA Overlay for Personal Communication Networks," IEEE J. Select. Area in Commun., vol. SAC-10, No. 4, pp. 655-668, May 1992.

[8] D.L. Schilling, K. Parsa, Z. Hadad, J. Garodnick, G. Lomp, D. Greico, "Broadband CDMA Overlay" ICCT Conference, Shanghi, China, June 1994.

[9] H. Taub and D.L. Schilling, " Principles of Communication Systems," 2nd ed: McGraw-Hill., New York, 1986.

[10] C.E. Cook and H.S. Marsh, " An Introduction to Spread Spectrum," IEEE Commun, Magazine, pp 8-16, March 1983.

[11] J.D. Parsons, "The Mobile Radio Propagation Channel", John Wiley & Sons, New York, 1992.

[12] R.A. Scholtz, "The origins of Spread Spectru Communications," IEEE Trans. Commun., vol 30, pp.822-854, may 1982.

[13] R.L. Pickholtz, D. L. Schilling, L. B. Milstein, "Theory of Spread Spectrum Commercial Communications", IEEE Trans. Commun.COM-30, pp 855-884, May 1982.

[14] R.W. Lucky, J. Salz, and E.J. Weldon Jr., "Principles of Data Communication", McGraw-Hill, New York:, 1968.

[15] J.G. Proakis, Digital Communications, 3rd ed., MacGraw-Hill, New York, 1989.

[16] T.S. Rappaport, C.D. McGillem, "UHF Fading in Factories," IEEE J. Select. Area in Commun., vol. SAC-7, No. 1, January 1989.

[17] J. Shapira, "Channel Characteristics for Land Cellular Radio, and Their Systems Implications," IEEE Antenna and Propagat. Mag., vol. 34, No. 4, August 1992.

[18] D.C. Cox and R.R. Murray ,"800-MHz Attenuation Measured in and around Houses," AT&T Tech. Journal., vol. 63, pp. 921-954, July 1984.

[19] D.C. Cox and R.P. Leck ,"Distribution of Multipath Delay Spread and Average Excess Delay for 910-MHz Urban Mobile Radio Paths," IEEE Trans. on Commun., vol. AP-23, No. 2, March 1976.

[20] -------, "Correlation Bandwidth and Delay Spread Multipath Propagation Statistics for 910-MHz Urban Mobile Radio Channels," IEEE Trans. on Commun., vol. com-23, No. 11, November 1975.

[21] -------, "910-MHz Urban Mobile Radio Propagation: Multipath Characteristics in New York City," IEEE Trans. on Commun., vol. com-21, November 1973.

[22] R.J.C. Bultitude, "Measured Characteristics of 800/900 MHz Fading Radio Channels with High Angle Propagation Through Moderately Dense Folidge," IEEE Commun. Mag., vol. 25, June 1987.

[23] R.J.C. Bultitude and G. K. Bedal, "Propagation Characteristics on Microcellular Urban Mobile Radio Channels at 910-MHz," IEEE J. Select. Area in Commun., vol. 7, No.1, pp. 31-39, January 1989.

[24] R.J.C. Bultitude, S. A. Mahmoud and W. A. Sullivan, "A Comparison of Indoor Radio Propagation Characteristics at 910 MHz and 1.75 GHz," IEEE J. Select. Area in Commun., vol. 7, No. 1, pp. 20-30, January 1989.

[25] J. Devasirvatham, "Time Delay Spread and Signal Level Measurements of 850-MHz Radio Waves in Building Environments," IEEE Trans. on Antennas and Propagat., vol. AP-34, pp. 1300-1308, November 1986.

[26] -------, "910-MHz Urban Mobile Radio Propagation: Multipath Characteristics in New York City," IEEE Trans. on Commun., vol. com-21, November 1973.

[27] -------, " Time Delay Spread Measurements of wideband radio signals within buildings," Electron letters, Vol. 20, No. 23, November 1984.

[28] C.S. Gardner and J.A. Orr, "Fading Effects on the Performance of a Spread Spectrum Multiple Access Communication System" IEEE Trans. on Commun., vol. com-237 No. 1, January 1979.

[29] J.G. Proakis and D.G. Manolakis, Introduction to Digital Signal Processing, MacMillan Publishing co., New York, 1988.

[30] D.A. Demery, "Wideband Characterization of UHF mobile radio

channels in Urban areas", Ph.D. Thesis, University of Liverpool, U.K., 1989.

[31] W.R. Young, L.Y. Lacy, "Echoes in transmission at 450 MHz from land-to-car radio units", Proc. IRE, March 1950, Vol 38, pp 255-258.

[32] S.S. Ghassemzadeh, V. Erceg, M. Taylor, D.L. Schilling, H. Arshad, "Indoor Propagation and Fading Characteristics of Spread Spectrum Signals at 2 GHz", Globecom 92, Tutorial Conference.